Journal of Zoological Systematics and Evolutionary Research
November 2021, Volume 59 Issue 8 Pages 1718-1753
https://doi.org/10.1111/jzs.12512
https://archimer.ifremer.fr/doc/00756/86788/

Deep Downunder: Integrative taxonomy of *Austrobela* , *Spergo* , *Theta* and *Austrotheta* (Gastropoda: Conoidea: Raphitomidae) from the deep sea of Australia

Criscione Francesco [1, *], Hallan Anders [1], Fedosov Alexander [2, 3], Puillandre Nicolas [3]

[1] Australian Museum Research Institute Sydney NSW, Australia
[2] A.N. Severtsov Institute of Ecology and Evolution of Russian Academy of Sciences Moscow ,Russia
[3] Institut de Systématique, Évolution, Biodiversité (ISYEB) Muséum National d'Histoire Naturelle CNRS Sorbonne Université EPHE Université des AntillesParis, France

* Corresponding author : Francesco Criscione, email address : francesco.criscione@austmus.gov.au

Abstract :

Recent sampling efforts in the deep seas of southern and eastern Australia have generated a wealth of DNA-suitable material of neogastropods of the family Raphitomidae. Based on this material, a molecular phylogeny of the family has revealed a considerable amount of genus and species level lineages previously unknown to science. These taxa are now the focus of current integrative taxonomic research. As part of this ongoing investigation, this study focuses on the genera Austrobela, Austrotheta (both Criscione, Hallan, Puillandre & Fedosov, 2020), Spergo Dall, 1895 and Theta Clarke, 1959. We subjected a comprehensive mitochondrial DNA dataset of representative deep-sea raphitomids to Automatic Barcode Gap Discovery, which recognized 24 primary species hypotheses (PSHs). Following additional evaluation of shell and radular features, as well as examination of geographic and bathymetric ranges, 18 of these PSHs were converted to secondary species hypotheses (SSHs). Based on the evidence available, the most likely speciation mechanisms involved were evaluated for each pair of sister SSHs, including niche partitioning. Eleven SSHs were recognized as new and their systematic descriptions are provided herein. Of these, four were attributed to Austrobela, one to Austrotheta, four to Spergo and two to Theta. While all new species are endemic to Australian waters, other species studied herein exhibit wide Indo-Pacific distributions, adding to the growing body of evidence suggesting that wide geographic ranges in deep-sea Raphitomidae are more common than previously assumed.

Keywords : biodiversity, deep sea, mtDNA, radula, shell, species delimitation

1 Introduction

Members of the 'turriform conoideans' [Caenogastropoda: Neogastropoda (Bouchet, Kantor, Sysoev, & Puillandre, 2011; Puillandre et al., 2011; Abdelkrim et al., 2018)] are well-known for their extensive shell homoplasy (Kantor, Puillandre, Olivera, & Bouchet, 2008; Kantor, Fedosov, & Puillandre, 2018; Criscione, Hallan, Puillandre, & Fedosov, 2021), although challenges associated with their systematics extend beyond shell morphology. For instance, turriform conoideans do generally not occur in readily accessible intertidal habitats and are typically rare, with many species known from single individuals only (Bouchet, Lozouet, & Sysoev, 2009; Criscione et al., 2021; Hallan, Criscione, Fedosov, & Puillandre, 2021). While already alluded to by Bouchet and Warén (1980), recent findings also suggest that several deep-sea species may be unusually widespread geographically, with some taxa also occupying considerable bathymetric and geographic ranges (e.g. Sánchez & Pastorino, 2020; Zaharias et al., 2020; Criscione et al., 2021; Hallan et al., 2021). With such complicating factors to their taxonomy, the notion that purely shell-based morphology can resolve the systematics of deep-sea turriform conoideans has therefore been largely abandoned in recent years, in favour of integrative approaches combining morpho-anatomical, genetic, and distribution data (Puillandre, Baylac, Boisselier, Cruaud, & Samadi, 2009; Puillandre, Fedosov, Zaharias, Aznar-Cormano, & Kantor, 2017; Zaharias et al., 2020). Owing to their unique venom apparatus, an apomorphic character to the Conoidea (Puillandre, Fedosov, & Kantor, 2015), there is significant impetus to characterise turriform conoidean diversity in order to facilitate further studies on their venom diversity (Lopez-Vera et al., 2004; Puillandre, Koua, Favreau, Olivera, & Stoecklin, 2012; Gonzales & Saloma, 2014; Criscione et al., 2021). However, due to the taxonomic challenges of the group as outlined above, the understanding of their diversity lags far behind that of the related Conidae (Puillandre et al., 2014) and Terebridae (Modica et al., 2019).

In the deep sea, notably in the Australasian region, recent research suggests that the family Raphitomidae is the most diversified conoidean family (MacIntosh et al., 2018; O'Hara et al., 2020; Criscione et al., 2021). Criscione et al. (2021) showed that widespread shell homoplasy among this fauna had led taxonomists to incorrectly attribute a considerable number of unrelated species to very few raphitomid genera (such as *Pleurotomella* Verril, 1872 and *Gymnobela* Verrill, 1884), some of which were shown to be polyphyletic. In constraining these genera, based on their support as clades and on diagnostic morphological

characters, Criscione et al. (2021) introduced a number of new genus-level taxa and described their type species. The same study also revealed a multitude of putatively undescribed species remaining to be tested through integrative taxonomy. Two subsequent studies commenced that task, describing a total of 11 species of the genera *Gladiobela* Criscione, Hallan, Puillandre & Fedosov, 2020 and *Pagodibela* Criscione, Hallan, Puillandre & Fedosov, 2020 (Hallan et al., 2021) and *Famelica* Bouchet and Warén, 1980 and *Rimosodaphnella* Cossman, 1916 (Criscione et al., in press.)

Based on a larger sampling size and on an integrative taxonomic approach, this study aims to test putative species as reported in Criscione et al. (2021) for four genera: *Austrobela* Criscione, Hallan, Puillandre & Fedosov, 2020, *Austrotheta* Criscione, Hallan, Puillandre & Fedosov 2020, *Spergo* Dall, 1895 and *Theta* Clarke, 1959. In the analysis of that study, these genera formed a monophyletic group (Criscione et al., 2021). Formal descriptions are here presented for newly recognised species. Furthermore, revised genus diagnoses and new anatomical and morphological data are introduced for both established and new taxa, which are discussed in terms of their diagnostic utility at the genus level. Finally, geographic and bathymetric distributions are presented for the taxa treated herein, and their biogeographic distributions are briefly discussed.

2 Materials and methods

2.1 Taxon sampling

The samples studied herein were selected among all deep-sea Raphitomidae ethanol-preserved material from the malacological collections of the Australian Museum, Sydney (AMS), the South Australian Museum, Adelaide (SAMA), the Tasmanian Museum and Art Gallery, Hobart, Australia (TMAG), the Western Australian Museum, Perth (WAM) and the Muséum national d'Histoire naturelle, Paris (MNHN). Most of the studied material has been collected off Australia during the expeditions IN2015_C01, IN2015_C02 (in the Great Australian Bight, GAB), IN2017_V03 (Tasman and Coral Seas) and IN2018_V06 (Tasmanian seamounts), targeting several Commonwealth Marine Reserves (CMR) among other sites. The remaining material has been sampled from other localities (mainly of the tropical and temperate Indian and Pacific Oceans), during a number of voyages that formed part of the Tropical Deep-sea Benthos programme of MNHN (https://expeditions.mnhn.fr/; Fig. 1, Table S1).

As a result of ongoing systematic research on the Conoidea at the AMS and MNHN, several hundreds of (mostly unpublished) sequences of two mitochondrial genes, cytochrome oxidase subunit I (*cox1*) and 16S ribosomal RNA (*16S*) were obtained (see methodology below) from a considerable number of largely undescribed representative raphitomid taxa. In order to assist with the selection of the study material, two pilot analyses were performed separately on two datasets including respectively all raphitomid *cox1* and *16S* sequences, using the neighbour-joining method (NJ) (Saitou & Nei, 1987) implemented in MEGA 7 (Kumar, Stecher, & Tamura, 2016). In particular, the datasets included *cox1* and *16S* sequences of the holotypes for the type species of several deep-sea raphitomid genera, including *Austrobela rufa* Criscione, Hallan, Puillandre & Fedosov, 2020 (GenBank ANs: MN983272 for *cox1*, MT395563 for *16S*) and *Austrotheta crassidentata* Criscione, Hallan, Puillandre & Fedosov, 2020 (MT260886 for *cox1*, MN985768 for *16S*), as well as sequences of non-topotypic specimens of *Theta lyronuclea* (Clarke, 1959) (type species of *Theta*) and sequences of well-recognisable species of *Spergo* [other than the type species, *S. glandiniformis* (Dall, 1895)].

According to the results of the NJ analyses, ingroup *cox1* or *16S* sequences (to be used in the molecular analysis - see below) were selected as follows:

1) sequences of any of the species of *Austrobela*, *Austrotheta*, *Theta* or *Spergo* listed above,
2) all sequences that were more closely related to the sequences of any of the species in 1) than to sequences of any other raphitomid genus in the larger dataset.

Sequences representing 37 deep-sea raphitomid species of 13 different genera, were selected to serve as outgroups (Table S1). Their choice was based on the phylogeny of Criscione et al. (2021), containing many southern and south-eastern Australian Raphitomidae, which established the phylogenetic framework for subsequent systematic studies on the family (Hallan et al., 2021; Criscione et al., in press).

Among the ingroup specimens, morphological examination was only conducted on those collected in Australian waters and some of those collected outside Australia (see Results). However, for samples outside Australia, examination of shell photographs was possible and thus utilised when necessary and appropriate. Geographic and bathymetric data were available for all ingroup specimens. Geographic distributions were assessed with reference to marine biogeographic realms as delimited in Costello et al. (2017). According to Bouchet,

Heros, Lozouet, and Maestrati (2008), when inferring bathymetric distributions of species from sampling depth intervals, only shallower depth values were considered, as there is no evidence that the species collected occurs beyond that value.

2.2 Molecular methods

Molecular work was performed in laboratories at two different Institutions (AMS and MNHN). Unless otherwise stated, the same methodology was followed by both laboratories. DNA was extracted from small pieces of foot muscle by use of a Bioline Isolate II Genomic DNA extraction kit for animal tissue, following the standard procedure of the manual (AMS) or using the Epmotion 5075 robot (Eppendorf), following the recommendations by the manufacturer (MNHN). Fragments of *cox1* and *16S* were amplified using the primer pairs LCO1490 (GGTCAACAAATCATAAAGATATTGG)/HCO2198 (TAAACTTCAGGGTGACCAAAAAATCA) for *cox1* (Folmer, Black, Hoeh, Lutz, & Vrijenhoek, 1994) and *16S*H (CCGGTCTGAACTCAGATCACG)/16LC (GTTTACCAAAAACATGGCTTC) for *16S* (Palumbi, 1996). PCR reactions were performed in volumes of 25 µl, containing 3 ng DNA, 1X Qiagen CoralLoad PCR Buffer, 2.5mM MgCl2, 0.25mM dNTP, 0.5mM of each primer, 0.5 µg/µl of BSA and 0.2 µl of Bioline MyTaq DNA polymerase. Amplification consisted of an initial denaturation step at 94 °C for 4 min, followed by 37 cycles of denaturation at 94 °C for 30 s, annealing at 50 °C (*cox1*) and 55 °C (*16S*) for 30 s, followed by extension at 72 °C for 1 min. The final extension was at 72 °C for 5 min. PCR products were purified and sequenced by the Macrogen (AMS) and Eurofins (MNHN) sequencing facilities. When necessary, chromatograms were manually corrected for misreads and forward and reverse strands were merged into one sequence file using CodonCode Aligner v. 9.0.1 (CodonCode Corporation, Dedham, MA). Sequence alignments were generated using MUSCLE as implemented in MEGA7 (Kumar et al., 2016). Sequences were deposited in GenBank (Table S1). Phylogenetic trees were generated using Maximum Likelihood (ML) and Bayesian inference (BI) methods. ML was performed using the program MEGA7 with Nearest-Neighbour-Interchange (NNI) as heuristic method and automatic generation of the initial tree. One thousand bootstrap replicates (BTSP) were performed to assess the topology support. The BI analysis was performed in MrBayes 3.2.6 (Ronquist & Huelsenbeck, 2003) and included 2 runs of 10^7 generations, with 4 chains each and a sampling frequency of one tree per 1,000 generations. Other parameters were set to default. After checking for

convergence (ESS>200) with Tracer (Rambaut, Drummond, Xie, Baele, & Suchard, 2018), a consensus tree was then calculated after discarding the first 25% trees as burn-in. Nodal support was assessed by values of Bayesian posterior clade probabilities (BPP). Prior to the model-based ML phylogenetic analyses, the TN93 model (Tamura & Nei, 1993) with gamma distribution and proportions of invariable sites (TN93+Γ+I) was identified as the best-fit model of sequence evolution for both gene fragments by means of the Bayesian Information Criterion as implemented in MEGA 7 (Kumar et al., 2016). According to MrBayes manual (p. 94), a priori model testing was not performed, and the GTR+G+I model was applied to the BI analysis. Uncorrected pairwise genetic distances were calculated using MEGA7 with the option 'pair-wise deletion of gaps'.

2.3 Morphological examinations

All studied samples consisted of bodies and their shells, from which they had been removed following the methodology described in Criscione et al. (2021). We studied shell morphology and (when possible) internal anatomy, including radular morphology. Shells of sequenced specimens were affixed to plasticine and positioned with their vertical axis parallel to the observation plane. Each shell was then photographed from above (frontal and lateral views) using a digital SLR camera. Maximum shell length (SL) and width (SW) were measured on digitised images using the calibrated ruler tool in Adobe Photoshop CC v.20.0.6. Measurements were rounded to the nearest 0.1 mm. The number of shell whorls was counted under a Leica MZ8 stereomicroscope, in accordance with Bouchet and Kantor (2004). While it was possible to obtain the number of teleoconch whorls (Wt) for almost all studied specimens, protoconch whorls could only be counted occasionally due to widespread erosion of the apex. When sufficient samples were available, morpho-spaces of individual species were compared through scatterplots of SW and SL.

Anatomical studies were conducted on animals removed from ethanol and briefly rehydrated in distilled water. Using standard dissection tools, the venom apparatus was excised and the radular sac isolated and placed on a glass slide; during this dissection process, head-foot, mantle, genital and (non-radula) foregut characters were examined where possible. After dissolution in diluted commercial bleach, clusters of hypodermic teeth were rinsed repeatedly in distilled water, then separated into individuals and ligament-connected pairs or smaller clusters. Subsequently, the glass stub was affixed to a carbon

adhesive placed on a 12 mm diameter aluminium mount. All samples were imaged at Macquarie University, Sydney, using a Phenom XL Scanning Electron Microscope. For radular descriptions we followed the terminology accepted and discussed by Kantor and Taylor (2000).

Species delimitation

The Automatic Barcode Gap Discovery (ABGD) (Puillandre, Lambert, Brouillet, & Achaz, 2012) was applied for primary species delimitation to a dataset including all *cox1* sequences. The web-based version of ABGD (https://bioinfo.mnhn.fr/abi/public/abgd/abgdweb.html) was used with a p-distance model. The relative gap width (X) was set to 1 and the other parameters left to default. Resulting ABGD groups were considered primary species hypotheses, henceforth referred to as PSHs. Following Puillandre, Modica, et al. (2012), conversion of PSHs to secondary species hypotheses (SSHs) was conducted through comparative examination of morphological characters as well as through evaluation of geographic and bathymetric distributions.

In particular, when converting individual PSHs to SSHs, the occurrence of the following conditions was assessed: (i) the PSH is a highly supported clade (BPP>0.98 and BS > 90%), (ii) all its constituent specimens share at least one distinctive morphological feature deemed not to be polymorphic or ecophenotypic, and without exhibiting intermediate forms, (iii) the PSH maintains genetic or morphological divergence and/or bathymetric partitioning when occurring in sympatry with another PSH. When available, species names were assigned to SSHs based on the current taxonomy. New species names were introduced when no names were available, and formal descriptions for these taxa are given in the systematic section below.

3 Results

3.1 Molecular studies

Molecular analyses were based on a total of 190 *cox1* sequences (158 newly generated and 32 GenBank-sourced) and 148 *16S* sequences (112 newly generated and 36 GenBank-sourced). Of the total sequences employed, 283 (153 *cox1* + 132 *16S*) constituted the ingroup and the remaining 55 (37 *cox1* and 18 *16S*), were used as outgroups.

In the vicinity of the barcode gap, the ABGD analysis of the *cox1* ingroup dataset consistently returned an initial partition with 23 PSHs. Among all PSHs, fourteen (A1–A5, S3–S6, U1–U2, T1–T3) contained exclusively Australian samples, two (A6 and S2) included samples from Australian seas and beyond, while the remaining seven (A7–A8, AA–AD and S1) encompassed sequences from outside Australian waters only.

Molecular analyses (BI and ML) were conducted on both single-gene datasets and on a dataset formed by concatenating all 190 *cox1* sequences and 128 *16S* sequences obtained from samples of the *cox1* dataset. In all analyses, one sequence was used for each cluster of identical sequences (CIS, Tables S2–S3) and identical haplotypes are labelled accordingly in the resulting trees (Figs 2–3, S1).

The trees generated with the *cox1* dataset (not shown) were very similar to that of the combined dataset (Figs 2, S1). As these latter trees provided higher support to the PSH clades, we refer to them in the below section detailing species delimitation.

The BI and ML analyses of the *cox1+16S* dataset generated trees with comparable topologies (Figs 2, S1). While deeper nodes were unstable across trees and often lacked support, only minor differences were observed in the relative position of individual sequences within some of the clades representing PSH-level relationships. In both analyses, four major genus-level clades were retrieved among the ingroup sequences, namely *Austrobela* (BPP=0.96, BTSP=56%), *Theta* (BPP=1, BTSP=99%), *Austrotheta* (BPP=1, BTSP=99%) and *Spergo* (BPP=1, BTSP=66%). These four generic clades included twelve, three, two and six PSHs respectively, mostly well-differentiated (in terms of branch lengths) and exhibiting moderate (BPP=0.95–0.98; BTSP=75–90%) to high (BPP >0.98; BTSP=>90%) values of nodal support.

No supported conflicting topologies were found between BI and ML trees obtained analysing the *16S* dataset, hence only the ML tree is shown here (Fig. 3). Based on a dataset of rather different composition (i.e. missing sequences of outgroup and of samples of A7, A8 and S1 as well as presence of 17 additional samples with no corresponding *cox1* sequence), this tree (Fig. 3) differed to some extent from the *cox1+16S* trees. In particular, clades corresponding to only 20 of the total PSHs were retrieved (although generally well-supported), with an additional clade (A9) recovered, formed by two identical *16S* sequences and for which no corresponding *cox1* sequence was available. Given the substantial topological congruence between *16S*- and *cox1*-based trees with respect to the PSH-level

clades (Figs 2–3), A9 is considered an additional PSH to undergo further testing for conversion to SSH.

In the *Austrobela* clade, the intra-PSH pairwise distances in *cox1* ranged from 0 to 0.5% (average=0.2 %) with inter-PSH distances ranging from 2.8 to 9.8 % (average=6.9%) (Table 1). The lowest inter-PSH distances were observed between A1 and A2 and the highest intra-PSH distances were found within A5. In the *Spergo* clade, the intra-PSH pairwise distances in *cox1* ranged from 0.2 to 0.8% (average=0.4 %) with inter-PSH distances ranging from 2.8 to 8.0 % (average=6.2 %) (Table 2). The lowest inter-PSH distances were observed between the pair S5/S6 and the highest intra-PSH distances were found within S2. In the *Theta* clade, the intra-PSH pairwise distances ranged from 0.3 to 0.6% (average=0.5%), whereas inter-PSH distances ranged from 3.3 to 4.9 % (average=4.1 %). The lowest inter-PSH distances were observed between T2 and T3 and the highest intra-PSH distances were found within T2. The distance between the two PSHs (one sequence each) in the *Austrotheta* clade was 3.1%. Genetic distances in *16S* within clades of *Austrobela*, corresponding to PSHs (Fig. 3), ranged from 0 to 0.2%, while distances between clades ranged from 0.2 to 3.1%. The lowest value of inter-PSH distance was recorded between A9 and A5 and the highest intra-PSH distance was measured for A3.

3.2 Morphological studies

Morphological observations refer to PSHs that are examined herein, and do not include PSHs assigned with a letter suffix (i.e., AB, AC, etc.). Considerable shell erosion affected the protoconchs of most specimen studied. As a consequence, protoconch sculpture could not be studied for *Spergo*. For *Theta* and *Austrotheta*, some sculptural detail could be inferred from heavily eroded protoconchs by careful examination using a microscope. However, these are not figured herein owing to their very poor quality. Due to the limited number of adult samples available for the other genera (see Table S1), the extent of intraspecific variability in shell features could be assessed in *Austrobela* only, albeit for just five PSHs: A1, A2, A3, A5, A6). SW/SL scatterplots (Fig. 4) could be generated for three of these PSHs only (A1–A3).

Differences in shell morphology among *Austrobela* species largely relate to sculptural elements, with the gross morphology in most PSHs consisting of a fusiform-biconical shape (Figs 5–7). When compared to the other PSHs, A6 and A7 (Fig. 7B, F) exhibit tall-spired shells

with 2–3 additional whorls. While shells of A6 were morphologically homogeneous, there was considerable intra-PSH variability for A1, A2, A3 and A5 (Figs 5; 6A–E, F–G - see Systematics for details on individual species). The protoconch (Fig. 8) is multispiral in all *Austrobela* PSHs, exhibiting sculpture of arcuate riblets in A1–A3 (Fig. 8A–D), diagonally cancellate sculpture in A4 and A6 (Fig. 8E–F) and with diagonally cancellate abapical portion with arcuate riblets on the adapical portion in A5 (Fig. 8G). No material of A7 and A8 was available for protoconch examination. The general radular morphology observed in all examined members of *Austrobela* consists of hypodermic teeth with two large, sharp distal barbs, a somewhat inflated lower portion of the shaft, and a thick ligament (Fig. 9). While virtually indistinguishable among most PSHs, radular teeth are somewhat different in A3 and A4. The tooth of A3 has a rather marked excavation of the ventral barb (when viewed laterally; Figs 9F, 10A), whereas the tooth of A4 is far longer than that of other PSHs (Fig. 9G).

The *Spergo* clade is comparatively heterogenous based on shell morphology, and all PSHs can readily be differentiated based on their shell features (Figs 11–12). *Spergo* PSHs exhibit shells ranging from large, elongate-fusiform with tall, cylindrical whorls in S5 (Fig. 11C), to rather small and fusiform-biconical in S3 (Fig. 11D). There are significant differences among PSHs in the presence and relative position of the shoulder, and while shells of all PSHs exhibit axial and spiral sculpture, there are notable differences in the arrangement and prominence of sculptural elements. The radulae in all but one studied PSH (S2, S4–S6; Fig. 13) consist of awl-shaped hypodermic teeth with a comparatively short, simple dorsal blade, a lateral process and a large, wide ligament. In S3, the tooth is significantly smaller, without a blade and a lateral process, and with a highly inflated base (Fig. 13C). In S5, there is considerable variability of tooth formation, ranging from straight and comparatively tightly rolled (*e.g.* Fig. 14A, E) to entirely unrolled (Fig. 14B).

In the *Theta* clade, all PSHs can be readily differentiated based on teleoconch morphology (Fig. 15D–F), ranging from distinctly shouldered with prominent axial tubercles in T1 to comparatively smooth with very weak to absent shoulder and rather convex teleoconch whorls in T2, with T3 exhibiting somewhat intermediate morphology. Two types of protoconch sculpture were exhibited by PSHs of *Theta*: arcuate riblets were present in T1 and T2, while T3 exhibited a (at least partly) diagonally cancellate pattern. In terms of the

radula (Fig. 16A–C), the hypodermic teeth with two comparatively weak barbs are arguably indistinguishable between T1 and T3, with somewhat weaker barbs in T2.

The two PSHs comprising the *Austrotheta* clade can be readily differentiated based on shell morphology (Fig. 15G–H), in that U1 exhibits long, sharp, weakly opisthocline axial ribs on early to mid teleoconch whorls, with U2 possessing a more distinct shoulder with tuberculate axial elements. The hypodermic teeth have only successfully been extracted for U1 (Fig. 16D), which possesses very thick and double-barbed teeth with extremely coarse basal texture and a very large ligament.

3.3 Geographic and bathymetric distributions

The recorded bathymetric range for *Austrobela* spans from 372 to 3235 metres, with *Spergo* exhibiting a very wide range from 318 to 4750 metres (Fig. 17). *Theta* is recorded between 2474 and 4890 metres, and *Austrotheta* between 2751 and 3389 metres.

In *Austrobela*, the sister PSHs A1 and A2 (Fig. 3) are known only from southern Australia, with the majority of records occurring in the GAB where they exhibit considerable geographic and bathymetric overlap (Figs 1, 17) between 965 and 1321 metres. Their sister taxon A3 (Fig. 3) occurs exclusively in the GAB with no bathymetric overlap with A1 and A2, with a reported range of 1535 to 2831 metres. In the GAB, A3 occurs in partial micro-sympatry with A5, the latter occupying a depth range between 1509 and 3235 metres, also extending eastward and up the eastern Australian coast to the Hunter Commonwealth Reserve (Figs 1, 17). Records of A4 and A9 are restricted to the eastern Australian coast, with A4 occurring between 1761 and 2429 metres depth, with records from the Central Eastern Marine Commonwealth Reserve and the Coral Sea Commonwealth Reserve. A9 is recorded at 2562 metres depth off Byron Bay, northern New South Wales (NSW).

With the exception of S2, all PSHs of the *Spergo* clade treated herein are recorded exclusively from the southeast Australian coast, from east of Tasmania northward to northern NSW. In terms of the bathymetric distribution PSHs of *Spergo* can be divided into three groups: S1 and S2 occur above 2000 metres, S5 and S6 are found between 2000 and 3000 metres, and S3 and S4 occur at depths below 3750 metres (Fig. 17). Only two PSHs, S3 and S4, have been recorded in micro-sympatry in the Bass Strait (Fig. 1E).

For the *Theta* clade, no clear bathymetric partitioning can be inferred due to the small sample size of T2 and T3, with all three PSHs recorded below 2500 metres (Fig. 17). T1

exhibits a wide bathymetric range between 2649 and 4890 metres, and with T2 and T3 recorded in 2677 to 2800 metres and at 2474 metres, respectively.

For the *Austrotheta* clade, both PSHs have been collected from single localities only: U1 from 2751 metres off eastern Tasmania, and U2 from 3389 metres in the GAB (Figs 1C–D, 17).

3.4 PSH to SSH conversion

Comparative examination of the morphological, geographic and bathymetric data available was employed to attempt the conversion of PSHs to SSHs. As generating morphological data for most species with distribution outside Australian waters was beyond the scope of this study, testing of four PSHs (i.e. AA–AD), out of the total of 23 retrieved by ABGD, was not attempted and these are pending further sampling and taxonomic investigation. Of the remaining 19 PSHs, 17 (16 retrieved by ABGD - namely A3–A8 S1–S6, T1–T3 and U1–U2 and one inferred from *16S* data – A9), satisfied the conditions described in the methodological section, while two PSHs (A1 and A2) did not. The evidence for PSHs to SSHs conversion is detailed below, where congeneric PSHs are compared with each other according to their relationships as resolved by the molecular analysis (Figs 2, 3 and S1).

In *Austrobela*, A1 and A2 corresponded to highly supported clades (BPP=100%, BTSP=99%; Figs 2, S1) in a sister relationship. Both exhibited very low intra-PSH genetic distance (average 0.01% and 0.02% respectively; Table 1) and moderate reciprocal genetic distance (average 2.8%; Table 1). Although both A1 and A2 could be often distinguished from all other PSHs by their combined dark orange, broad, distinctly shouldered teleoconch whorls with few wide axial ribs (Fig. 5) and protoconch with arcuate riblets (Fig. 8A–C), no morphological features could be used to readily distinguish the two. Furthermore, their bathymetric (Fig. 17) and geographic ranges overlap extensively, with numerous occurrences of micro-sympatry (i.e. the two PSHs were found in the same trawl haul) (Fig. 1B–D). Rather than supporting the conversion into separate SSHs, the evidence produced indicates that A1 and A2 may be two mitochondrial lineages within the same SSH (A1/2).

Clade A3 was highly supported (BPP=1 and BTSP=99%), exhibiting values of intra-PSH genetic distances (average 0.4%; Table 1) well below values of reciprocal between-PSH genetic distance with its most closely related PSHs (4.4% with A1 and 5.3% with A2; Table 1).

The distinctive, virtually unsculptured white teleoconch (Fig. 6A–E), the protoconch

sculpture of very closely set arcuate ribs (Fig. 8D) and the excavated adapical opening of the hypodermic teeth (Figs 9F, 10A) shared by its constituent samples, set A3 apart from all other PSHs, including the microsympatric A1 and A5 (Fig. 1B).

In the ML analysis of the combined dataset (Fig. S1), samples of A5 are sister to the only sample of A4 (AMS C.519338), from which they exhibited values of genetic differentiation (average=3.3%; Table 1) that were notably higher than values measured between themselves (average=0.5%). They both occurred in the same marine realm (Coral Sea - Fig. 1D) and at a comparable depth (Fig. 17). However, A4 can be readily differentiated from A5 by its much more shouldered and sculptured shell (Fig. 6H), by its diagonally cancellate protoconch and by its distinctively more elongate hypodermic teeth (Fig. 8E). This latter feature is not found in any of the other congeneric PSHs.

In the Coral Sea (Fig. 1D), the sister pair A4/A5 co-occurred and were closely related with A6. This latter PSH received low BPP support (0.94) but exhibited low values of intra-PSH genetic distance (average=0.3%; Table 1) and moderately high values of genetic differentiation from both A4 and A5 (4.2% and 2.9% respectively; Table 1). The shell of A6 (Fig. 7B) is markedly more elongate than shells of both A4 and A5 (Figs 6F–H) and it is found at shallower depth than the latter two PSHs (Fig. 17).

The analysis of the *16S* dataset (Fig. 3) revealed a sister relationship between A5 and A9, that occur at the same depth range. However, despite being sympatric in the Coral Sea realm, these two PSHs maintain considerable morphological differentiation. In particular, A9 differs from A5 in overall shell shape and colour (Fig. 6F–G, I) and protoconch sculpture (diagonally cancellate vs. diagonally cancellate and with arcuate ribs; Fig. 8G–8H).

Two further PSHs, A7 and A8, were recorded at much shallower depths (Fig. 17) outside Australian waters (Table S1). Although A7 received phylogenetic statistical support in the ML analysis only (BTSP=88%; Fig. S1), it exhibited low intra-PSH genetic distance (0.3%, Table 1) and moderate values of inter-PSH distance (3.0%) with its closely related PSHs, AD (Table 1). The geographic and bathymetric ranges of the two PSHs overlap in the South Pacific (Table S1, Fig. 17); but their morphological distinctiveness could not be assessed, due to the lack of shell or radular data for AD. Although A7 is here tentatively regarded as a distinct SSH from AD, it is not unlikely that the two PSHs would prove to be conspecific, once further data is available. A8 was highly supported (BPP=1 and BTSP=100%) and exhibited high levels of genetic differentiation (>7.1%, Table 1) from all other PSHs in the *Austrobela* clade. It is

found well outside the focus area of this paper (Caribbean Sea) and its shell exhibits a characteristic 'speckled' colouration, not found in other congeners. These elements are considered sufficient to warrant its conversion to SSH.

In *Spergo*, two well-supported PSHs, S1 (BPP=1; BTSP=99%) and S2 (BPP=0.98; BTSP=91%), forming a sister relationship, exhibited low values of intra-PSH genetic distance (average=0.3% for S1 and 0.8% for S2; Table 2) but were separated by moderately high inter-PSHs distance (average=2.8%; Table 2). They occur at much shallower depths than all other congeneric PSHs, from which they can be differentiated by a more prominent axial sculpture. Samples of S2 were collected in the Coral and northern Tasman Sea (Fig. 1E) and in the South China Sea, where they co-occur with samples of S1 (Table S1). Although the radulae of S1 and S2 have not been studied here, their shells are markedly distinct (i.e. more elongate and with less pronounced axial ribs in S2, Fig 12B).

A strongly supported PSH clade (BPP=1 and BTSP=100%), S3, was sister to the S1/S2 pair in the *cox1+16S* tree (Fig. 2). It exhibited low values of intra-PSH genetic distance (0.2%; Table 2) and was separated from all other congeneric PSHs by comparatively high values (>6.7%; Table 2) of genetic distance. Along with its genetic distinctiveness, S3 could be readily separated from other PSHs in *Spergo* mainly by its extremely reduced venom apparatus and extremely small teeth, bearing neither barbs nor a blade (Fig. 13C).

Despite its low BPP support (0.90), S4 exhibited low intra-PSH genetic distance (0.6%; Table 2) and was separated from the closely related S5 and S6 by relatively high genetic distance (4.2 and 3.4% respectively; Table 2). In the South Australia realm, S4 co-occurs with S5 (Fig. 1E), where it occupies a clearly distinct bathymetric range (Fig. 17). Furthermore, S4 can be readily differentiated from all congeneric PSHs by a combination of its distinctively thin shell with a curved siphonal canal (Fig. 11B). The sister pair S5/S6 were both highly supported (BPP=1, BTSP=99%) and exhibited little intra-PSH genetic distance (0.3 and 0.5% respectively; Table 2). These were separated by the lowest inter-PSHs genetic distance (2.8%; Table 2) of all PSHs in *Spergo*. Their distribution is geographically disjunct (Fig. 1E) and bathymetrically overlapping (Fig. 17). However, S5 and S6 differ considerably in both shell colour and shape (respectively red and elongate vs. white and broad) and whorl profile (cylindrical vs convex) (Fig. 11C, E). In addition, these two PSHs also differ in radula features, with S5 having loosely rolled teeth (Fig. 13A) and S6 exhibiting more tightly rolled ones (Fig. 13E). Given their low genetic divergence, S5 and S6 could be (in theory) considered

geographically distinct populations of a single species. However, the morphological differentiation observed was higher than that expected between potential ecophenotypes. Hence, S5 and S6 are considered distinct SSHs.

Within *Theta*, T1 was highly supported (BPP=1; BTSP=98%), exhibited low values of intra-PSH genetic distance (average=0.3%) and comparatively high levels of genetic differentiation from both T2 (4.9%) and T3 (4.2%). This PSH occurs in deeper waters than both T2 and T3 (Fig. 17) and can be distinguished from these by its much broader shell bearing coarse, prominent axial ribs on all whorls (Fig. 15D). In particular, T1 possesses a different protoconch sculpture (of arcuate riblets) from that of T3 (at least partly diagonally cancellate). The difference in shell morphology between T1 and T2 (Fig. 15D, F) is maintained in spite of their co-occurrence in the South Australia realm (Fig. 1C).

The inter-PSHs genetic distance separating T2 (BPP=1; BTSP=99%) and T3 (one sample only) was the lowest of all PSHs in *Theta* (3.3%; Table 2). Their distribution is geographically disjunct (Fig. 1C) and bathymetrically overlapping (Fig. 17). However, T2 and T3 differ considerably in the sculpture of both teleoconch (respectively unsculptured vs. bearing axial ribs; Fig. 15E–F) and protoconch (with arcuate ribs vs. at least partly diagonally cancellate). and these differences are deemed sufficient for their conversion to SSH.

Despite their moderate inter-PSHs genetic distance (3.3%), both PSHs of *Austrotheta* (U1 and U2, each represented by one specimen only) were converted into SSHs, based on their difference in shell features (such as relative size, teleoconch whorl profile and sculpture) (Fig. 15G–H) and their disjunct bathymetric distributions (Fig. 17). The observed divergence was present in spite of their co-occurrence in the South Australia realm (Fig. 1C–D).

3.5 Assigning names to SSHs

A search was conducted for all names available and potentially applicable to the eighteen SSHs resulting from the conversion process described above. By consulting the relevant literature on Raphitomidae (Clarke, 1959; Bouchet & Warén, 1980; Sysoev, 1997; e.g. Bouchet & Sysoev, 2001; Sysoev & Bouchet, 2001; Kantor & Taylor, 2002; Sánchez & Pastorino, 2020; Criscione et al., 2021) and by comparison of molecular and morphological data available on type specimens with the data generated on sequenced specimens, we found eight names applicable to eight SSHs. Two of these SSHs, A1/2 and U1, comprised the type material of respectively *Austrobela rufa* (Fig. 5A) and *Austrotheta crassidentata* (Fig.

15H) and could therefore be respectively assigned to these species. The remaining six SSH, namely A6, A7, A8, S1, S2 and T1, included specimens whose shells closely resembled the holotypes of respectively *Gymnobela procera* Sysoev & Bouchet, 2001 (Fig. 7A), *Gymnobela micraulax* Sysoev, 1997 (Fig. 7E), *Gymnobela pyrrhogramma* (Dautzenberg & Fischer, 1896) (Fig. 6J), *Gymnobela sibogae* (Schepman, 1913) (Fig. 11F), *Spergo fusiformis* (Kuroda & Habe, 1961) (Fig. 12A) and *Theta lyronuclea* (Fig. 15A). Shells of specimens of all five SSH also exhibited patterns of morphological variation which were consistent with those reported in the literature (see Bouchet & Warén, 1980; Sysoev & Bouchet, 2001; Kantor & Taylor, 2002; Sánchez & Pastorino, 2020; Criscione et al., 2021). Therefore, these SSHs were attributed to these species. This required the formal transfer (as hereby proposed) of the first three species to *Austrobela* as *Austrobela procera* n. comb., *Austrobela micraulax* n. comb. and *Austrobela pyrrhogramma* n. comb and of the fourth species to *Spergo* as *Spergo sibogae* orig. comb. As no available names could be found for the remaining eleven SSHs, new taxon names were assigned: namely *A. levis* n. sp. (A3), *A. sagitta* n. sp. (A4), *A. obliquicostata* n. sp. (A5) and *A. regia* n. sp. (A9) (for *Austrobela*); *S. parvidentata* n. sp. (S3), *S. tenuiconcha* n. sp. (S4), and *S. castellum* n. sp. (S5) and *S. annulata* n. sp. (S5) (for *Spergo*); *T. polita* n. sp. (T2) and *T. microcostellata* n. sp. (T3) (for *Theta*) as well as *Austrotheta wanbiri* n. sp. (U2) (for *Austrotheta*). Formal taxonomic descriptions of these newly recognised species are provided below.

3.6 Systematics

General remarks

If not stated otherwise, holotypes are dissected ethanol-preserved specimens on which all systematic descriptions are based. Shell whorls counts (approximated to one decimal unit) are reported with reference to intact whorls only. When applicable, the expression ‘at least’ is used in combination with the whorl count to indicate potential additional missing whorls that could not be counted. Shell and head-foot colouration reported in the descriptions are based on observations performed prior to fixation, and thus may not be fully reflected in the illustrations provided (Figs 5–8, 11–12, 15).

Measurements of radular features, mainly the length of the adapical opening and the dorsal blade, are given as ratios of the length of the shaft. The ‘shaft’ is here defined as the entire

length of the tooth minus the base. This is done to ensure consistency with the terminology used in Criscione et al. (2021).

Superfamily Conoidea Fleming, 1822

Family Raphitomidae Bellardi, 1875

Genus *Austrobela* Criscione, Hallan, Puillandre and Fedosov, 2020 (Criscione et al., 2021; p. 983)

Type species: *Austrobela rufa* Criscione, Hallan, Puillandre and Fedosov, 2020 by original designation (PSHs A1–A2).

Other species: *A. levis* n. sp., *A. micraulax* (Sysoev, 1997) (Fig. 7E; Sysoev, 1997; p. 338–339, figs 47–48), *A. obliquicostata* n. sp., *A. procera* (Sysoev & Bouchet, 2001) (Fig. 7A; Sysoev & Bouchet, 2001; p. 312–313; figs 131–133, 172), *A. pyrrhogramma* (Dautzenberg & Fischer, 1896) (Fig. 6J; Dautzenberg & Fischer, 1896; p. 415–416; pl. 17, fig. 6–8), *A. regia* n. sp., *A. sagitta* n. sp.

Diagnosis

Shell fusiform, thin. Protoconch multispiral, orange. Protoconch sculpture varying from diagonally cancellate to bearing widely distanced to closely set arcuate ribs, or combination of diagonally cancellate (abapical) and arcuate (adapical). Teleoconch red orange, cream or white, suture impressed. Whorl profile medium- to very broad, with wide, concave to oblique subsutural ramp, clearly demarcated from whorl periphery. Lower portion of whorl cylindrical or convex. Subsutural ramp sculpture of dense arcuate growth lines, reflecting shape of anal sinus. Teleoconch axial sculpture absent or of ribs below subsutural ramp; spiral sculpture of fine, sometimes flattened cords or shallow grooves; microsculpture of growth lines. Last adult whorl evenly convex, clearly to very clearly demarcated from rather straight, subcylindrical to tapering siphonal canal.

Aperture elongate, from about 2/5 to half of total shell length; outer lip thin, unsculptured. Inner lip with distinct callus and with or without spiral cords extending onto rather straight columella; callus whitish, red orange with or without a darker transversal band. Anal sinus wide, moderately deep to deep, L-shaped.

Cephalic tentacles muscular, subcylindrical to cylindrical; eyes large. Rhynchodeal introvert rather thin-walled, densely folded. Venom apparatus extremely large, occupying majority of rhynchocoel. Radula of hypodermic teeth with two large, sharp distal barbs; lower portion of shaft somewhat inflated; base broad; ligament thick.

Remarks

Prior this study, the type species *A. rufa* was the only described *Austrobela* species. Here, the total number of species is increased to eight, following the description of four new species and the transfer to *Austrobela* of further three species previously included in different genera. The current genus distribution appears disjunct, with most species occurring in the Indo-Pacific (three realms, Fig. 1A, B, D) and one (*A. pyrrhogramma*) in the Caribbean Sea (Fig. S1). However, the picture of the genus diversity and distribution emerging here is far from complete, due to narrow geographic focus of this study. It is almost certain that a comprehensive revision of *Austrobela* (with access to data from taxa not treated here) would result in an increase of its species number and in a considerable expansion of its geographic range. Our results indicate that up to four additional species from outside Australian waters could be added to *Austrobela* once morphological data is available for PSHs AA–AD (Fig. 2). Further molecular data would be also necessary to evaluate the genus placement of further 9 deep-sea raphitomid species (currently included in *Gymnobela*, *Xanthodaphne* Powell, 1942 and *Theta*) that exhibit conchological and (when available) radular features very similar to those observed in *Austrobela*.

One of these species, *G. nivea* Sysoev, 1990 (Fig. 18F; Sysoev, 1990, fig. 3.7) occurs in the Nazca and Salas y Gomez Ridges off the coast of Chile. Another species, *G. gypsata* (Watson, 1881) (Fig. 18A; Dell, 1963, figs 10–11) was described from (off) New Zealand. Two more species, *G. ceramensis* (Schepman, 1913) (Fig. 18H; Schepman, 1913, pl. 30, fig. 3) and *G. dubia* (Schepman, 1913) (Fig. 18C; Schepman, 1913, pl. 30, fig. 8) were described for the Ceram Sea (off E Indonesia). One species, *X. pyrropelex* (Barnard, 1963) (Barnard, 1963, fig. 2c; Sysoev, 1996, figs 16-18, 20), is found off the South African Cape region. Of the further four species described for the Atlantic, two are from the NE, namely *G. fulvotincta* (Dautzenberg & H. Fischer, 1896) (Fig. 18B; Bouchet & Warén, 1980, figs 109, 251) and *Theta chariessa* (Watson, 1881) (Fig. 15C; Bouchet & Warén, 1980, fig. 129 - but not 130)

and two are from the NW, namely *G. filifera* (Dall, 1881) (Fig. 18D; Dall, 1889, pl. 12, fig. 9) and *G. petiti* Garcia, 2005 (Fig. 18E; Garcia, 2005, figs 17–19).

Austrobela exhibits a fusiform, lightly sculptured shell, typical of taxa attributed tentatively to *Gymnobela* by earlier studies (e.g. Sysoev, 1990, 1996, 1997; Sysoev & Bouchet, 2001). As a result of a predominantly conchological approach, *Gymnobela* s. l., became a "dumpster", later shown to be an assemblage of a number of evolutionary distinct genus-level lineages, including *Austrobela* (Criscione et al., 2021). Its thin-walled, often semitranslucent, lightly sculptured shells with longer siphonal canal differentiate *Austrobela* from other genera once encompassed by *Gymnobela*, which also differ each by a set of additional shell characters, such as: smaller size and weaker spiral sculpture (*Theta*, *Fusobela* Criscione, Hallan, Puillandre & Fedosov, 2020 and *Gladiobela*), keeled, shorter and broader whorls (*Pagodibela*), more robust, chalky shells ('*Gymnobela' ioessa* Sysoev, 1997 and some other species conventionally placed in *Gymnobela*). While the two-barbed hypodermic tooth of *Austrobela* is very similar to that of *Theta*, it exhibits notably more prominent distal barbs (Figs 9 and 16).

Austrobela rufa Criscione, Hallan, Puillandre & Fedosov, 2020 (PSHs A1, A2)
(Figs 5, 8A–C, 9A–B, 10D)

Austrobela rufa - (Criscione et al., 2021; p. 983–984, figs 3F, 5E, 6D)

Material examined

Holotype. Australia, GAB, (-35.15, 134.11), IN2015_C02_131, 965–1077 m, AMS C.571709.

Paratypes. Australia, Tasmania, Flat area south of Brians, (-44.24, 147.29), IN2018_V06_169,1443–1422 m, 1 wet (TMAG E59197); St Helens flat, (-41.21, 148.8), IN2018_V06_184, 1221–1202 m, 1 wet (AMS C.271201), 1 wet (AMS C.574588), (TMAG E45585), 1 wet (TMAG E45586), 1 wet (TMAG E59223). GAB, (-35.34, 134.05), IN2015_C02_134, 1509–1544 m, 1 wet (AMS C.532691), 1 wet (AMS C.571699); (-35.15, 134.11); IN2015_C02_131, 965–1077 m, 1 wet (AMS C.571786), 1 wet (AMS C.571787); (-34.82, 132.69), IN2015_C02_167, 1015–998 m, 1 wet (AMS C.532677); (-34.78, 131.73), IN2015_C01_099, 1323–1340 m, 1 wet (AMS C.483801), 1 wet (AMS C.483802), 1 wet (AMS C.571668); (-34.74, 131.84), IN2015_C01_108, 1350–1321 m, 1 wet (SAMA D44253), 1 wet (SAMA D67742), 1 wet (SAMA D67745); (-34.71, 132.53), IN2015_C01_114, 994–980 m, 1 wet (AMS C.571679), 1 wet (AMS C.571781); (-34.67, 132.48), IN2015_C01_117, 1016–1014

m, 1 wet (AMS C.571681), 1 wet (AMS C.571784), 1 wet (AMS C.483817); (-33.52, 130.27), IN2015_C02_382, 978–1013 m, 1 wet (AMS C.571680), 1 wet (AMS C.571790), 1 wet (AMS C.571791); (-33.52, 130.27), 1 wet (AMS C.571792), 1 wet (AMS C.571793), 1 wet (AMS C.571796), 1 wet (AMS C.571799), 1 wet (AMS C.571801), 1 wet (AMS C.571803), 1 wet (AMS C.571804), 1 wet (AMS C.571805), 1 wet (AMS C.571806), 1 wet (AMS C.571807), 1 wet (AMS C.571808).

Other material. Australia, Tasmania, St Helens flat, (-41.21, 148.8), IN2018_V06_184, 1221–1202 m, 1 wet (AMS C.271202), 1 wet (AMS C.557076), 1 wet (TMAG E45587); GAB, (-35.15, 134.11), IN2015_C02_131, 965–1077 m, 1 wet (AMS C.532684); 1 wet (AMS C.571664), 1 wet (AMS C.571788), 1 wet (AMS C.571789), 1 wet (AMS C.571756), 1 wet (AMS C.575584); (-34.82, 132.69), IN2015_C02_167, 1015–998 m, 1 wet (AMS C.571670); (-34.74, 131.84), IN2015_C01_108, 1350–1321 m, 1 wet (SAMA D67743), 1 wet (SAMA D67744); (-34.71, 132.53), IN2015_C01_114, 994–980 m, 1 wet (AMS C.483826); (-34.67, 132.48), IN2015_C01_117, 1016–1014 m, 1 wet (AMS C.571785); (-33.93, 131.06), IN2015_C02_196, 1021–1033 m, 1 wet (AMS C.532702); (-33.72, 130.67), IN2015_C02_292, 1010–1011 m; (-33.52, 130.27), IN2015_C02_382, 978–1013 m, 1 wet (AMS C.532874), 1 wet (AMS C.571794), 1 wet (AMS C.571795), 1 wet (AMS C.571797), 1 wet (AMS C.571798), 1 wet (AMS C.571800), 1 wet (AMS C.571802), 1 wet (AMS C.571809).

Remarks

The examination of comparatively large amount of material available for this species revealed significant intraspecific variability in general shell size, shape and sculpture. Shells of adult specimens of *A. rufa* range from very large (> 40 mm, Fig. 5F–G) to relatively small (<30 mm, Fig. 5H–I), from comparatively broad (Fig. 5B–D) to more elongate (Fig. 5E) and from heavily sculptured (Fig. 5B, F) to almost smooth (Fig. 5E, H–I). Such heterogeneity in shell features does not have any correlation with phylogeny, geography or bathymetry. For instance, three paratype specimens [AMS C.271201 (Fig. 5G), AMS C.574588 (Fig. 5F) and TMAG E59223 (not figured)] possessed remarkably large shells, well above the species average (green circles on the upper left in Fig. 4). These specimens were all collected at the same site on St Helen's flat, where also other specimens of average size, clustering in the same PSH (A1), were collected.

Austrobela levis n. sp. (PSH A3)

(Figs 6A–E, 8D, 9F, 10A)

Material examined

Holotype: Australia, GAB, (-34.074, 129.182), IN2015_C01_064, 2649–2803 m (AMS C.571693).

Paratypes: Australia, GAB, (-35.54, 132.676), IN2015_C02_155, 1942–1926 m, 1 wet (= ethanol-preserved specimen); (AMS C.532671); (-35.009, 130.317), IN2015_C02_227, 2848–2831 m, 1 wet (AMS C.532710); (-34.625, 130.28), IN2015_C02_449, 2007–2067 m, 1 wet (AMS C.532883), 1 wet (AMS C.571695); (-35.798, 132.693), IN2015_C02_151, 2773–2677 m, 1 wet (AMS C.571616); (-35.558, 134.083), IN2015_C02_137, 1927–1995 m, 1 wet (AMS C.571694); 1 wet (AMS C.571813); (-34.072, 130.267), IN2015_C02_435, 1570–1535 m, 1 wet (SAMA D44145); (-35.202, 131.629), IN2015_C01_054, 1912–1836 m, 1 wet (SAMA D44143).

ZooBank registration: http://zoobank.org/urn:lsid:zoobank.org:act:EB55708D-8C49-411F-90E5-3952BDF26ABF

Etymology

In reference to its unsculptured shell, derived from ‘levis’ (Latin=smooth). Adjective of feminine gender.

Distribution

This new species is known from bathyal depths in the GAB (Fig. 1B).

Description

Shell (SL=29.4, SW=12.0 mm), fusiform, chalky-white, with polished surface. Protoconch cyrthoconoid, multispiral, of at least three evenly convex orange whorls, with sculpture of dense arcuate riblets. Teleoconch of 5.4 uniformly whitish whorls. Early teleoconch whorls with clear angulation at about mid-height of whorl, separating wide straight subsutural ramp from whorl periphery. Late whorls with gradual transition from subsutural ramp to more convex periphery. Sculpture of shallow striae and very fine collabral growth lines. Shell

base convex, clearly demarcated from long, tapering siphonal canal. Striae becoming denser towards siphonal canal, resulting in finely lyrate sculpture. Aperture elongate, about half length of shell. Outer lip thin, unsculptured, evenly convex below subsutural ramp, and attenuated towards tip of siphonal canal in its lower portion; inner lip smooth, with thin callus. Siphonal canal wide and deep.

Animal (based on AMS C.532671) uniform cream. Cephalic tentacles cylindrical, with blunt tips; large eyes situated at their outer base. Penis large, thick, evenly tapering toward pointed tip.

Radula (Fig. 9F, 10A) of hypodermic, relatively straight, somewhat loosely rolled marginal teeth, attaining 300 µm in length. Tip with two barbs of roughly equal size, of which barb anterior to adapical opening occurs slightly more distal from tip, strongly excavated, commonly curved in profile (Fig. 10A); adapical opening opening subterminal posterior to ventral barb, elongate, approximately 1/12–1/15 of shaft length, somewhat depressed in profile. Base swollen, texture somewhat coarse; ligament narrow, small.

Remarks:

This species is very similar to *A. rufa* in overall shell morphology but can be readily differentiated based on its comparatively smooth, whitish shell. The hypodermic tooth has a somewhat shorter adapical opening than the two former species, and with the barb on the side of the adapical opening more excavated and curved in profile, and with a notable depression where the opening is situated (Fig. 9F).

This species bears notable similarity to the South African *X. pyrropelex*, in that both taxa exhibit comparatively smooth, elongate shells with a moderately steep, wide subsutural ramp and a protoconch sculpture of arcuate riblets (Barnard, 1963; Sysoev, 1996). Furthermore, (Barnard, 1963, fig. 2c) illustrated the radula which shows a double-barbed hypodermic tooth with a somewhat inflated lower shaft, which is similar to that of *Austrobela* (Fig. 9). As Barnard (1963) provided a relatively simple line illustration, there is limited detail upon which to make further comparison with *Austrobela,* such as the morphology of the adapical and basal openings, basal texture, and ligament. We also note that Barnard (1963) reported that the eyes are very small or absent in *X. pyrropelex*, whereas *A. levis* n. sp., as all other *Austrobela* spp. examined herein, possess large eyes. Criscione et al. (2021) suggested that the presence and/or relative size of the eyes appeared

comparatively consistent at the genus-level in deep-sea Raphitomidae. Owing to the lack of detail in the line drawing by Barnard (1963), the radula cannot be readily compared to that of *Austrobela* apart from noting that they are at least superficially similar. The divergent eye morphology, however, does suggest that *X. pyrropelex* and *A. levis* n. sp. are not conspecific. While shells of *A. levis* n. sp. exhibit conserved sculptural features, they vary in shell size and particularly large forms (Fig. 6E) are not uncommon. The presence of these forms does not appear to reflect any phylogenetic or geographic/bathymetric pattern.

Austrobela obliquicostata n. sp. (PSH A5)

(Figs 6F–G, 8G, 9D)

Material examined:

Holotype: Australia, GAB, (-35.54, 132.67), IN2015_C02_155, 1942 m, 1 wet (SAMA D67741).

Paratypes: Australia, GAB, (-35.798, 132.69), IN2015_C02_151, 2773–2677 m, 1 wet (AMS C.571645), 1 wet (AMS C.532869); (-35.345, 134.045), IN2015_C02_134, 1509–1544 m, 1 wet (AMS C.571710); (-35.54, 132.67), IN2015_C02_155, 1942–1926 m, 1 wet (SAMA D44141); (-35.009, 130.317), IN2015_C02_227, 2848–2831 m, 1 wet (SAMA D44164); (-34.452, 129.492), IN2017_C01_197, 3350–3235 m, 1 wet (AMS C.571728), 1 wet (AMS C.571729), 1 wet (AMS C.572173); NSW, off Bermagui, (-36.355, 150.644), IN2017_V03_044, 2821–2687 m, 1 wet (AMS C.482317); NSW, Hunter CMR, (-32.575, 153.162), IN2017_V03_070, 2595–2474 m, 1 wet (AMS C.571644).

ZooBank registration: http://zoobank.org/urn:lsid:zoobank.org:act:95629EDD-2DBC-46DC-A74F-FADF8D05FBE5

Etymology

In reference to its shell sculpture of opisthocline ribs, derived from ‘obliquus’ (Latin=oblique) and ‘costatus’ (Latin=bearing ribs). Composite adjective of feminine gender.

Distribution

Known for the GAB and for off the south-eastern coast of Australia.

Description

Shell (Fig. 6F) (SL= 27.7, SW=10.5 mm), thin-walled, semi-translucent, broadly fusiform, with strongly shouldered whorls. Protoconch multispiral of four light to reddish orange whorls. Protoconch II whorls evenly convex, with arcuate riblets on adapical half to two-thirds of whorl, with diagonally cancellate sculpture below. Teleoconch of 5.8 whitish whorls; first whorl nearly cylindrical; subsequent whorls strongly shouldered, with wide weakly concave subsutural ramp. Sculpture of prominent, evenly interspaced, notably opisthocline ribs on whorl periphery, best pronounced at shoulder and barely reaching lower suture. Spiral sculpture of regular, slightly undulate striae, indistinct on subsutural ramp, and well-pronounced on whorl periphery. Subsutural ramp with fine, densely set collabral growth lines, some forming short regularly spaced raised riblets bordering upper suture. Last adult whorl with approximately 20 ribs of regularly decreasing prominence below shoulder. Shell base gently convex, continued into long, straight and slender siphonal canal. Aperture elongate, about half of length of shell. Outer lip thin, unsculptured; inner lip smooth, with thin callus on columella. Anal sinus wide, moderately deep, L-shaped.

Animal uniform whitish cream. Cephalic tentacles moderately short, stubby, broad; eyes situated on outer side of tentacles, approximately 1/3–1/4 from their bases.

Proboscis yellowish, cylindrical, blunt, with latitudinal folds in wall; radular sac large, elongate; venom gland extremely long and convoluted, colourless, filled with whitish substance; muscular bulb lustrous, yellowish, large.

Radula (based on paratype AMS C.571644, Fig. 9D) of relatively straight to slightly undulating, loosely rolled hypodermic teeth, attaining 200 µm in length. Tip with two barbs of approximately equal size, ventral barb situated more distal from tip than dorsal barb; adapical opening posterior to ventral barb, elongate, approximately 1/8 of length of shaft. Base swollen, with somewhat coarse texture; ligament thick.

Remarks

This species overlaps geographically and bathymetrically with *A. levis* throughout much of its range. However, the latter has not been recorded outside of the GAB. Of the *Austrobela* species, these are among the two taxa most readily distinguished based on their shell morphology; *A. levis* n. sp. possesses a comparatively smooth shell with a rounded shoulder,

whereas *A. obliquicostata* n. sp. has marked axial sculpture and a prominent, angulated shoulder. Furthermore, the protoconch of *A. levis* n. sp. possesses a sculpture of arcuate riblets (Fig. 8B), as opposed to the combination of these elements with more typical diagonally cancellate sculpture observed in *A. obliquicostata* n. sp. (Fig. 8E).

While most specimens of *A. obliquicostata* n. sp. exhibit shells with typical sculptural features and size, some specimens differed in colouration and general shape and exhibited cream-coloured and particularly elongate shells (Fig. 6G). Such variability does not appear to correlate with either phylogeny or geographic/bathymetric distribution.

Austrobela regia n. sp. (PSH A9)

(Figs 6I, 8H, 9E, 10B,H)

Material examined:

Holotype: Australia, NSW, off Byron Bay, (-28.677, 154.203), IN2017_V03_090, 2587–2562 m, (AMS C.571682).

Paratype: As per holotype, 1 wet (AMS C.519374).

ZooBank registration: http://zoobank.org/urn:lsid:zoobank.org:act:F9B67DF8-D865-4ADD-8FDA-4B259637DFC1

Etymology

In reference to its elegant spiral sculpture, resembling a crown, derived from ‘regium’ (Latin=regal). Adjective of feminine gender.

Distribution

Known for the type locality only, off Byron Bay, NSW, Australia.

Description

Shell (Fig. 6I) (SL= 28.9, SW=12.6 mm) thin, broadly fusiform, with strongly shouldered whorls. Protoconch (Fig. 8H) multispiral, light orange, eroded, with at least 3.5 whorls, with dense diagonally cancellate sculpture. Teleoconch of 5.9 whitish to amber whorls, spiral sculpture of many wavy spiral grooves, about half width of their interspaces, and extending

across axial sculpture, consisting of distinct ribs, forming starkly angulated periphery and extending to base in early whorls, then gradually becoming subobsolete to obsolete at base of mature whorls. Microsculpture of bi-sinuose growth lines, forming regularly placed cordlets with finer striae in their interspaces, most distinct at sinus then graduating toward subobsolete at periphery. Suture deep, adpressed; subsutural ramp moderately steep (approx. 55–60°), concave on early whorls, and rather straight on last whorl; sinus wide, subsutural, broadly U-shaped, widely arcuate, deep. Aperture elongate-pyriform, about equal in length to spire, outer lip thin, rounded anterior to subsutural ramp and evenly tapering toward moderately long siphonal canal; inner lip smooth, whitish posteriorly, graduating to orange to reddish brown anteriorly.

Animal uniform cream; cephalic tentacles of medium length, broad at base, evenly tapering toward blunt tip; eyes situated on outer side, approximately ¼ from base.

Radula (Figs 9E, 10B) consisting of long, rather thick, loosely rolled, relatively straight to lightly curved hypodermic teeth exceeding 300 µm in length; tip with two prominent barbs (Fig. 8B) of which the dorsal is somewhat larger and more distal from tip; adapical opening situated immediately posterior to dorsal barb, somewhat elongate; base swollen, texture rather coarse. Ligament thick, rather short (Fig. 8H).

Remarks

This new species can be distinguished from other *Austrobela* spp. on the basis of the following combined features: a wide, concave to straight subsutural ramp; prominent axial ribs forming starkly pronounced shoulder; a densely diagonally cancellate protoconch, and comparatively long hypodermic teeth. In shell proportions and whorl profile *A. regia* n. sp. is closely comparable to *A. sagitta* n. sp., but the latter species possesses a much lighter shell, with denser ribs and more widely spaced grooves. The shell of the holotype of *A. regia* n. sp. (Fig. 6I) bears multiple scars, indicating a series of unsuccessful predatory attacks (see Vermeij, 1982 and references therein). Although most Australian deep-sea raphitomids possess thin-walled shells (Criscione et al., 2021) with no apparent adaptations conferring resistance to predators, they rarely show signs of destructive predation attempts. This could be interpreted as a sign of overall low predatory pressure in the habitats occupied. However, the fact that marks of at least three attacks have been found for one specimen suggests that encounters with predators may still be frequent.

Austrobela sagitta n. sp. (PSH A4)

(Figs 6H, 8E, 9G)

Material examined:

Holotype: Australia, Central Eastern CMR, (-30.098, 153.899), IN2017_V03_086, 2429–2518 m, (AMS C.519338).

Paratype: Australia, Coral Sea CMR, (-23.631, 154.66), IN2017_V03_128, 1770–1761 m, 1 wet (AMS C.519400).

ZooBank registration: http://zoobank.org/urn:lsid:zoobank.org:act:FF4F714B-6C7D-4072-BCB7-426D07F4A0EF

Etymology

In reference to its very long and straight hypodermic teeth, derived from 'sagitta' (Latin=arrow). Noun in apposition.

Distribution

This species is recorded from Coral Sea, Queensland (1770 m) and off the coast of northern NSW (2429 m).

Description

Shell (Fig. 6H) (SL= 25.0, SW=11.3 mm) broadly fusiform, thin-walled, with glossy surface. Protoconch multispiral, cyrthoconoid, of four orange whorls. PII whorls evenly convex, with fine, diagonally cancellate sculpture throughout height of whorl. Protoconch-teleoconch transition well-defined, with opisthocline boundary. Teleoconch of 5.2 whorls, uniformly white, with distinct suture. Whorls rather broad, with wide, distinctly to slightly concave subsutural ramp and well-pronounced shoulder situated slightly below mid-height of whorl. Subsutural ramp sculptured with regular collabral riblets. Below, axial sculpture of strong, sharp, densely set, weakly opisthocline ribs, thicker at whorls periphery; clearly arcuate on penultimate and last whorls, and obsolete at its base. Spiral sculpture of regular fine, wavy grooves, about half width of their interspaces, extending across axial sculpture. Siphonal canal long, slender, tapering. Aperture large, elongate-pyriform, about half length of shell,

outer lip thin, opisthocline; inner lip white, smooth except for extensions of few spiral cords of siphonal canal inside aperture. Anal sinus wide, deep, u-shaped.

Animal uniform cream, cephalic tentacles of medium length, broad, blunt; eyes rather large, situated at outer base of cephalic tentacles.

Proboscis broad, blunt; radular sac extremely large; venom gland very long, convoluted; muscular bulb large, bean-shaped, lustrous.

Radula (Fig. 9G) consisting of very long, relatively straight hypodermic teeth, exceeding 600 µm in length. Tip with two barbs of approximately equal size, of which ventral barb more distal from tip; adapical opening posterior to ventral barb, elongate, approximately 1/17 length of shaft; base swollen, texture rather indistinct; basal opening large. Ligament comparatively long, moderately thick.

Remarks

This species can be differentiated from other Australian *Austrobela* spp. by its significantly longer hypodermic tooth (Fig. 9G). A comparison of *A. sagitta* n. sp. with the very similar *A. regia* n. sp. is provided under the remarks to this latter species. Kantor and Taylor (2002) figured a similarly elongate tooth for the Atlantic *Austrobela pyrrhogramma*: however, our molecular analyses (Figs 2–3) suggest these two taxa are not closely related. In terms of shell morphology, *A. sagitta* n. sp. can be differentiated from *A. pyrrhogramma* by its significantly broader shell, and from the other Australian spp. by its multiple prominent axial ribs that extend across the periphery to the lower suture and about half-way across the base of last adult whorl (Fig. 6H). *A. sagitta* n. sp. can also readily be separated from *A. rufa, A. levis* and *A. obliquicostata* by its fine, diagonally cancellate protoconch, which in the two former species bears arcuate riblets, whereas in the latter one the abapical portion is coarsely diagonally cancellate, above which arcuate riblets are present. *A. sagitta* n. sp. differs from *Theta lyronuclea* in its more pronounced and numerous axials, which remain distinctive throughout the height of whorl periphery, while vanishing quickly below shoulder on late whorls of *T. lyronuclea*.

Austrobela sagitta, *A. regia* n. sp. and *A. procera* n. sp. are the only species of this genus occurring in Australia that are not known from the GAB.

Austrobela procera (Sysoev and Bouchet, 2001) n. comb. (PSH A6)

(Figs 7A–B, 8F, 9C)

Gymnobela procera Sysoev and Bouchet, 2001, p. 312, figs 131–133, 172

Distribution

New Caledonia, Norfolk Ridge, Loyalty Ridge, Wallis and Futuna and East and West Tropical Australia.

Remarks

This species was previously known for its shell only and all specimens studied herein for this species exhibit typical features (Sysoev & Bouchet, 2001). The radula of *A. procera* is illustrated for the first time in the present study (Fig. 9C) and is typical of the genus. The penis (based on AMS C.571647) is very long, narrow with no obvious glands or swellings, with a small distal seminal papilla. Large eyes are situated at the outer lower bases of moderately long, cylindrical cephalic tentacles. The protoconch differs from *A. rufa, A. levis* n. sp. and *A. obliquicostata* n. sp. in its fine, diagonally cancellate sculpture throughout the height of the whorls (Fig. 8F) but it is not readily differentiated from that of *A. sagitta* n. sp. However, *A. procera* differs from *A. sagitta* n. sp. by its notably more elongate shell (Fig. 7A–B).

Genus *Spergo* Dall, 1895 (Dall, 1895; p. 680)

Type species *Mangilia glandiniformis* Dall, 1895 (Fig. 11A; Dall, 1895, p. 681–683, pl. 24, figs 1–2) by subsequent designation (Dall, 1918, p. 331)

Other species: *S. aithorrhis* Sysoev & Bouchet, 2001 (Fig. 12C; Sysoev & Bouchet, 2001, p. 303–305, figs 9, 121–124, 170), *S. annulata* n. sp., *S. castellum* n. sp., *S. fusiformis* (Kuroda & Habe, 1961) (Fig. 12A; Habe, 1961, p. 81, pl. 40, fig. 9, app. 30; Sysoev & Bouchet, 2001, p. 302-303, figs 8, 115–120), *S. parunculis* Stahlschmidt, Chino & Fraussen, 2015 (Fig. 12C; Stahlschmidt, Chino, & Fraussen, 2015, p. 9-10, figs 10–20), *S. parvidentata* n. sp., *S. sibogae* Schepman, 1913 (Fig. 11F; Schepman, 1913, p. 448–449, pl. 30, fig. 9; Sysoev & Bouchet, 2001, p. 306, fig. 125–128), *S. tenuiconcha* n. sp.

Diagnosis

Shell large, fusiform to elongate-fusiform, walls solid, opaque to moderately thin. Protoconch multispiral. Teleoconch white, cream or dark orange; whorl profile slender to medium broad, evenly-convex or with well-defined shoulder; whorl portion below subsutural ramp short to very tall, cylindrical to convex. Subsutural ramp varying from indistinct to wide, concave; suture impressed. Spiral sculpture evenly developed throughout whorl height, or below subsutural ramp; of cords, often regularly spaced. Axial sculpture of opisthocline ribs, usually weak and/or confined to early whorls. Microsculpture of growth lines, most prominent on subsutural ramp with slightly to moderately raised cordlets present at regular to uneven intervals, reflecting shape of anal sinus. Last adult whorl evenly convex to distinctly shouldered below subsutural ramp, not clearly demarcated from moderately long, evenly tapering siphonal canal. Aperture elongate-pyriform, from about one third to over half of shell length; outer lip thin, unsculptured; inner lip with distinct, rather wide whitish (with or without dark orange stain), cream or yellowish callus. Anal sinus wide, shallow, u-shaped.

Animal colour variable (greyish, pink, whitish). Head broad to very broad, blunt; cephalic tentacles broad, short, tapering, with medium to large eyes situated at outer basal part. Rhynchocoel capacious, Proboscis short, broad to very broad. Venom apparatus well-formed to greatly reduced; venom gland moderately long to short; muscular bulb elongate to very elongate. Radula of hypodermic teeth. Teeth rolled, loosely rolled to entirely unrolled, straight to curved or bent, barbs absent; no blade or with short dorsal blade; adapical opening elongate of variable length; base swollen, lateral process distinct to absent; external base with medium coarse sculpture; basal opening subcircular, large to very large. Ligament broad.

Remarks

Prior to this study the genus included five species, namely the type species *Spergo glandiniformis* (from off Hawaii), *S. aithorrhis* Sysoev & Bouchet, 2001 (Norfolk Ridge), *S. parunculis* Stahlschmidt, Chino & Fraussen, 2015 (Mozambique Channel), *S. fusiformis* (Kuroda & Habe, 1961) (West Pacific) and *S. nipponensis* Okutani & Iwahori, 1992 (Japan Sea) (Okutani & Iwahori, 1992, figs 65–66). However, the description of the holotype of the latter species (Okutani & Iwahori, 1992, p. 264) mentions the presence of an operculum, which is absent in all Raphitomidae. For this reason, *S. nipponensis* is herein formally

removed from *Spergo.* The number of remaining species is here doubled and the genus distribution further extended to cover six different realms (9, 13, 15, 16, 26 and 29 of Costello et al., 2017) across the Indian (not shown) and the Pacific Oceans (Fig. 1E *partim*). In order to confirm the boundaries of the genus *Spergo*, molecular data needs to be generated for species not studied here, in particular, for the type species. There is a plethora of species, currently placed in different genera, but sharing some shell and radular features with the species of *Spergo* and whose affinities to *Spergo* should be evaluated. Among them are the Antarctic *Xanthodaphne pastorinoi* Kantor, Harasewych & Puillandre, 2016 (Kantor, Harasewych, & Puillandre, 2016, fig. 16), *Gymnobela africana* Sysoev, 1996 from (off) E Africa (Fig. 18M; Sysoev, 1996, figs 109–111), the N Pacific *Gymnobela oculifera* Kantor & Sysoev, 1986 (Fig. 18L; Kantor & Sysoev, 1986, figs 1A, 2A, 3), the NE Atlantic *Bathybela nudator* (Locard, 1897) (Fig. 18K; Bouchet & Warén, 1980, figs 16, 133) and the NW Atlantic *Gymnobela emertoni* (Verrill & S. Smith, 1884) (see below remarks under *S. tenuicostata*).

Spergo was traditionally, regarded as part of an informal “complex” or “group” of nominal genera (Sysoev & Bouchet, 2001; Stahlschmidt et al., 2015), which were considered evolutionarily related based on their shell similarity. However, analysis of molecular data have revealed considerable homoplasy in shell features and resolved this artificial group into a number of unrelated genus-level lineages (Criscione et al., 2021). Among these lineages, *Spergo* is characterised by species with large shells featuring a shallow anal sinus, weak spiral cords and with short awl-shaped radular teeth. While the combination of shell characters is sufficient to differentiate *Spergo* from most raphitomid genera, the examination of the radula is necessary to distinguish this genus from the conchologically similar *Pontiothauma* E. A. Smith, 1895, *Nodothauma* Criscione, Hallan, Puillandre & Fedosov, 2020 and *Abyssobela* Kantor & Sysoev, 1989.

Due to erosion, the protoconch has not been studied in any *Spergo* species other than the type series of *S. glandiniformis* (Dall, 1895, p. 680.). Thus, the assumption that a multispiral protoconch is a feature shared by *Spergo* species (see diagnosis above) is pending confirmation.

Spergo castellum n. sp. (PSH S5)

(Figs 11C, 13A, 14)

Material examined:

Holotype: Australia, Victoria, East Gippsland CMR, (-37.792, 150.382), IN2017_V03_035, 2338–2581 m, (AMS C.482148).

Paratype: Australia, Tasmania, Freycinet CMR, (-41.731, 149.12), IN2017_V03_004, 2820–2751 m, 1 wet (AMS C.519290).

ZooBank registration: http://zoobank.org/urn:lsid:zoobank.org:act:5BACDBB2-0A37-4097-BAFB-67D1BFA93EBC

Etymology: In reference to the cylindrical, high wall-like appearance of the whorl periphery, derived from 'castellum' (Latin=castle). Noun in apposition.

Distribution

Known only from two localities; East Gippsland Commonwealth Marine Reserve, Victoria, and Freycinet Commonwealth Marine Reserve (Fig. 1E)

Description. Shell (Fig. 11C) (SL=66.4 mm, SW= 24.8 mm), elongate-fusiform, with high spire; walls solid, opaque. Protoconch eroded. Teleoconch of 7.7 uniform white whorls; whorl profile slender, with well-defined shoulder at approximately adapical third of whorl, whorl base very tall, cylindrical to weakly convex. Subsutural ramp wide; suture impressed. Spiral sculpture below subsutural ramp of cords, rather regularly spaced on early whorls, more irregularly placed on mature whorls. Axial sculpture of twenty or more weak opisthocline ribs, largely confined to shoulder area and rapidly becoming obsolete below shoulder and on last whorl. Microsculpture of growth lines, most prominent on subsutural ramp with slightly raised cordlets present at uneven intervals, reflecting shape of anal sinus. Last adult whorl evenly convex below subsutural ramp, not clearly demarcated from long, evenly tapering siphonal canal. Aperture elongate, approximately 40% of shell length; outer lip thin, unsculptured; inner lip with distinct, rather wide yellowish callus. Anal sinus wide, moderately deep, u-shaped.

Animal greyish; head broad, blunt; penis narrow, moderately large, with seminal papilla. Cephalic tentacles broad, stubby, somewhat tapering to blunt tip. Large eyes situated at outer basal part.

Rhynchocoel walls covered in thick layer of dark red matter. Inside of oesophagus covered in thick layer of charcoal matter. Proboscis very broad (retracted); venom gland moderately long, convoluted; muscular bulb elongate, semi-transparent.

Radula (Fig. 14) of hypodermic, somewhat loosely rolled to entirely unrolled, rather straight to curved or bent, teeth attaining 140 µm in length; barbs absent; dorsal blade approximately 1/5 of length of shaft; adapical opening rather elongate, highly variable in length; base lightly swollen, distinct lateral process; external base with coarse sculpture; basal opening subcircular, very large. Ligament broad, rather large.

Remarks

The distinct, cylindrical whorls with high periphery of this species make it rather distinct among its congeners. It bears some resemblance to *Nodothauma magnifica* Criscione, Hallan, Fedosov & Puillandre, 2020; however, it can be separated from the latter by its distinctly shouldered, cylindrical whorls, taller spire, a comparatively lower aperture (as a ratio of its total length), a less defined siphonal canal, and in its white colouration in contrast to the orange-brown *N. magnifica.* Furthermore, these taxa can readily be differentiated anatomically, as *N. magnifica* does not possess a radula and venom apparatus. A high proportion of the hypodermic teeth encountered in the holotype exhibit unusual characteristics for Raphitomidae, with some entirely unrolled and trough-shaped (Fig. 14), similar to members of the Mangeliidae (see Bouchet et al., 2011), whereas other exhibit various degrees of unrolling, or where one tooth is contained by another.

Spergo castellum n. sp., as with *S. annulata* n. sp. and *S. fusiformis,* possesses a dark matter (possibly epithelium, see Kantor & Taylor, 2002) inside the rhynchocoel, lining the rhynchodeum walls. A similar appearing matter is seen also in *N. magnifica*, in some species of *Teretiopsis* Kantor & Sysoev, 1989 and in a number of other raphitomids (Kantor & Taylor, 2002; Criscione et al., 2021).

Spergo tenuiconcha n. sp. (PSH S4)

(Figs 11B, 13B)

Material examined:

Holotype: Australia, Victoria, East Gippsland CMR, (-38.479, 150.185), IN2017_V03_032, 3850–3853 m, (AMS C.482142).

Paratypes: As per holotype, 1 wet (AMS C.571636), 1 wet (AMS C.571658); Australia, Tasmania, Flinders CMR, (-40.473, 149.397), IN2017_V03_015, 4114–4139 m, 1 wet (AMS C.519392); NSW, Jervis CMR, (-35.114, 151.469), IN2017_V03_053, 3952–4011 m, 1 wet (AMS C.482310).

ZooBank registration: http://zoobank.org/urn:lsid:zoobank.org:act:2DC536C6-AB42-4C93-989C-A8FA3BBC4EF0

Etymology

In reference to its thin shell, derived from ‘tenuis’ (Latin=thin) and ‘concha’ (Latin=shell). Noun in apposition.

Distribution

Known for off the south-eastern coast of Australia (Fig. 1E).

Description

Shell (Fig. 11B) (SL= 42.4, SW=20.3), fusiform, thin, opaque. Protoconch eroded. Teleoconch of at least 5.5 yellowish whorls; whorl profile medium broad, with well-defined shoulder approximately at its mid-height in spire whorls, becoming rounded on penultimate- and subobsolete on last adult whorl. Subsutural ramp very wide, deeply concave in early teleoconch whorls, becoming straight to somewhat convex in mature whorls; suture impressed. Axial sculpture of about 15 low ribs, largely confined to shoulder area, on early teleoconch whorls, becoming subobsolete to absent in later whorls. Spiral sculpture below subsutural ramp of about 8 grooves (30+ on last adult whorl), forming dense pairs on mature whorls; each groove or pair of grooves separated by wide interspace, becoming weaker and less regularly set toward base of last adult whorl. Microsculpture of collabral growth lines, most prominent on subsutural ramp with slightly raised cordlets at regular intervals (rather strong on early teleoconch whorls), reflecting shape of anal sinus. Last adult

whorl evenly convex below subsutural ramp, tapering evenly toward long siphonal canal. Aperture elongate-pyriform, approximately 60% of total shell length; outer lip thin, unsculptured; columella recurved with distinct whitish callus, pinkish in upper third (pink area also on base of last whorl). Anal sinus wide, moderately deep, u-shaped.

Anatomy (based on AMS C.571636).

Animal uniform pink; head very broad, with thick, muscular walls, blunt; cephalic tentacles thick, muscular, rather short, tapering, with large eyes on outer base. Penis situated well-posterior of cephalic tentacle, muscular, *cox1*ling clockwise, bearing gland-like swellings on distal quarter.

Proboscis pink, of moderate size, broad, rather conical; radular sac long, opening into buccal mass posterior to right side of proboscis; venom gland moderately large, whitish, convoluted, muscular bulb moderately large, very long, lustrous pink, bending abruptly at middle, pointing posteriorly.

Radula (Fig. 13B) of hypodermic type, teeth attaining approximately 140 µm in length, mostly straight but somewhat curved distally, rather broad; barbs absent; dorsal blade approximately 1/5 of length of shaft; adapical opening elongate, about 1/5 of length of shaft; base slightly inflated, with distinct lateral process; base texture rather coarse; basal opening large, subcircular. Ligament wide, rather long.

Remarks

This species can be differentiated from its congeners and other raphitomids by its distinctly recurved columella, and with the last adult whorl being rather cylindrical below the shoulder (Fig. 11B) until it tapers toward the siphonal canal.

In terms of shell morphology, *S. tenuiconcha* n. sp. bears some similarity to the Atlantic *G. emertoni* in having a rather cylindrical portion below the shoulder, a tall aperture (as a ratio of total shell length), and a distinct shoulder in early to penultimate whorls. Bouchet and Waren (1980) and Kantor and Taylor (2002) both figure the shell and radula of material identified as *G. emertoni*. While figured shells are similar in gross morphology to *S. tenuiconcha* n. sp.*,* they have more conical outline of spire, compared to the more gradate spire of *S. tenuiconcha* n. sp.. Furthermore, the radulae illustrated for *G. emertoni* differ markedly in the two publications. Bouchet and Warén (1980, fig. 21) figure a line drawing showing a double-barbed tooth, while Kantor and Taylor (2002, fig. 3l) illustrate a

photograph of a shorter, broader *Spergo*-like tooth with no barbs. However, further molecular data and radular studies are required to decide about the assignment of *G. emertoni* to *Spergo* as well as its relationship with *S. tenuiconcha* n. sp.

Spergo parvidentata n. sp. (PSH S3)

(Figs 11D, 13C)

Material examined:

Holotype: Australia, Tasmania, Flinders CMR, (-40.473, 149.397), IN2017_V03_015, 4114–4139 m, 1 wet (AMS C.519401).

Paratypes: As per holotype, 1 wet, (AMS C.571654); Australia, Tasmania, Bass Strait, (-39.552, 149.553), IN2017_V03_030, 4197–4133 m, 1 wet, (AMS C.519331), 1 wet, (AMS C.571669); Victoria, East Gippsland CMR, (-38.479, 150.185), IN2017_V03_032, 3850–3853 m, 1 wet, (AMS C.571652); NSW, off Bermagui, (-36.351, 150.914), IN2017_V03_043, 4753–4750 m, 1 wet, (AMS C.571707); off Newcastle, (-33.441, 152.702), IN2017_V03_065, 4280–4173 m, 1 wet, (AMS C.519367), 1 wet, (AMS C.571667), 1 wet, (AMS C.571716).

ZooBank registration: http://zoobank.org/urn:lsid:zoobank.org:act:5EB9BD05-6A52-4429-B455-78B3B01357E9

Etymology

In reference to the small size of its hypodermic teeth, derived from ‘parvus’ (Latin=small) and ‘dentatus’ (Latin=bearing teeth). Composite adjective of feminine gender.

Distribution

Known for off the south-eastern coast of Australia (Fig. 1E).

Description

Shell (Fig. 11D) (SL=20.4, SW=9.4 mm), fusiform, moderately thin, semi-translucent. Protoconch eroded. Teleoconch of 4.8 light yellow whorls; whorl profile medium broad, with well-defined shoulder approximately at its mid-height to abapical third. Subsutural ramp very wide, concave to rather straight; suture impressed. Axial elements of about 15

low ribs, most prominent on shoulder, gradually weakening toward suture on early teleoconch whorls, becoming subobsolete to absent in later whorls. Spiral sculpture below subsutural ramp of 5 regularly set cords, separated by rather deep grooves. On last adult whorl first spiral cord after shoulder slightly swollen; in total 24 cords, rounded adapically and becoming progressively wider, flat and oblique towards siphonal canal. Microsculpture of collabral growth lines, most prominent on subsutural ramp with slightly raised cordlets at regular intervals (rather strong on early teleoconch whorls), reflecting shape of anal sinus. Last adult whorl evenly convex below shoulder, not clearly demarcated from long siphonal canal. Aperture elongate-pyriform, approximately 60% of total shell length; outer lip thin, unsculptured; inner lip recurved with whitish callus. Anal sinus wide, medium deep, broadly u-shaped.

Anatomy (based on paratypes AMS C.571707, AMS C.571716 and AMS C.571652). Animal whitish to pinkish; head very broad; cephalic tentacles medium long, broad, subcylindrical to cylindrical, tip blunt; small eyespots situated at their outer lower bases Penis large, muscular. Venom apparatus extremely small; venom gland thin, short; muscular bulb very elongate.

Radula (based on paratype AMS C.571667, Fig. 13C) of hypodermic type, short, attaining 30 µm in length, loosely rolled, gradually tapering from base of shaft toward sharpened tip; adapical opening elongate, narrow. No apparent blade, barbs absent. Base swollen, somewhat broader than basal portion of shaft, lateral process or spur absent. Basal opening large, subcircular, situated obliquely relative to orientation of tooth; basal texture coarse. Ligament moderately large.

Remarks

When compared to the *Spergo* species treated herein, *S. parvidentata* n. sp. can be differentiated from *S. fusiformis* and *S. castellum* by its smaller size and from *S. annulata* n. sp. and *S. tenuiconcha* n. sp. by its shouldered whorl periphery. This species also differs from other congeners by the morphology of the hypodermic teeth (Fig. 13C), which lacks a dorsal blade and a basal process, and rarely exceed 30 µm in length.

Spergo annulata n. sp. (PSH S6)

(Figs 11E, 13E)

Material examined

Holotype: Australia, NSW, off Byron Bay, (-28.677, 154.203), IN2017_V03_090, 2587–2562 m, (AMS C.519333).

Paratype: Australia, NSW, Hunter CMR, (-32.575, 153.162), IN2017_V03_070, 2595–2474 m, 1 wet (AMS C.571638).

ZooBank registration: http://zoobank.org/urn:lsid:zoobank.org:act:7B600648-C2C8-406F-B8FA-560B36B73AB9

Etymology

In reference to its shell sculpture of deep spiral grooves, derived from ‘annulatus’ (Latin=‘bearing rings’). Adjective of feminine gender.

Distribution

Known from northern NSW, Australia.

Description

Shell (11E) (SL=20.7, SW=9.8 mm) fusiform, rather thin-walled, orange, semi-translucent. Protoconch eroded. Teleoconch of at least six orange-brown whorls; whorl profile medium broad, with weakly defined shoulder approximately at its mid-height in early teleoconch whorls, becoming obsolete on subsequent whorls. Subsutural ramp on early spire whorls very wide, concave to straight, subobsolete to absent in subsequent whorls; suture impressed. Axial elements of low, rather indistinct, densely set ribs on early teleoconch whorls, spanning height of whorl below subsutural ramp, becoming subobsolete to absent in later whorls. Spiral sculpture below subsutural ramp of deep grooves, evenly interspaced on early spire whorls, and paired subsequently; each pair separated by wide rounded spiral cord, single on penultimate whorl, and bipartite on last whorl. Spiral cords becoming weaker, flatter and less regularly set toward base of last adult whorl. Microsculpture of collabral growth lines, traceable throughout whorl height, but most prominent on subsutural ramp, forming slightly raised cordlets at regular intervals (very prominent on early teleoconch whorls. Last adult whorl evenly convex below very weak subsutural ramp,

weakly demarcated from long siphonal canal. Aperture elongate-pyriform, more than 60% of total shell length; outer lip thin, unsculptured; columella rather straight, with wide whitish callus, distinct burnt-orange vertical stain on lower half. Anal sinus wide, rather shallow, weakly u-shaped.

Cephalic tentacles short, stubby; large eyes situated at their outer lower bases. Rhynchocoel large, capacious, lined with porous dark reddish-brown epithelium. Venom apparatus small, far retracted into posterior rhynchocoel; muscular bulb small, elongate; venom gland thin rather small; radular sac small, filled with reddish teeth. Proboscis broad, short. Oesophagus (based on AMS C.571638) very thick.

Radula (based on paratype AMS C.571638, Fig. 13E) of hypodermic, somewhat loosely rolled to semi-unrolled, rather straight teeth attaining 100 µm in length; barbs absent; dorsal blade approximately 1/5 of length of shaft; adapical opening rather elongate, highly variable in length); base lightly swollen, with distinct lateral process; external base with coarse sculpture; basal opening subcircular, very large. Ligament broad, rather large.

Remarks

This new species can be differentiated from its congeners by its orange shell with distinct spiral grooves, evenly convex last adult whorl, and its comparatively long, straight columella with a dark orange vertical stain (Fig. 11E). It is rather similar to *S. tenuiconcha* n. sp., but the latter bears less prominent spiral sculpture, a more acute shoulder in early to penultimate whorl, and a whitish, curved columella (Fig. 11B).

Spergo fusiformis (Kuroda & Habe, 1961) (PSH S2)

(Figs 12A–B, 13D)

Pontiothauma fusiforme Kuroda & Habe in Habe, 1961: 81, pl. 40, Fig. 10, Appendix: 30.

Remarks

As no published radular or other anatomical data are available for this species, details are provided herein based on specimen AMS C.482154: Animal greyish white, head broad, blunt; cylindrical, medium length cephalic tentacles, with eyes on outer lower base. Rhynchocoel capacious, internal walls covered in dark red matter. Muscular bulb extremely small, elongate, semi-transparent; venom gland thin, small; radular sac small; proboscis

broad, sphincter surrounded by green filamentous/lamellate structure. Internal oesophagus also lined with dark matter.

Radula (Fig. 13D) of hypodermic, somewhat loosely rolled, rather straight teeth attaining 100 µm in length; barbs absent; dorsal blade approximately 1/4of length of shaft; adapical opening elongate; base lightly swollen, distinct lateral process; external base with coarse sculpture; basal opening subcircular, very large. Ligament broad, rather large.

Genus *Theta* Clarke, 1959 (Clarke, 1959; p. 234)

Type species *Pleurotomella* (*Theta*) *lyronuclea* Clarke, 1959 by original designation (Fig. 15A; Clarke, 1959, p. 234, pl. 13, figs 1–2).

Other species. *T. chariessa* (R. B. Watson, 1881) (Fig. 15C; Watson, 1881, p. 458-460, fig. 2; 1886, p. 352-353, pl. 20, fig. 6; Bouchet & Warén, 1980, p. 59-61, figs. 14, 129–130, 254–255), *T. microcostellata* n. sp., *T. polita* n. sp., *T. vayssierei* (Dautzenberg, 1925) (Fig. 15B; Dautzenberg, 1925, p. 1, fig. 2; Bouchet & Warén, 1980, p. 59, figs 126–127, 253).

Diagnosis

Shell biconical- to elongate fusiform, semi-translucent to opaque. Protoconch multispiral (moderately to heavily eroded in observed material); sculpture of arcuate riblets throughout, or riblets limited to upper portion of whorls and diagonally cancellate below. Teleoconch with distinctly shouldered to rounded whorls; axial sculpture ranging from weak, present largely in mid-whorls, to bearing sharply opisthocline or orthocline axial ribs in most or all whorls, vanishing below shoulder or present more or less from shoulder to suture; spiral sculpture of weak, indistinct cords; last whorl cylindrical to evenly convex below indistinct to wide subsutural ramp. Siphonal canal moderately long to long, rather straight. Aperture large, pyriform, moderately broad to narrow, about half of shell length. Anal sinus rather shallow to comparatively deep, wide, u-shaped. Radula of hypodermic, slightly curved teeth with two blunt to moderately sharp distal barbs; adapical opening rather long; base broad, angular, lateral process indistinct; basal opening large; ligament broad.

Remarks

Prior to this work, *Theta* consisted of three accepted species: the type species *T. lyronuclea* [from off the Bermuda Islands (Clarke, 1959) and possibly from S Australia (this study but also Criscione et al., 2021), *T. vayssierei* (Dautzenberg, 1925) and *T. chariessa* (R. B. Watson, 1881) [both from the N Atlantic (Bouchet & Warén, 1980)]. With the addition of the two species described here from Australia, *Theta* currently encompasses a total of five species. However, the genus placement of *T. vayssierei* and *T. chariessa* (exhibiting *Austrobela*-like features - see above) remains to be tested molecularly. Thus delimited, the genus exhibits a disjunct Atlantic/Pacific distribution. Arguably, a complete picture of the genus diversity and distribution depends on the availability of molecular data on additional species and it is beyond the scope of this study. Taxa such as *Pleurotomella argeta* Dall, 1890 from (off) the Galapagos Islands (Fig. 18G; Dall, 1890, pl. 6, fig. 5), *Gymnobela latistriata* Kantor & Sysoev, 1986 from the NW Pacific (Fig. 18I; Kantor & Sysoev, 1986, figs 1B-E, 2B, 4), *Typhlosyrinx chrysopelex* Barnard, 1963 from (off) the Cape Point region, S Africa (Barnard, 1963, figs 3g–h; Sysoev, 1996, fig. 6), '*Gymnobela' camerunensis* Thiele, 1925 from (off) W Africa (Thiele, 1925, pl. 28, fig. 20) and *G. homeotata* (Watson, 1886) from the mid-Atlantic (Fig. 18J; Watson, 1886, pl. 26, fig. 12; Bouchet & Warén, 1980, figs 18, 199, 240), exhibit shell and (when available) radular characters that are close to *Theta*, and so affinity of these species to *Theta* needs further evaluation.

Theta shares a number of features with other genera in the informal group *Gymnobela s.l.* (Criscione et al., 2021) from which it can be distinguished by a thinner, more glossy, greyish semitransparent shell, with axial sculpture often limited to the whorl upper portion and a double-barbed hypodermic tooth (which is similar to that of *Austrobela* – see above).

Theta lyronuclea (Clarke, 1959) (PSH T1)

(Figs 10E–F; 15A, D; 16A)

Pleurotomella (*Theta*) *lyronuclea* Clarke, 1959 - Clarke (1959, p. 233–235, pl. 13, figs 1-2)

Gymnobela lyroniclea [sic] (misspelling) - Sysoev (2014, p. 148)

Material examined:

Australia, GAB, (-36.069, 132.637), IN2015_C01_016, 4602–4612 m, 1 wet, (AMS C.487451), 1 wet, (AMS C.571655), 1 wet, (AMS C.571708); (-35.794, 131.711), IN2015_C01_026, 4576–4459 m, 1 wet, (AMS C.487453); (-34.074, 129.182), IN2015_C01_064, 2649–2803 m, 1 wet,

(AMS C.483790); (-35.009, 130.317), IN2015_C02_227, 2848–2831 m, 1 wet, (SAMA D44171); (-35.852, 131.977), IN2017_C01_175, 3930–4250 m, 1 wet, (AMS C.572169; (-35.811, 131.71), IN2017_C01_179, 4741–4618 m, 1 wet, (SAMA D67752), (SAMA D67753); (-35.523, 130.351), IN2017_C01_182, 4890–5032 m, 1 wet, (AMS C.571733), 1 wet, (AMS C.572171); (-34.452, 129.492), IN2017_C01_197, 3235–3350 m, 1 wet, (AMS C.572172); NSW, off Bermagui, (-36.351, 150.914), IN2017_V03_043, 4763–4750 m, 1 wet, (AMS C.571718); Jervis CMR, (-35.114, 151.469), IN2017_V03_053, 3952–4011 m, 1 wet, (AMS C.482290).

Remarks

This species was described based on a single shell collected off the Bermuda Islands by the M/V *Theta* of the Lamont Geological Observatory and its description was accompanied by the illustration of the shell (Clarke, 1959, pl. 13, figs 1-2). A photograph of the shell and a line drawing of the radula were figured for an additional specimen from the NE Atlantic (Bouchet & Warén, 1980, figs 13, 128). Sequences obtained from specimens of *T. lyronuclea* from Australia are included in the phylogenies of Criscione et al. (2021) as well as in that of this study. The description of the radula and the anatomy of this species, reported below, is based on these specimens.

Radula (based on AMS C.571733; Figs 10E–F; 13A) of hypodermic, slightly curved teeth exceeding 200 µm, with two moderately sharp distal barbs (Fig. 10E), dorsal barb smaller; adapical opening moderately long (Fig. 10F), about 1/5 of length of shaft; base broad, angular, indistinct lateral process; basal opening large; ligament broad.

Anatomy (based on AMS C.487453 and AMS C.482290). Males with extremely large, muscular penis. Eyes moderately large, albeit may be in part covered by epidermis, situated at outer lower base of moderately long, cylindrical tentacles which may bear a longitudinal furrow.

As already pointed out by Criscione et al. (2021), the remarkably wide distribution of *T. lyronuclea* (as currently understood) remains molecularly untested and a scenario of two morphologically-cryptic species cannot at present be ruled out.

Theta polita n. sp. (PSH T2)

(Figs 10G, I; 15E, 16B)

Material examined:

Holotype: Australia, GAB, (-35.818, 134.109), IN2015_C02_141, 2852–2800 m (AMS C.532711).

Paratypes: Australia, GAB, (-35.798, 132.693), IN2015_C02_151, 2773–2677 m, 1 wet (AMS C.532868); 1 wet (AMS C.571696).

ZooBank registration: http://zoobank.org/urn:lsid:zoobank.org:act:ADD9935E-63BE-4C18-80BA-4097EF19D685

Etymology

In reference to its unsculptured shell, derived from 'politus' (Latin=smooth). Adjective of feminine gender.

Distribution

Known for the GAB (Fig. 1C)

Description

Shell (Fig. 15E) (SL=23.1, SW=10.1), fusiform, thin-walled, with glossy surface. Protoconch orange, cyrtoconoid, of at least three evenly convex orange whorls, with sculpture of arcuate riblets. Teleoconch of 5 uniformly whitish whorls. Whorl profile moderate to rather broad, evenly convex to somewhat angulated; subsutural ramp approximately 60°, straight to lightly concave; sinus wide, rounded, subsutural, rather deep. Spiral sculpture absent; axial sculpture obsolete or of weak arcuate ribs, appearing as a series of nodules about mid-height of second whorl; microsculpture of bi-sinuose growth lines throughout whorl height, short and deeply convex at sinus, in places regularly arranged low riblets, long and slightly concave below. Last whorl evenly convex, clearly demarcated from the straight, moderately long, tapering siphonal canal. Aperture large, about half of shell length, ovate. Outer lip thin, convex along most of its length, with anterior portion attenuated towards tip of siphonal canal; inner lip smooth, with thin, narrow, white callus.

Radula [based on holotype (not figured) and paratype AMS C.532868 (Fig. 16B)] of hypodermic, rather straight teeth exceeding 200 µm in length, with two rather blunt distal barbs (Fig. 10G); adapical opening moderately long, about 1/5 of length of shaft; base

broad, angular; lateral process indistinct; basal opening large; ligament broad, very thick (Fig. 8I).

Venom gland long, convoluted; muscular bulb large, bean shaped.

Remarks

This species can be readily distinguished from all other congeners by its markedly convex whorls and virtually absent sculpture. The holotype (Fig. 15E) superficially resembles the paratype of *T. vayssierei* (Bouchet & Warén, 1980, fig. 127), which however differs by the presence of prominent tubercles on the periphery of the earlier whorls and by distinct dense spiral striae across the spire. *T. polita* n. sp. is also similar to *Austrotheta crassidentata* (Fig. 15H). While minor features, such as the overall size and canal length, allow differentiating these two species, the difference in protoconch sculpture (respectively arcuate vs diagonally cancellate) provides a reliable distinctive character. Albeit not immediately accessible, the different morphology of the hypodermic tooth (Fig. 16B, D) is an additional character separating the two species. The shell of *T. polita* n. sp. is remarkably similar to that of the holotype of *Pleurotomella argeta* (Fig. 18G) and the two species cannot be separated based on shell features only. Due to the lack of molecular data on *P. argeta*, the hypothesis of a trans-oceanic *Theta* species (*argeta*+*polita*) remains untested. *Theta polita* n. sp. is also superficially similar to *Xanthodaphne cladara* Sysoev, 1997, which differs by its protoconch sculpture with a combination of arcuate riblets and diagonally cancellate pattern and by its finely reticulate teleoconch sculpture (Sysoev, 1997, p. 343, figs 8, 51–52).

Theta microcostellata n. sp. (PSH T3)

(Figs 15F, 16C)

Material examined:

Holotype: Australia, NSW, Hunter CMR, (-32.575, 153.162), IN2017_V03_070, 2595–2474 m, (AMS C.571657).

ZooBank registration: http://zoobank.org/urn:lsid:zoobank.org:act:9DB5C008-9796-45F0-BE1C-2F032F3DA269

Etymology

In reference to the finely ribbed pattern created by its prominent growth lines, derived from ‘micros’ (ancient Greek=small) and ‘costellatus’ (scientific Latin=finely ribbed or ridged). Adjective of feminine gender.

Distribution

Known only from the type locality.

Description

Shell (Fig. 15F) (SL=19.9, SW=8.8 mm), fusiform, rather thin-walled. Protoconch, of at least two orange whorls, with diagonally cancellate sculpture remaining on lower part of last whorl. Teleoconch of 4.8 uniformly yellowish-white whorls. Whorl profile subcylindrical to rather broad, with distinct shoulder in all early to median teleoconch whorls and rounded shoulder in last adult whorl; suture deep; subsutural ramp lightly concave; sinus rather narrow, rounded, subsutural, rather shallow. Spiral sculpture represented by indistinct cords on the shell base; axial sculpture of strong sharp orthocline ribs on spire whorls (about 20 on penultimate whorl); microsculpture of marked bi-sinuose growth lines throughout whorl height, forming distinct, raised riblets on subsutural ramp. Aperture large, pyriform, about half of shell length, opening posteriorly to medium length, rather broad, siphonal canal; outer lip thin, simple, orthocline; inner lip smooth, with rather thick, broad, white callus. Radula (Fig. 16C) of hypodermic, slightly curved teeth of approximately 240 µm in length, with two barbs, dorsal barb smaller, rather blunt; adapical opening moderately long, about 1/5–1/6 of length of shaft; base medium broad, with gentle slope, lateral process indistinct; basal opening large; ligament broad.

Animal uniform cream. Eyes large, situated about ¼ dorsal to outer base of cephalic tentacles. Cephalic tentacles broad, blunt, of medium length. Venom apparatus large; venom glad long, coiled; muscular bulb elongate, lustrous, extremely large; proboscis short, blunt, large.

Remarks

This is currently the only *Theta* species known to have a (at least partly) diagonally cancellate protoconch sculpture. Its adult shell can be differentiated from most other congeners by the small size and the elongate shape as well as by its subcylindrical whorls. The shell of *T. microcostellata* n. sp. (Fig. 15F) superficially resembles that of *Austrotheta wanbiri* n. sp. (Fig. 15G), which is however smaller and more elongate, and has wider and less numerous axial ribs.

Genus *Austrotheta* Criscione, Hallan, Fedosov and Puillandre, 2020 (Criscione et al., 2021; p. 985–986)

Type species *Austrotheta crassidentata* Criscione, Hallan, Fedosov and Puillandre, 2020 by original designation. (PSH U1)

Other species. *Austrotheta wanbiri* n. sp.

Diagnosis

Shell fusiform, semi-translucent to opaque. Protoconch multispiral; sculpture of arcuate cordlets on upper portion of whorls and diagonally cancellate below. Teleoconch with distinctly shouldered to rounded whorls, bearing sharp opisthocline or orthocline axial ribs in most or all whorls; last whorl cylindrical to evenly convex below narrow subsutural ramp, with or without undulating striae throughout its height. Siphonal canal straight, moderately long to long. Aperture elongate to wide, about half of shell length. Anal sinus rather shallow, u-shaped. Radula (based on type species only) of very thick, cylindrical hypodermic teeth, bearing two weak barbs and with very short adapical opening. Base very broad, with extremely coarse external sculpture. Ligament very large.

Remarks

Two species only, the type species *A. crassidentata* and a further species (described below), are included in this South Australian endemic genus. The South African *Typhlosyrinx subrosea* Barnard, 1963 shares with them distinctive shell and radula features (Barnard, 1963, fig. 3a–d; Sysoev, 1996, figs 25–27) and molecular data (when available) may confirm its inclusion in *Austrotheta*. Species of *Austrotheta* are very similar to those of *Theta* in shell characters (see e. g. Fig. 15E vs. H and Fig. 15F vs. G) but differ in their hypodermic tooth (Fig. 16A–C vs. D).

Austrotheta wanbiri n. sp. (PSH U2)

(Figs 15G)

Material examined:

Holotype: Australia, GAB, (-34.574, 129.572), IN2017_C01_198, 3389–3540 m, (AMS C.572174).

ZooBank registration: http://zoobank.org/urn:lsid:zoobank.org:act:B2ABF2BF-4A7C-47D9-B714-A82118BF3AFD

Etymology

In reference to its occurrence in the GAB, derived from 'wanbiri' (Aboriginal Australian language Mirning = sea coast).

Distribution

Known only from the type locality in the GAB.

Description

Shell (Fig. 15G) (SL=15.9, SW=6.5) fusiform, rather thick-walled, opaque. Protoconch broken, orange, multispiral (at least 1.5 whorls), with arcuate cordlets on adapical half to two-thirds of whorl, with diagonally cancellate sculpture below. Teleoconch of 4.3 whorls; subsutural ramp distinctly concave; teleoconch whorls with prominent shoulder on early whorls, situated at adapical third of whorl, more rounded in last whorl; whorl periphery subcylindrical, slightly more convex in last whorl. Early teleoconch whorls with 14 rounded, orthocline axials, reaching lower suture, and producing prominent nodules at shoulder. Later whorls only with nodules becoming weaker on last whorl. Spiral sculpture absent. Microsculpture of collabral growth lines, forming distinct, raised riblets on subsutural ramp. Last adult whorl subcylindrical below subsutural ramp, with long, slender siphonal canal. Aperture rather narrow, pyriform, about half of shell length. Inner lip with whitish callus, rather straight. Outer lip thin, unsculptured. Anal sinus rather shallow, weakly u-shaped. Anatomy and radula unknown.

Remarks

This species can be readily differentiated from *A. crassidentata* by its smaller and more slender shell, bearing more numerous and more prominent axial ribs. For a comparison with *Theta microcostellata* n. sp. (Fig. 15F), see remarks to this latter species.

4 Discussion

4.1 Phylogenetic relationships and genus-level systematics

The five-gene phylogeny of Criscione et al. (2021) established the phylogenetic framework upon which the new genera *Austrobela* and *Austrotheta* were recognised and described, and it is shown herein that there is strong support in both BI and ML analyses for their monophyly, as is the case for *Spergo* and *Theta* (Figs 2–3).

The integrity of these genera is corroborated by morpho-anatomical, notably radular, features diagnostic for each genus. The radula of *Austrobela* is characterised by hypodermic teeth with two large, sharp distal barbs, commonly with a thickened cylindrical basal half of the shaft, and with a rather solid, thick ligament (Fig. 9). While double-barbed teeth appear to be less common than awl-shaped teeth in Australian deep-sea raphitomids (see Criscione et al., 2021), this configuration is not unique to *Austrobela.* Members of the closely related *Theta* also exhibit double-barbed teeth (see below), but they are encountered also, among others, in the more distantly related *Typhlosyrinx* Thiele, 1925 (Bouchet & Sysoev, 2001) and *Pontiothauma* (Pace, 1903). However, the barbs are particularly prominent in *Austrobela,* also when compared to *Theta* (Figs 9–10, 16). Furthermore, all PSHs of the *Austrobela* clade here examined possess an extremely large venom apparatus that occupies the majority of the body haemocoel, and all possess large eyes. Criscione et al. (2021) reported the presence and size of eyes to be a useful diagnostic character at the genus level for deep-sea raphitomids. In terms of shell morphology, members of *Austrobela* can be characterised by their primarily fusiform shells with a prominent shoulder and subcylindrical whorl periphery, a straight columella and a large aperture, which in most PSHs is about equal in length to that of the spire (Figs 5–7). Three discrete types of protoconch sculpture are found in the clade: a sculpture of arcuate ribs (*A. rufa* and *A. levis*), the typical raphitomid diagonally cancellate sculpture (*A. sagitta*, *A. procera* and *A. micraulax*), and a combination of the two former types, where arcuate ribs on the adapical portion are changed by cancellate sculpture on

lower whorl portion (*A. obliquicostata*) (Fig. 8). While the sculpture of arcuate ribs is unusual among the Raphitomidae, it is not unique to members of *Austrobela* – it is also seen in *Theta lyronuclea*, and Clarke (1959) considered this sculpture to warrant the erection of the (then) subgenus *Theta.* The taxa with arcuate ribs on the protoconch (*A. rufa* and *A. levis*) formed a strongly supported clade in Criscione et al. (2021) (there labelled *Austrobela rufa* n. gen. n. sp., *A.* n. gen. sp. 2 and *A.* n. gen. sp. 3), suggesting some phylogenetic signal to this sculptural feature.

Members of the *Spergo* clade primarily exhibit loosely rolled, awl-shaped hypodermic teeth with a short distal blade and a rather narrow base with a distinct lateral process (Figs 13–14). The very loosely rolled teeth encountered in some *Spergo*, notably in *Spergo castellum* (Fig. 14), are unusual within the Raphitomidae. One individual, in particular, exhibited teeth unrolled to a variable extent, including an entirely unrolled tooth, similar to those seen in species of the *Hemilienardia ocellata* (Jousseaume, 1883) complex (Fedosov, Stahlschmidt, Puillandre, Aznar-Cormano, & Bouchet, 2017) as well as in the mangeliid *Benthomangelia* Thiele, 1925 (see Bouchet et al., 2011) where the outer margins do not overlap at any point (Fig. 14B). Examples of teeth entirely contained within others were also observed (Fig. 14A, C), as were distinctly bent teeth (Fig. 14D). This same individual also exhibited teeth that are more typical, albeit loosely rolled (Fig. 14E).

Our phylogenetic analyses (Figs 2, S1) indicated the inclusion within the ingroup of one outgroup taxon, '*Gymnobela' yoshidai* (Kuroda & Habe, 1962), type species of *Speoides* Kuroda & Habe, 1962. This nominal genus was synonymised with *Gymnobela,* when a broader concept was adopted for this latter taxon (Sysoev & Bouchet, 2001). With the boundaries of *Gymnobela* currently restricted by combined morphology and genetics (Criscione et al., 2021), the current placement of *Speoides yoshidai* is untenable. A synonymy of *Speoides* with *Theta* would be supported by their strong phylogenetic relationship and their morphological similarity (see Bouchet & Warén, 1980, p. 59). However, the genetic distance between *Speoides* and *Theta* is comparable to that separating other genera in the trees (Figs 2, S1). In addition, some of these genera (particularly *Austrobela*) exhibit a degree of morphological similarity with *Speoides* comparable to that observed between this latter taxon and *Theta*. For these reasons, a definite answer about the taxonomic status of *Speoides* must await evaluation of morphological and combined mitochondrial and nuclear molecular data.

4.2 Bathymetric and geographic patterns

Most species of *Austrobela* treated herein occur within an area corresponding approximately to the South Australia marine realm of Costello *et al.* (2017). The highest species diversity is recorded in the GAB, where three species are recorded: *A. rufa*, *A. levis* and *A. obliquicostata*, the latter also occurring on the east Australian coast (Fig. 1B–D). The evidence produced indicated that two distinct mitochondrial haplotypes (corresponding to A1 and A2), sharing virtually identical morphology, coexist within *A. rufa*, without showing any apparent geographic or bathymetric partitioning. This pattern may have been generated by a hypothetical scenario of transitory vicariance and subsequent contact of the diverged populations as observed in another deep-water neogastropod *Amalda hilgendorfi* (Martens, 1897) (Kantor, Castelin, Fedosov, & Bouchet, 2020). However, this scenario also is rather speculative, as, in the deep sea, the rapid rise and fall of a geographic barrier is an extremely rare event. The genetic divergence observed may also be the ongoing result of niche partitioning, following (for instance) exploitation of different resources (prey, microhabitat, etc.) as observed in Zvonareva et al. (2020). However, this will remain untested until more information is available on the ecology of *Austrobela* species and on the exact microhabitat composition of the portion of seafloor where the two divergent lineages occur. Whatever the underlying mechanism responsible, assessing whether A1 and A2 indeed represent indeed a pair of cryptic species requires testing the occurrence of recombination by sequencing a suitable nuclear marker.

There is clear bathymetric partitioning between *A. rufa* and the closely related *A. levis* (Fig. 14) and speciation as a result of partitioning into separate bathymetric niches could therefore explain their genetic distinction. This is in agreement with the bathymetric separation observed for some other turriform conoidean sister taxa, such as for members of *Gladiobela* Criscione, Hallan, Puillandre and Fedosov, 2020 (Hallan et al., 2021), *Lophiotoma* T. L. Casey, 1904 (Puillandre et al., 2017) and *Cryptogemma* Dall, 1918 (Turridae) (Zaharias et al., 2020). While the radulae are slightly different in these species (Fig. 9A–B, F), nothing is known of their prey preference so whether this is a potential factor in their differentiation remains unknown.

Only two of the new Australian *Austrobela* species do not occur in the GAB, namely *A. sagitta* and *A. regia*, neither of which is recorded outside of Australia. However, as these

two taxa occur further north, with *A. sagitta* extending into the Coral Sea (Fig. 1D) future deep-sea sampling may reveal distributions beyond Australian waters (particularly for the latter). This study reports a range extension for *A. procera*, not previously recorded in Australia [with records from both (off) Western Australia and the east coast (Fig. 1A, D)] and in Taiwan and the Tuamotu archipelago (Table S1). The type locality of *A. procera* is the Loyalty Ridge, and it is recorded as far east as Wallis and Futuna (Sysoev & Bouchet, 2001). While it remains to be proven by means of molecular data that the material throughout this range is conspecific, the new records indicate that this may be a widespread species. There is growing evidence of wide distributions in several deep sea conoideans species (Zaharias et al., 2020; Hallan et al., 2021) and further sampling and systematics work will likely reveal additional widespread taxa. Criscione et al. (2021) reported *Theta lyronuclea* from Australia, although the topotypic Caribbean population has never been sequenced (Clarke, 1959). A record of *T. lyronuclea* from Argentina by Sánchez and Pastorino (2020) (albeit not molecularly confirmed) lends more confidence to that species assignment, as their provision of both radular and penial anatomy reveals considerable similarity to the Australian material. Pending molecular confirmation linking the Caribbean, South Atlantic and Australian populations, there is therefore compelling morphological and anatomical evidence of *T. lyronuclea* as a widespread, transoceanic species. Due to the limited material of *T. microcostellata* and *T. polita*, we cannot infer much about any potential bathymetric zonation among *Theta* species, nor discuss the biogeography of the two latter. This is also the case for the species of *Austrotheta* treated herein. While any inference of rarity will inevitably, to some extent, be an artefact of sampling, there is evidence that many turriform conoidean species are comparatively rare based on their scarcity in reasonably well-sampled areas (Castelin et al., 2011). Bouchet et al. (2009) noted this for the New Caledonian fauna, and Hallan et al. (2021) for some species of the deep-sea genus *Gladiobela. Theta microcostellata, T. polita, Austrotheta crassidentata* and *A. wanbiri* may therefore represent additional relatively rare species, as the regions in which they have been collected are comparatively well-sampled (MacIntosh et al., 2018; O'Hara et al., 2020), with a diverse raphitomid fauna (Criscione et al., 2021). Conversely, most *Austrobela* species studied here, notably *A. rufa*, *A. levis* and *A. obliquicostata*, can be considered relatively common, as is the case for *Theta lyronuclea.*

In Australian waters, species of *Spergo* have only been recorded from the east coast (Fig. 1E) with none recorded in the GAB despite comparable sampling efforts (MacIntosh et al., 2018). This notable pattern requires further study to be explained.

Acknowledgments

This work has been made possible through financial support from the Australian Government (ABRS grant RF217-57, principal investigator FC). The participation of AF was supported by the Russian Science Foundation (grant 19-74-10020 to AF). The participation of NP was also supported by funding from the European Research Council (ERC) under the European Union's Horizon 2020 research and innovation programme (grant agreement No.865101).

Voyages in the GAB were part of: (a) the GAB Research Program [GABRP – a collaboration between BP, CSIRO, the South Australian Research and Development Institute (SARDI), the University of Adelaide, and Flinders University] and (b) the GAB Deepwater Marine Program (GABDMP – a CSIRO led research program sponsored by Chevron Australia]. Funding for the 'Eastern Abyss' voyage (IN2017_V03) was provided by the Marine Biodiversity Hub (MBH), supported through the Australian Government's National Environmental Science Program (NESP). The 'Tasmanian seamounts' voyage (IN2018_V06) was sponsored by the CSIRO Marine National Facility (MNF), the NESP MBH and Parks Australia. The authors wish to thank the CSIRO MNF for its support in the form of sea time onboard, support personnel, scientific equipment and data management. We also thank the scientific staff and crew who participated in all voyages generating the samples studied herein.

The MNHN samples used in this study originates from shore-based expeditions (KARUBENTHOS 2015, PAPUA NIUGINI; PI Philippe Bouchet) and deep-sea cruises (AURORA 2007, BIOMAGLO, BIOPAPUA, CONCALIS, EBISCO, KANADEEP, NANHAI 2014, NORFOLK 2, SALOMON 2, TAIWAN 2014, TARASOC, TERRASSES, ZHONGSHA 2015; PIs Philippe Bouchet, Tin-Yam Chan, Laure Corbari, Nicolas Puillandre, Sarah Samadi, Wei-Jen Chen, Bertrand Richer de Forges) conducted by MNHN, Pro-Natura International (PNI) and Institut de Recherche pour le Développement as part of the Our Planet Reviewed and the Tropical Deep-Sea Benthos programs. Funders and sponsors included a bilateral cooperation research funding from the Taiwan Ministry of Science and Technology (MOST 102-2923-B-002-001-MY3, PI Wei-Jen Chen) and the French National Research Agency (ANR 12-ISV7-0005-01, PI Sarah Samadi), the Total Foundation, Prince Albert II of Monaco Foundation, Stavros Niarchos Foundation, and Richard Lounsbery Foundation. All expeditions operated under the regulations then in force in the countries in question and satisfy the conditions set by the Nagoya Protocol for access to genetic resources (expeditions.mnhn.fr). We would

like to express our gratitude to Mandy Reid, Alison Miller and Jennifer Caiza (AMS) for assistance with registration and databasing of material, to Barbara Buge (MNHN for the sample preparation, and to Andrea Crowther (SAMA, Adelaide), Simon Grove and Kirrily Moore (TMAG, Hobart), Lisa Kirkendale and Corey Whisson (WAM, Perth). Adam Baldinger (MCZ, Cambridge MA), Michel Dagnino and Michèle Bruni (MOM, Monaco), Jeroen Goud and Bram van der Bijl (NCBN, Leiden), Kazunori Hasegawa (NSMT, Tokyo), Andreia Salvador and Kevin Webb (NHMUK, London), Ellen Strong (USNM, Washington) and Alexander Sysoev (ZMMU, Moscow) are thanked for providing photographs of the types of previously described species. Thanks are also due to Sue Lindsay and Chao Shen (Macquarie University, Sydney) for assisting with SEM work. Finally, Ben and Janine Travaglini (Mornington, Vic) are thanked for producing photographs of some of the specimens studied here.

References

Abdelkrim, J., Aznar-Cormano, L., Fedosov, A. E., Kantor, Y. I., Lozouet, P., Phuong, M. A., . . . Puillandre, N. (2018). Exon-Capture-Based Phylogeny and Diversification of the Venomous Gastropods (Neogastropoda, Conoidea). *Molecular Biology and Evolution, 35*(10), 2355-2374. doi:10.1093/molbev/msy144

Barnard, K. H. (1963). Deep sea Mollusca from West of Cape Point, South Africa. *Annals of the South African Museum, 46*, 407-453.

Bouchet, P., Heros, V., Lozouet, P., & Maestrati, P. (2008). *A quarter - century of deep-sea malacological exploration in the South and West Pacific: where do we stand? How far to go?*

Bouchet, P., & Kantor, Y. I. (2004). New Caledonia: The major centre of biodiversity for volutomitrid molluscs (Mollusca: Neogastropoda: Volutomitridae). *Systematics and Biodiversity, 1*(4), 467-502. doi:10.1017/S1477200003001282

Bouchet, P., Kantor, Y. I., Sysoev, A. V., & Puillandre, N. (2011). A new operational classification of the Conoidea (Gastropoda). *Journal of Molluscan Studies, 77*(3), 273-308. doi:10.1093/mollus/eyr017

Bouchet, P., Lozouet, P., & Sysoev, A. V. (2009). An inordinate fondness for turrids. *Deep-Sea Research Part II Topical Studies in Oceanography, 56*(19-20), 1724-1731.

Bouchet, P., & Sysoev, A. V. (2001). Typhlosyrinx-like tropical deep-water turriform gastropods (Mollusca, Gastropoda, Conoidea). *Journal of Natural History, 35*(11), 1693-1715. doi:10.1080/002229301317092405

Bouchet, P., & Warén, A. (1980). Revision of the north east Atlantic bathyal and abyssal Turridae (Mollusca, Gastropoda). *Journal of Molluscan Studies Supplement, 8*, 1-119.

Castelin, M., Puillandre, N., Lozouet, P., Sysoev, A. V., de Forges, B. R., & Samadi, S. (2011). Molluskan species richness and endemism on New Caledonian seamounts: Are they enhanced compared to adjacent slopes? *Deep Sea Research Part I: Oceanographic Research Papers, 58*(6), 637-646. doi:https://doi.org/10.1016/j.dsr.2011.03.008

Clarke, A. H. (1959). New abyssal mollusks from off Bermuda collected by the Lamont geological Observatory Research vessels. *Proceedings of the Malacological Society of London, 38*, 231-238.

Costello, M. J., Tsai, P., Wong, P. S., Cheung, A. K. L., Basher, Z., & Chaudhary, C. (2017). Marine biogeographic realms and species endemicity. *Nature Communications, 8*(1), 1057. doi:10.1038/s41467-017-01121-2

Criscione, F., Hallan, A., Puillandre, N., & Fedosov, A. (2021). Where the snails have no name: a molecular phylogeny of Raphitomidae (Neogastropoda: Conoidea) uncovers vast unexplored diversity in the deep seas of temperate southern and eastern Australia. *Zoological Journal of the Linnean Society, 191*(4), 961-1000. doi:10.1093/zoolinnean/zlaa088

Dall, W. H. (1889). Reports on the results of dredgings, under the supervision of Alexander Agassiz, in the Gulf of Mexico (1877-78) and in the Caribbean Sea (1879-80), by the U. S. Coast Survey Steamer 'Blake'. XXIX-Report on the Mollusca. Part II. Gastropoda and Scaphopoda. *Bulletin of the Museum of Comparative Zoölogy at Harvard College, 18*, 1-492.

Dall, W. H. (1890). Preliminary Report on the Collection of Mollusca and Brachiopoda obtained in 1887-88. vn. Scientific Results of Explorations by the U.S. Fish. Commission Steamer 'Albatross.'. *Proceedings of the United States National Museum, xii*, pp. 219-362.

Dall, W. H. (1895). Report on the Mollusca and Brachiopoda dredged in deep water, chiefly near the Hawaiian Islands, with illustrations of hitherto unfigured species from Northwest America. *Proceedings of the United States National Museum., 17*, 675-733.

Dall, W. H. (1918). Notes on the nomenclature of the mollusks of the family Turritidae. *Proceedings of the United States National Museum., 54*(2238), 313-333. doi:10.5479/si.00963801.54-2238.313

Dautzenberg, P. (1925). Mollusques nouveaux provenant des croisières du Prince Albert Ier de Monaco. *Bulletin de l'Institut Océanographique de Monaco, 457*, 1-12.

Dautzenberg, P., & Fischer, H. (1896). Campagnes scientifiques de S. A. le Prince Albert Ier de Monaco. Dragages effectues par l'Hirondelle et par la Princesse Alice, 1888-1895... I-Mollusques, Gasteropodes including Polyplacophora. *Memoires de la Societe Zoologique de France, ix*, pp. 395-498.

Dell, R. K. (1963). Notes on some New Zealand Mollusca in the British Museum. *Transactions of the Royal Society of New Zealand Zoology, 3*, 171-177.

Fedosov, A. E., Stahlschmidt, P., Puillandre, N., Aznar-Cormano, L., & Bouchet, P. (2017). Not all spotted cats are leopards: evidence for a Hemilienardia ocellata species complex (Gastropoda: Conoidea: Raphitomidae). *European Journal of Taxonomy, 268*, 1-20.

Folmer, O., Black, M., Hoeh, W., Lutz, R., & Vrijenhoek, R. (1994). DNA primers for amplification of mitochondrial cytochrome c oxidase subunit I from diverse metazoan invertebrates. *Molecular Marine Biology and Biotechnology, 3*(5), 294-299.

Garcia, E. F. (2005). Six new deep-water molluscan species (Gastropoda: Epitoniidae, Conoidea) from the Gulf of Mexico. *Novapex, 6*, 79-87.

Gonzales, D. T. T., & Saloma, C. P. (2014). A bioinformatics survey for conotoxin-like sequences in three turrid snail venom duct transcriptomes. *Toxicon, 92*, 66-74.

Habe, T. (1961). Coloured illustrations of the shells of Japan (II). Hoikusha, Osaka. xii + 183 + 42 pp., 66 pls.

Hallan, A., Criscione, F., Fedosov, A., & Puillandre, N. (2021). Few and far apart: integrative taxonomy of Australian species of Gladiobela and Pagodibela (Conoidea : Raphitomidae) reveals patterns of wide distributions and low abundance. *Invertebrate Systematics, 35*(2), 181-202. doi:https://doi.org/10.1071/IS20017

Kantor, Y. I., Castelin, M., Fedosov, A., & Bouchet, P. (2020). The Indo-Pacific Amalda (Neogastropoda, Olivoidea, Ancillariidae) revisited with molecular data, with special emphasis on New Caledonia. *European Journal of Taxonomy*(706). doi:10.5852/ejt.2020.706

Kantor, Y. I., Fedosov, A. E., & Puillandre, N. (2018). New and unusual deep-water Conoidea revised with shell, radula and DNA characters. *Ruthenica, 28*, 47-82.

Kantor, Y. I., Harasewych, M. G., & Puillandre, N. (2016). A critical review of Antarctic Conoidea (Neogastropoda). *Molluscan Research, 36*(3), 153-206.

Kantor, Y. I., Puillandre, N., Olivera, B. M., & Bouchet, P. (2008). Morphological proxies for taxonomic decision in turrids (Mollusca, Neogastropoda): a test of the value of shell and radula characters using molecular data. *Zoological Science (Tokyo), 25*(11), 1156-1170. doi:10.2108/zsj.25.1156

Kantor, Y. I., & Sysoev, A. V. (1986). A new genus and new species from the family Turridae (Gastropoda, Toxoglossa) in the northern part of the Pacific Ocean. *Zoologicheskii Zhurnal, 65*(4), 485-498.

Kantor, Y. I., & Taylor, J. D. (2000). Formation of marginal radular teeth in Conoidea (Neogastropoda) and the evolution of the hypodermic envenomation mechanism. *Journal of Zoology (London), 252*(2), 251-262. doi:10.1017/s0952836900009985

Kantor, Y. I., & Taylor, J. D. (2002). Foregut anatomy and relationships of raphitomine gastropods (Gastropoda: Conoidea: Raphitominae). *Bollettino Malacologico, 38*, 83-110.

Kumar, S., Stecher, G., & Tamura, K. (2016). MEGA7: Molecular Evolutionary Genetics Analysis Version 7.0 for Bigger Datasets. *Mol Biol Evol, 33*(7), 1870-1874. doi:10.1093/molbev/msw054

Lopez-Vera, E., de la Cortera, E. P. H., Maillo, M., Riesgo-Escovar, J. R., Olivera, B. M., & Aguilar, M. B. (2004). A novel structural class of toxins: the methionine-rich peptides from the venoms of turrid marine snails (Mollusca, Conoidea). *Toxicon, 43*(4), 365-374. doi:10.1016/j.toxicon.2003.12.008

MacIntosh, H., Althaus, F., Williams, A., Tanner, J. E., Alderslade, P., Ahyong, S. T., . . . Wilson, R. S. (2018). Invertebrate diversity in the deep Great Australian Bight (200–5000 m). *Marine Biodiversity Records, 11*(1), 23. doi:10.1186/s41200-018-0158-x

Modica, M. V., Gorson, J., Fedosov, A. E., Malcolm, G., Terryn, Y., Puillandre, N., & Holford, M. (2019). Macroevolutionary Analyses Suggest That Environmental Factors, Not Venom Apparatus, Play Key Role in Terebridae Marine Snail Diversification. *Systematic Biology, 69*(3), 413-430. doi:10.1093/sysbio/syz059

O'Hara, T. D., Williams, A., Ahyong, S. T., Alderslade, P., Alvestad, T., Bray, D., . . . Bax, N. J. (2020). The lower bathyal and abyssal seafloor fauna of eastern Australia. *Marine Biodiversity Records, 13*(1), 11. doi:10.1186/s41200-020-00194-1

Okutani, T., & Iwahori, A. (1992). Noteworthy Gastropods Collected from Bathyal Zone in Tosa Bay by the R/V Kotaka-Maru in 1987 and 1988. *Venus (Japanese Journal of Malacology), 51*(4), 235-268. doi:10.18941/venusjjm.51.4_235

Pace, S. (1903). On the Anatomy of the Prosobranch genus Pontiothauma E. A. Smith. *Journal of the Linnean Society Zoology, xxviii*, pp. 455-462.

Palumbi, S. R. (1996). *Nucleic acids 2: the polymerase chain reaction*: Sinauer Associates, Inc.

Puillandre, N., Baylac, M., Boisselier, M. C., Cruaud, C., & Samadi, S. (2009). An integrative approach to species delimitation in Benthomangelia (Mollusca: Conoidea). *Biological*

Journal of the Linnean Society, 96(3), 696-708. doi:10.1111/j.1095-8312.2008.01143.x

Puillandre, N., Bouchet, P., Duda, T. F., Kauferstein, S., Kohn, M., Olivera, B., . . . Meyer, C. (2014). Molecular phylogeny and evolution of the cone snails (Gastropoda, Conoidea). *Molecular Phylogenetics and Evolution, 78*. doi:10.1016/j.ympev.2014.05.023

Puillandre, N., Fedosov, A. E., & Kantor, Y. I. (2015). Systematics and Evolution of the Conoidea. In P. Gopalakrishnakone & A. Malhotra (Eds.), *Evolution of Venomous Animals and Their Toxins* (pp. 1-32). Dordrecht: Springer Netherlands.

Puillandre, N., Fedosov, A. E., Zaharias, P., Aznar-Cormano, L., & Kantor, Y. I. (2017). A quest for the lost types of Lophiotoma (Gastropoda: Conoidea: Turridae): integrative taxonomy in a nomenclatural mess. *Zoological Journal of the Linnean Society, 181*(2), 243-271. doi:10.1093/zoolinnean/zlx012

Puillandre, N., Kantor, Y. I., Sysoev, A. V., Couloux, A., Meyer, C., Rawlings, T., . . . Bouchet, P. (2011). The dragon tamed? A molecular phylogeny of the Conoidea (Gastropoda). *Journal of Molluscan Studies, 77*(3), 259-272. doi:10.1093/mollus/eyr015

Puillandre, N., Koua, D., Favreau, P., Olivera, B. M., & Stoecklin, R. (2012). Molecular Phylogeny, Classification and Evolution of Conopeptides. *Journal of Molecular Evolution, 74*, 297-309.

Puillandre, N., Lambert, A., Brouillet, S., & Achaz, G. (2012). ABGD, Automatic Barcode Gap Discovery for primary species delimitation. *Molecular Ecology, 21*, 1864-1877.

Puillandre, N., Modica, M. V., Zhang, Y., Sirovich, L., Boisselier, M. C., Cruaud, C., . . . Samadi, S. (2012). Large-scale species delimitation method for hyperdiverse groups. *Molecular Ecology, 21*(11), 2671-2691.

Rambaut, A., Drummond, A. J., Xie, D., Baele, G., & Suchard, M. A. (2018). Posterior Summarization in Bayesian Phylogenetics Using Tracer 1.7. *Systematic Biology, 67*(5), 901-904. doi:10.1093/sysbio/syy032

Ronquist, F., & Huelsenbeck, J. P. (2003). MrBayes 3: Bayesian phylogenetic inference under mixed models. *Bioinformatics, 19*(12), 1572-1574. doi:10.1093/bioinformatics/btg180

Saitou, N., & Nei, M. (1987). The neighbor-joining method: a new method for reconstructing phylogenetic trees. *Molecular Biology and Evolution, 4*(4), 406-425.

Sánchez, N., & Pastorino, G. (2020). The North Atlantic Conoidean Gastropod Theta lyronuclea (Raphitomidae) in Deep-Waters of the Southwestern Atlantic. *Malacologia, 63*(1), 33-40, 38.

Schepman, M. M. (1913). The Prosobranchia of the Siboga Expedition. Part V. Toxoglossa, with a supplement. *Siboga-Expeditie, 49*, 365-452.

Stahlschmidt, P., Chino, M., & Fraussen, K. (2015). A new Spergo species (Conoidea: Raphitomidae) from the Mozambique Channel. *Miscellanea Malacologica:, 7*.

Sysoev, A. V. (1990). Gastropods of the family Turridae (Gastropoda: Toxoglossa) of the Nasca and Sala-y-Gomez underwater ridges. *Trudy Instituta Okeanologii Akademii Nauk SSSR, 124*, 245-260.

Sysoev, A. V. (1996). Taxonomic notes on South African deep-sea conoidean gastropods (Gastropoda: Conoidea) described by K.H. Barnard, 1963. *Nautilus, 110*(1), 22-29.

Sysoev, A. V. (1997). Mollusca Gastropoda: new deep-water turrid gastropods (Conoidea) from eastern Indonesia. *Memoires du Museum National d'Histoire Naturelle, 172*, 325-355.

Sysoev, A. V. (2014). Deep-sea fauna of European seas: An annotated species check-list of benthic invertebrates living deeper than 2000 m in the seas bordering Europe. Gastropoda. *Invertzool, 11*, 134-155. doi:10.15298/invertzool.11.1.14

Sysoev, A. V., & Bouchet, P. (2001). New and uncommon turriform gastropods (Gastropoda: Conoidea) from the South-West Pacific. *Memoires du Museum National d'Histoire Naturelle, 185*, 271-320.

Tamura, K., & Nei, M. (1993). Estimation of the number of nucleotide substitutions in the control region of mitochondrial DNA in humans and chimpanzees. *Mol Biol Evol, 10*(3), 512-526. doi:10.1093/oxfordjournals.molbev.a040023

Thiele, J. (1925). Gastropoden der Deutschen Tiefsee-Expedition. II Teil. Wissenschaftliche Ergebnisse der Deutschen Tiefsee-Expedition auf dem Dampfer "Valdivia". *Wissenschaftliche Ergebnisse der Deutschen Tiefsee-Expedition, 17*(2), 35-382.

Vermeij, G. J. (1982). Unsuccessful Predation and Evolution. *The American Naturalist, 120*(6), 701-720. doi:10.1086/284025

Watson, R. B. (1881). Mollusca of H.M.S. 'Challenger' Expedition.—Part X. *Journal of the Linnean Society of London, Zoology, 15*(88), 457-475. doi:10.1111/j.1096-3642.1881.tb00377.x

Watson, R. B. (1886). Report on the Scaphopoda and Gastropoda collected by H.M.S. 'Challenger' during the Years 1873-76. *Zoology Challenger Expedition, 15*(42), 756 pp.

Zaharias, P., Kantor, Y. I., Fedosov, A. E., Criscione, F., Hallan, A., Kano, Y., . . . Puillandre, N. (2020). Just the once will not hurt: DNA suggests species lumping over two oceans in deep-sea snails (Cryptogemma). *Zoological Journal of the Linnean Society, 190*(2), 532-557. doi:10.1093/zoolinnean/zlaa010

Zvonareva, S., Mekhova, E., Hoang, D., Nguyen, T., Vo, H., & Fedosov, A. (2020). Diversity and relationships of shallow water Ovulidae (Mollusca:Gastropoda) of Vietnam. *Archiv für Molluskenkunde, 149*, 113-146. doi:10.1127/arch.moll/149/113-146

Figure legends

Figure 1. Distribution of taxa studied herein in Australian waters. Thin lines mark limits among marine realms (numbered as in Costello et al., 2017). (a) Map of the South Australia realm (#26) and Tropical Australia/Coral Sea realm (#16) (*sensu* Costello et al., 2017), with indication of the areas (in the GAB and along the South-Eastern coast - shaded) containing records of samples studied. (b) Records of sequenced specimens of *Austrobela* in the Great Australian Bight (numbered circles). (c) Records of sequenced specimens of *Theta* (numbered triangles) and *Austrotheta* (numbered diamonds) in the Great Australian Bight. (d) Records of sequenced specimens of *Austrobela* (numbered circles), *Theta* (numbered triangles) and *Austrotheta* (numbered diamond) along the Australian South-Eastern coast. (e) Records of sequenced specimens of *Spergo* (numbered squares) along the Australian South-eastern coast. Numbers in shapes indicate PSHs/species of: *Austrobela* (circles: 1 – A1/*A. rufa*, 2 – A2/*A. rufa*, 3 – A3/*A. levis*, 4 – A4/*A. sagitta*, 5 – A5/A*. obliquicostata*, 6 – A6/*A. procera,* 9 – A9/*A. regia*); *Spergo* (squares: 2 – S2/*S. fusiformis*, 3 – *S. parvidentata*, 4 – S4/*S. tenuiconcha*, 5 – S5/*S. castellum*, 6 – S6/*S. annulata*); *Theta* (triangles: 1 – T1/*T. lyronuclea*, 2 – T2/*T. polita*, 3 – T3/*T. microcostellata*) and *Austrotheta* (diamonds: 1 – U1/*A. crassidentata*, 2 - U2/ *A. wanbiri*). Records of micro-sympatry (see text) are indicated by numbers and shapes connected by '+'. Scalebars = 5000 km (a), 1000 km (b –e).

Figure 2. Bayesian consensus phylogram (BI) based on analyses of the *cox1+16S* sequences dataset. Clades containing congeneric species in the outgroup are collapsed. Numbers above branches indicate nodal support by Bayesian posterior probabilities (BPP). Numbers below PSH nodes indicate nodal support (%) by bootstrap (BTSP) resulting from the ML analysis of Fig. S1. BPP values of 1 and BTSP values of 100% are represented by asterisks. Support values within PSH are omitted. Voucher details on clusters of identical sequences (CIS - numbers in brackets) are given as supplementary material (Table S2). Names of species described herein, and sequences of Australian samples are in bold. Vertical bars mark distinct PSHs as delimited by ABGD on the corresponding *cox1* dataset. Samples whose shells are figured or CIS containing figured shells are underlined. For A5, the holotype, SAMA D67741is figured. Shells of congeneric species are in scale.

Figure 3. Maximum likelihood (ML) tree based on analyses of the *16S* sequences dataset. Clades containing congeneric species in the outgroup are collapsed. Numbers near branches indicate nodal support (%) by ML bootstrap (BTSP. Support values for clades below the PSH/species level are omitted. Voucher details on clusters of identical sequences (CIS - numbers in brackets) are given as supplementary material (Table S3). Names of species described herein, and sequences of Australian samples are in bold. Vertical bars mark distinct primary species hypotheses (PSHs) as delimited by the ABGD method on the corresponding *cox1* dataset.

Figure 4. Scatter plot of SW and SH ratios with Wt for measured shells of the *Austrobela*. PSHs A1, A2, A3, with 68% confidence ellipses drawn for each PSHs.

Figure 5. Shells of *Austrobela rufa* Criscione et al., 2020 (PSHs A1-A2). (a) Holotype AMS C.571709 (A1); (b) AMS C.571756 (A2); (c) AMS C.532684 (A2); (d) Paratype AMS C.571699 (A1); (e) Paratype AMS C.483802 (A1); (f) Paratype AMS C.574588 (A1); (g) Paratype AMS C.271201 (A1); (h) Paratype SAMA D44253 (A1); (i) Paratype SAMA D67742 (A1). Scale bar = 10 mm.

Figure 6. Shells of *Austrobela* PSHs/species studied herein. (a) A3/*Austrobela levis* n. sp., holotype AMS C.571693; (b) A3/*Austrobela levis* n. sp., paratype AMS C.532671; (c) A3/*Austrobela levis* n. sp., paratype AMS C.571694; (d) A3/*Austrobela levis* n. sp., paratype AMS C.571813; (e) A3/*Austrobela levis* n. sp., paratype SAMA D44145; (f) A5/*Austrobela obliquicostata* n. sp., holotype SAMA D67741; (g) A5/*Austrobela obliquicostata* n. sp., paratype AMS C.532689; (h) A4/*Austrobela sagitta* n. sp., holotype AMS C.519338; (i) A9/*Austrobela regia* n. sp. holotype AMS C.571682; (j) *Austrobela pyrrhogramma* (Dautzenberg & Fischer, 1896) n. comb., holotype MOM INV-18477; (k) A8/*Austrobela pyrrhogramma* (Dautzenberg & Fischer, 1896) n. comb., MNHN IM-2013-61353 . Scale bar = 10 mm.

Figure 7. Shells of *Austrobela* PSHs/species studied herein. (a) *Austrobela procera* (Sysoev & Bouchet, 2001), holotype MNHN IM-2000-3188; (b) A6/*Austrobela procera* (Sysoev & Bouchet, 2001) n. comb., AMS C.519339; (c) *Austrobela* AB, MNHN IM-2009-13538; (d)

Austrobela AA, MNHN IM-2013-61625; (e) *Austrobela micraulax* (Sysoev, 1997) n. comb., holotype MNHN IM-2000-3091; (f) A7/*Austrobela micraulax* (Sysoev, 1997) n. comb., MNHN IM-2013-9837; (g) *Austrobela* AD, MNHN IM-2009-29317; (h) *Austrobela* AC, IM-2007-38756. Scale bar = 10 mm.

Figure 8. Larval shells of *Austrobela* PSHS/species studied herein. (a) A1/*Austrobela rufa* Criscione et al., 2020 holotype AMS C. 571709; (b) A1/*Austrobela rufa* Criscione et al., 2020 paratype AMS C.571681; (c) A2/*Austrobela rufa* Criscione et al., 2020, AMS C.571756; (d) A3/*Austrobela levis* n. sp., paratype AMS C.532883; (e) A4/*Austrobela sagitta* n. sp., paratype AMS C.519400; (f) A6/*Austrobela procera* (Sysoev & Bouchet, 2001) n. comb., AMS C.519275; (g) A5/*Austrobela obliquicostata* n. sp., paratype AMS C.572173; (h) A9/*Austrobela regia* holotype AMS C.571682. Scale bar = 1 mm.

Figure 9. Hypodermic teeth of *Austrobela* PSHs/species studied herein. (a) A1/*Austrobela rufa* Criscione et al., 2020, paratype AMS C.571679; (b) A2/*Austrobela rufa* Criscione et al., 2020, AMS C. C.575584; (c) A6/*Austrobela procera* (Sysoev & Bouchet, 2001) n. comb., AMS C.519339; (d) A5/*Austrobela obliquicostata* n. sp., paratype AMS C.571644; (e) A9/*Austrobela regia* holotype AMS C.571682; (f) A3/*Austrobela levis* n. sp., holotype AMS C.571693; (g) A4/*Austrobela sagitta* n. sp., holotype AMS C.519338. Scale bar = 200 µm.

Figure 10. Radular details of *Austrobela* and *Theta* spp. (a) A3/*Austrobela levis* n. sp., holotype AMS C.571693; (b) A9/*Austrobela regia* holotype AMS C.571682; (c) A1/*Austrobela rufa* Criscione et al., 2020 paratype AMS C.574588; (d) A2/*Austrobela rufa* Criscione et al., 2020 AMS C.575584; (e) T1/*Theta lyronuclea* (Clarke, 1959), AMS C.571733; (f) T1/*Theta lyronuclea* (Clarke, 1959), AMS C.571733; (g) T3/*Theta polita* n. sp., paratype AMS C.532868 (h) A9/*Austrobela regia* holotype AMS C.571682; (i) T3/*Theta polita* n. sp., holotype AMS C.571657; (j) A2/*Austrobela rufa* Criscione et al., 2020, AMS C.571670. Scale bar = 20 µm. Abbreviations: ao = adapical opening; bo = basal opening; db = dorsal barb; evb = edge of ventral barb; lig = ligament; tw = tooth wall; vb = ventral barb.

Figure 11. Shells of *Spergo* PSHS/species studied herein. (a) *Spergo glandiniformis* (Dall, 1895), holotype USNM 107013; (b) S4/*Spergo tenuiconcha* n. sp., holotype AMS C.482142;

(c) S5/*Spergo castellum* n. sp. holotype AMS C.482148; (d) S3/*Spergo parvidentata* n. sp., holotype AMS C.519401; (e) S6/*Spergo annulata* n. sp., holotype AMS C.519333; (f) *Spergo sibogae* (Schepman, 1913), holotype NBCNL ZMA.MOLL.136847; (g) S1/*Spergo sibogae* (Schepman, 1913), MNHN IM-2009-16933; (h) S1/*Spergo sibogae* (Schepman, 1913), MNHN IM-2013-61655. Scale bar = 20 mm.

Figure 12. Shells of *Spergo* PSHs/species studied herein. (a) *Spergo fusiformis* (Habe, 1962), holotype NSMT MoR 49751; (b) S2/*Spergo fusiformis* (Habe, 1962), AMS C.482154; (c) *Spergo aithorrhis* Sysoev & Bouchet, 2001, holotype MNHN IM-2000-2742; (d) *Spergo parunculis* Stalschmidt, Chino & Fraussen, 2015, holotype MNHN IM-2000-30150. Scale bar = 20 mm.

Figure 13. Hypodermic teeth of *Spergo* PSHs/species studied herein. (a) S5/*Spergo castellum* n. sp., paratype AMS C.519290; (b) S4/*Spergo tenuiconcha* n. sp., holotype AMS C.482142; (c) S3/*Spergo parvidentata* n. sp., paratype AMS C.571667; (d) S2/*Spergo fusiformis* (Habe, 1962), AMS C.482154; (e) S6/*Spergo annulata* n. sp., paratype AMS C.571638. Scale bar = 50 µm (9A, B, D & E); 30 µm (9C).

Figure 14. Variation in tooth formation in S5/*Spergo castellum* n. sp., holotype AMS C.482148. (a) Teeth exhibiting medium to high degree of unrolling, with two bottom teeth entangled (with one encapsulated within the other); (b) entirely unrolled tooth; (c) entangled teeth; (d) bent, possibly poorly sclerotized teeth (e) moderately to tightly rolled, straight teeth; (f) cluster of teeth with interconnecting ligaments, showing one entirely unrolled tooth. Scale bar = 100 µm.

Figure 15. Shells of *Theta* and *Austrotheta* PSHs/species studied herein. (a) *Theta lyronuclea* (Clarke, 1959), holotype MCZ 218184; (b) *Theta vayssierei* (Dautzenberg, 1925), holotype MOM INV-18405; (c) *Theta chariessa* (Watson, 1881), syntype NHMUK 1887.2.9.1098; (d) T1/*Theta lyronuclea* (Clarke, 1959), AMS C.571655; (e) T3/*Theta polita* n. sp., holotype AMS C.571657; (f) T2/*Theta microcostellata* n. sp., holotype AMS C.532711; (g) U2/*Austrotheta wanbiri* n. sp., holotype AMS C.572174; (h) U1/*Austrotheta crassidentata* Criscione et al., 2020, holotype AMS C.519302. Scale bar = 5 mm (a), 10 mm (b-h).

Figure 16. Hypodermic teeth of *Theta* and *Austrotheta* PSHs/species studied herein. (a) T1/*Theta lyronuclea* (Clarke, 1959), AMS C.571733; (b) T2/*Theta polita* n. sp., paratype AMS C.532868; (c) T3/*Theta microcostellata* n. sp., holotype AMS C.571657; (d) U1/*Austrotheta crassidentata* Criscione et al., 2020, holotype AMS C.519302. Scale bar = 100 µm.

Figure 17. Bathymetric ranges of taxa studied herein as inferred from records of sequenced specimens. Species represented by a single record are indicated by a circle.

Figure 18. Shells of types of species of Raphitomidae showing typical traits of the genera studied herein. (a) *Pleurotoma gypsata* Watson, 1881, syntype NHMUK 1887.2.9.979; (b) *Pleurotoma fulvotincta* Dautzenberg & Fischer, 1896, syntype MOM INV-18461; (c) *Pleurotomella dubia* Schepman, 1913, syntype NBCN ZMA.MOLL.136881; (d) *Pleurotoma filifera* Dall, 1881, holotype USNM 596209; (e) *Gymnobela petiti* Garcia, 2005, holotype ANSP 412715; (f) *Gymnobela nivea* Sysoev, 1990, holotype ZMMU Lc-5737; (g) *Pleurotomella argeta* Dall, 1890, holotype UNSM 96552; (h) *Pleurotomella ceramensis* Schepman, 1913, syntype ZMA.MOLL.137936; (i) *Gymnobela latistriata* Kantor & Sysoev, 1986, holotype ZMMU Lc-22341; (j) *Clathurella homeotata* Watson, 1886, holotype NHMUK 1887.2.9.1115; (k) *Thesbia nudator* Locard, 1897, holotype MNHN IM-2000-3131; (l) *Gymnobela oculifera* Kantor & Sysoev, 1986; (m) *Gymnobela africana* Sysoev, 1996, holotype NHMUK 1993114. Scale bar = 3 mm (k), 5 mm (e-f), 10 mm (a-d, h-i, j, l), 12.5 mm (g, k, m).

Supporting information

Figure S1. ML tree based on a concatenated *cox1+16S* dataset.
Table S1. List of sequenced material and accession numbers.
Table S2. List of samples sharing identical concatenated *cox1+16S* sequences.
Table S3. List of samples sharing identical concatenated *16S* sequences.
Additional data S1. Alignment of the concatenated *cox1+16S* dataset in FASTA format.

Table 1. Intra- and inter-PSHs/specific genetic differentiation of *cox1* sequences in *Austrobela* by means of p-distances. Intra-PSH/specific distances shaded. Maximum and minimum values of inter-PSHs/specific distance in bold. Inset: minimum, maximum and average intra- and inter-PSHs/specific p-distances within *Austrobela*. Species codes: lev, *A. levis*.; mic, *A. micraulax* n. sp; obl, *A. obliquicostata* n. sp; pro, *A. procera* n. sp; pyr, *A. pyrrogramma* n. sp.; ruf, *A. rufa*; sag, *A. sagitta* n. sp; Codes of species described herein in bold.

	A1/ruf	A2/ruf	**A3/lev**	**A4/sag**	**A5/obl**	A6/pro	A7/mic	A8/pyr	AA	AB	AC	AD
A1/ruf	0.001									min	max	mean
A2/ruf	**0.028**	0.002							within	0.000	0.005	0.002
A3/lev	0.044	0.053	0.004						between	0.028	0.098	0.069
A4/sag	0.060	0.068	0.057	0.002								
A5/obl	0.053	0.061	0.043	0.033	0.005							
A6/pro	0.053	0.060	0.046	0.042	0.029	0.003						
A7/mic	0.059	0.060	0.057	0.076	0.060	0.061	0.003					
A8/pyr	0.086	0.082	0.071	0.086	0.075	0.075	0.086	0.000				
AA	0.073	0.067	0.068	0.070	0.067	0.061	0.073	0.081	-			
AB	0.085	**0.098**	0.071	0.082	0.075	0.080	0.082	0.077	0.082	0.002		
AC	0.089	0.095	0.075	0.079	0.075	0.074	0.083	0.084	0.084	0.036	-	
AD	0.071	0.072	0.070	0.081	0.066	0.069	0.030	0.096	0.073	0.085	0.089	-

Table 2. Intra- and inter-PSHs/specific genetic differentiation of *cox1* sequences in *Spergo* by means of p-distances. Intra-PSH/specific distances shaded. Inset: minimum, maximum and average intra- and inter-PSHs/specific p-distances within *Spergo*. Maximum and minimum values of inter-PSHs/specific distance are in bold underlined. Species codes: ann, *S. annulata* n. sp.; cas, *S. castellum* n. sp; fus, *S. fusiformis.;* par, *S. parvidentata* n. sp; sib, *S. sibogae*; ten, *S. tenuiconcha* n. sp. Codes of species described herein in bold.

	S1/sib	S2/fus	**S3/par**	**S4/ten**	**S5/cas**	**S6/ann**
S1/sib	0.003					
S2/fus	0.029	0.008				
S3/par	0.075	0.075	0.002			
S4/ten	0.070	0.065	0.067	0.006		
S5/cas	0.075	0.072	0.069	0.042	0.003	
S6/ann	**<u>0.080</u>**	0.072	0.072	0.034	**<u>0.028</u>**	0.005

	min	max	mean
within	0.002	0.008	0.004
between	0.028	0.080	0.062

Data Availability Statement

The data that support the findings of this study are openly available in GenBank at https://www.ncbi.nlm.nih.gov/genbank/, accession numbers: EU015650, EU015736, FJ868138, HQ401584, HQ401682, HQ401707, MN983163-81, MN983183-84, MN983186-90, MN983198, MN983201-12, MN983272, MN985714-22, MN985733-34, MN985736-37, MN985743-47, MN985755, MN985758-68, MN985770-71, MT081415, MT256968, MT260886, MT393752, MT394302-20, MT394322-30, MT394332, MT394334-36, MT394338-47, MT394349-75, MT394378, MT394380, MT394383, MT394385-94, MT394396-97, MT394399-400, MT394402-14, MT395513-17, MT395519-34, MT395536-47, MT395549, MT395551-57, MT395559-61, MT395563-73, MT395575-602, MT395604, MT395607, MT395609, MT395612, MT395614-23, MT395625-26, MT395628, MT395629, MT395631-42, MT888638-93.

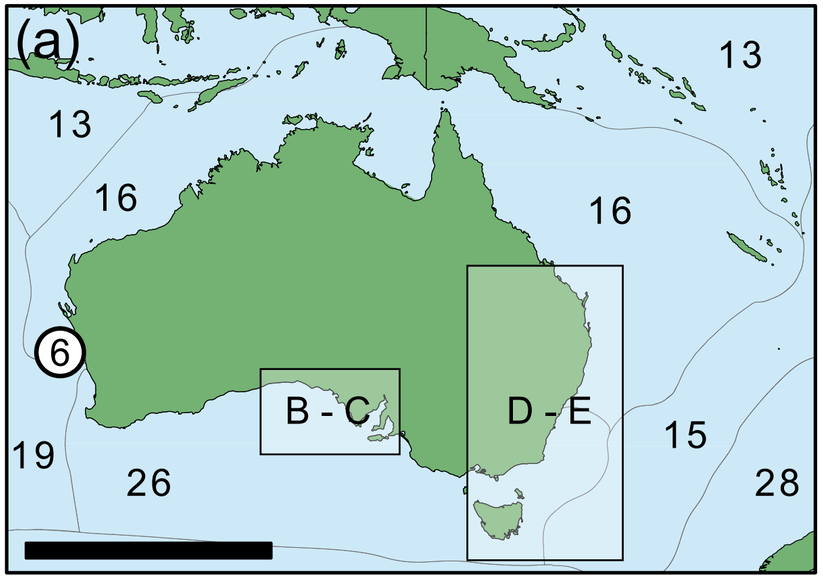
(a)
13
13
16
16
6
B - C
D - E
15
19
26
28

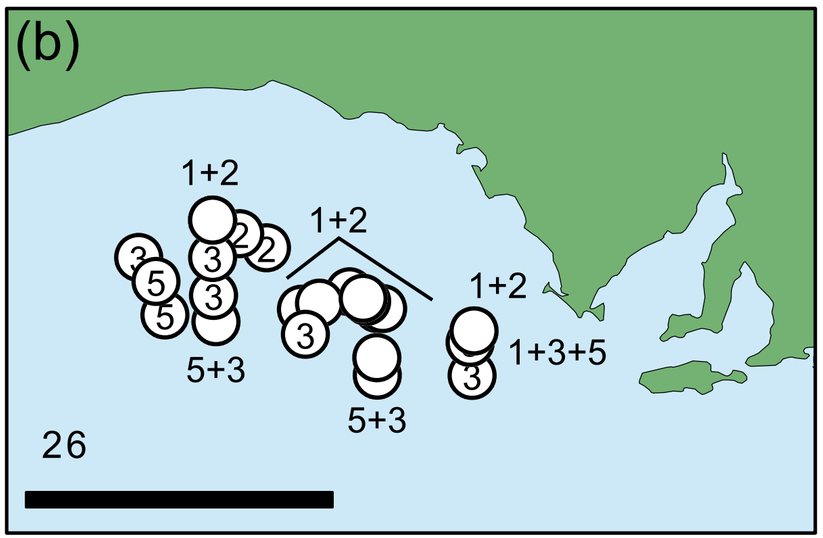
(b)
1+2
1+2
1+2
1+3+5
5+3
5+3
26

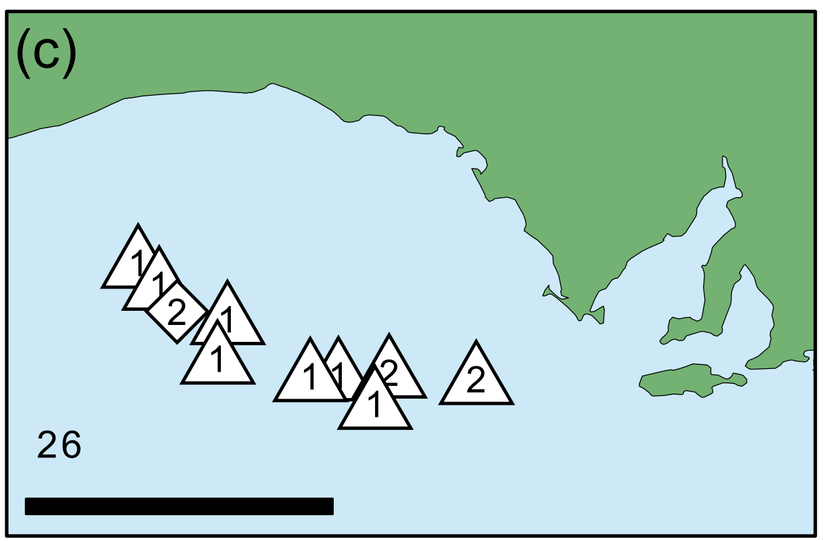
(c)
26

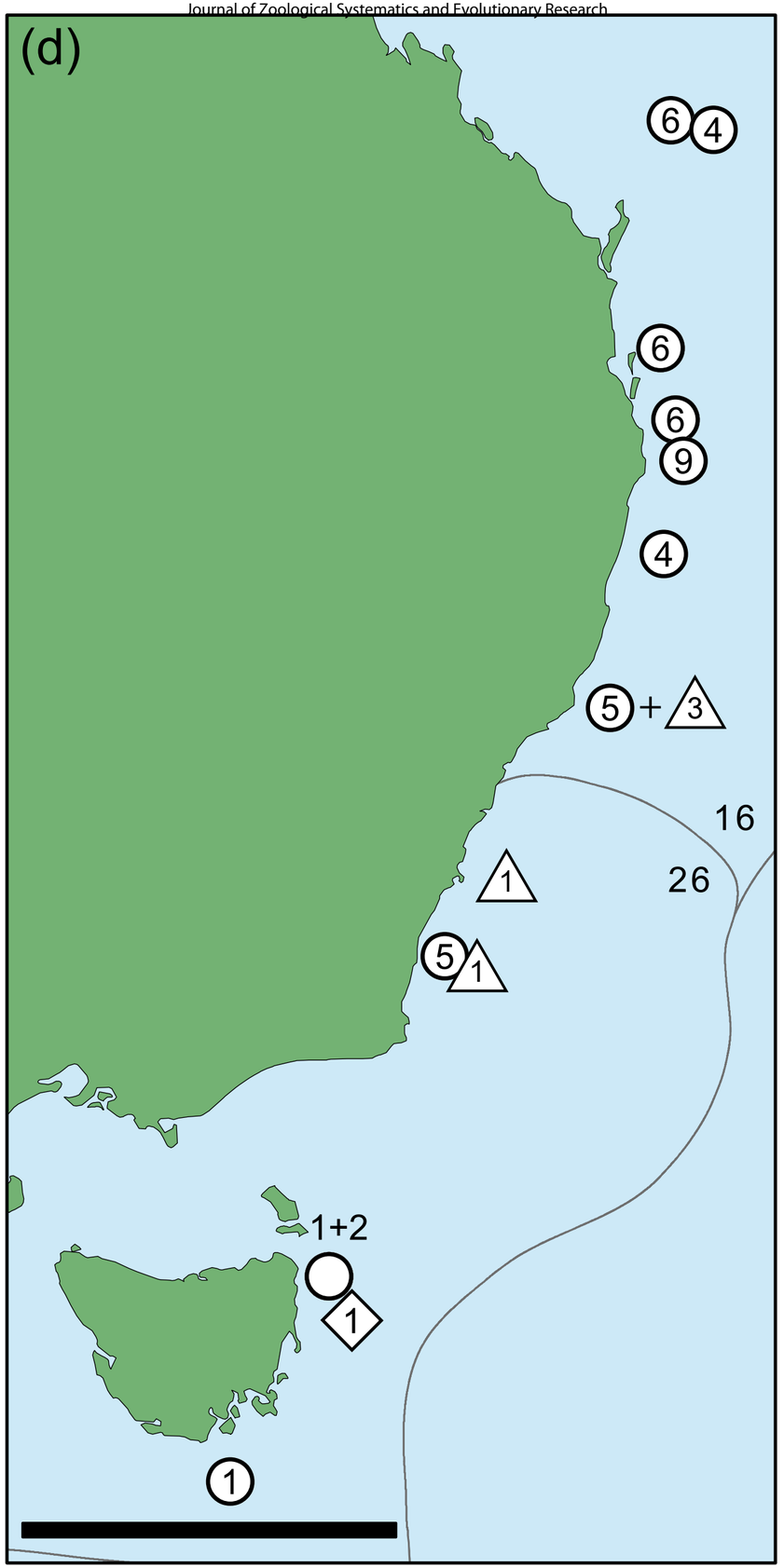
(d)
6
4
6
6
9
4
5
3
16
1
26
5
1
1+2
1
1

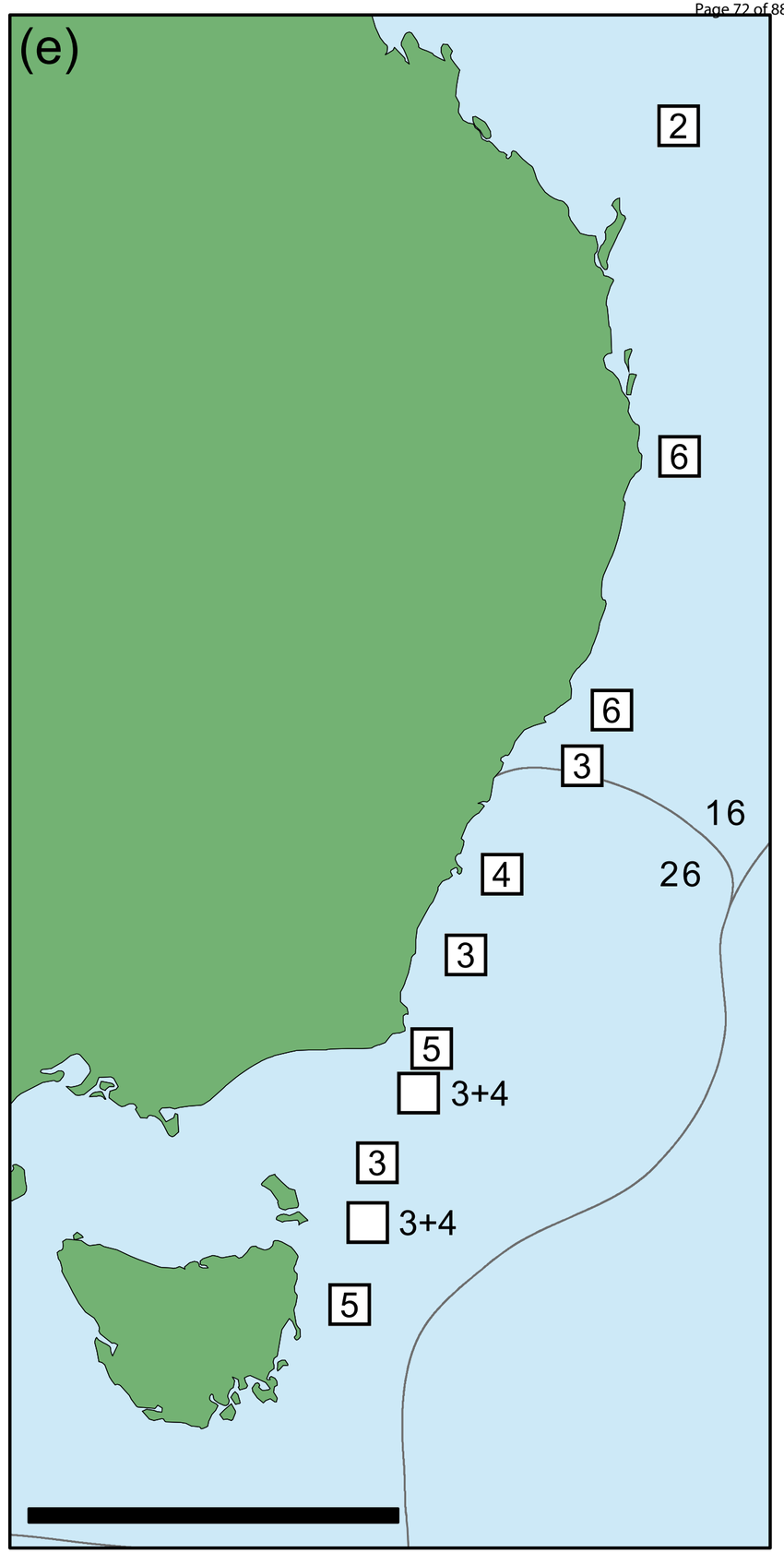
(e)
2
6
6
3
16
4
26
3
5
3+4
3
3+4
5

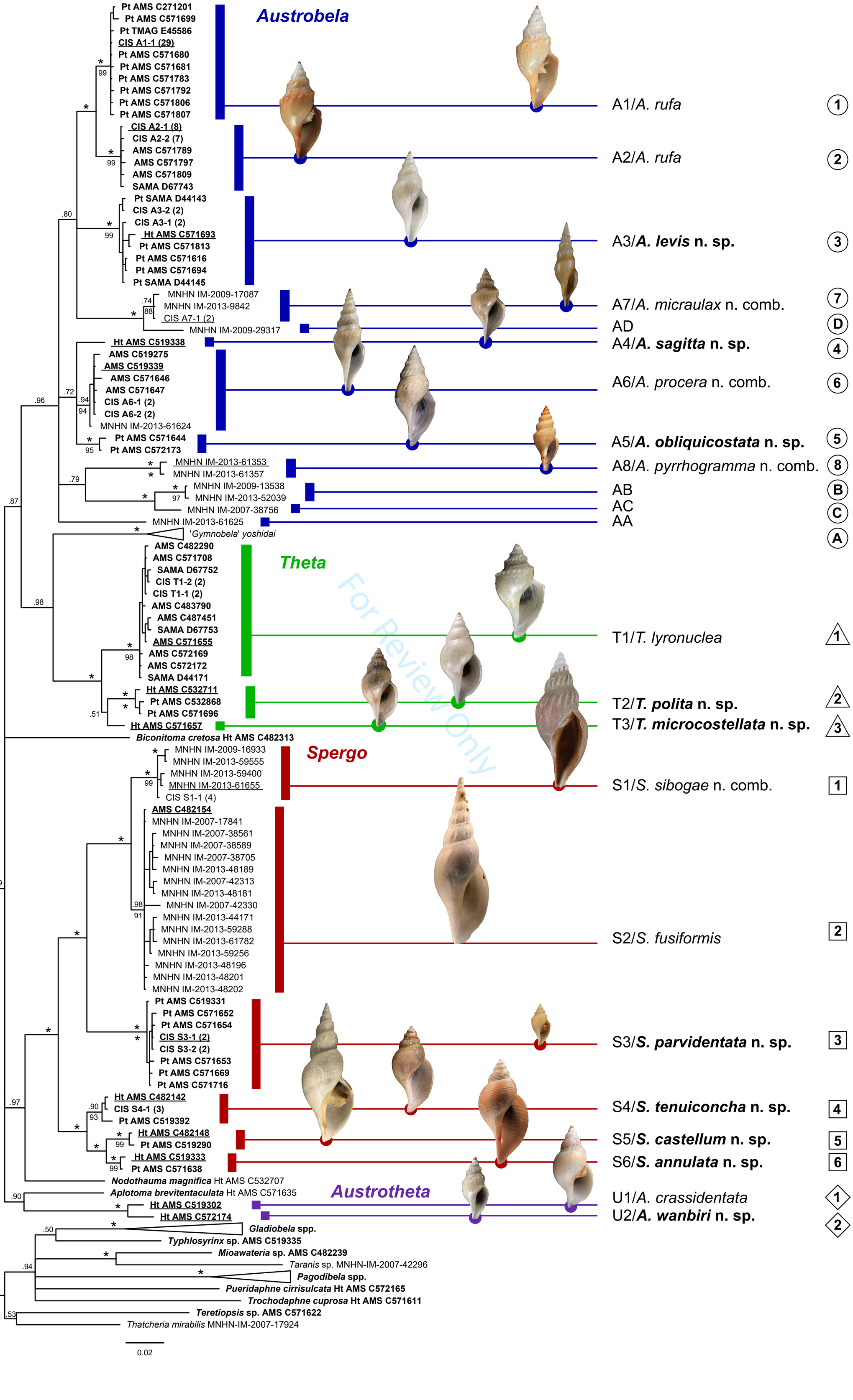

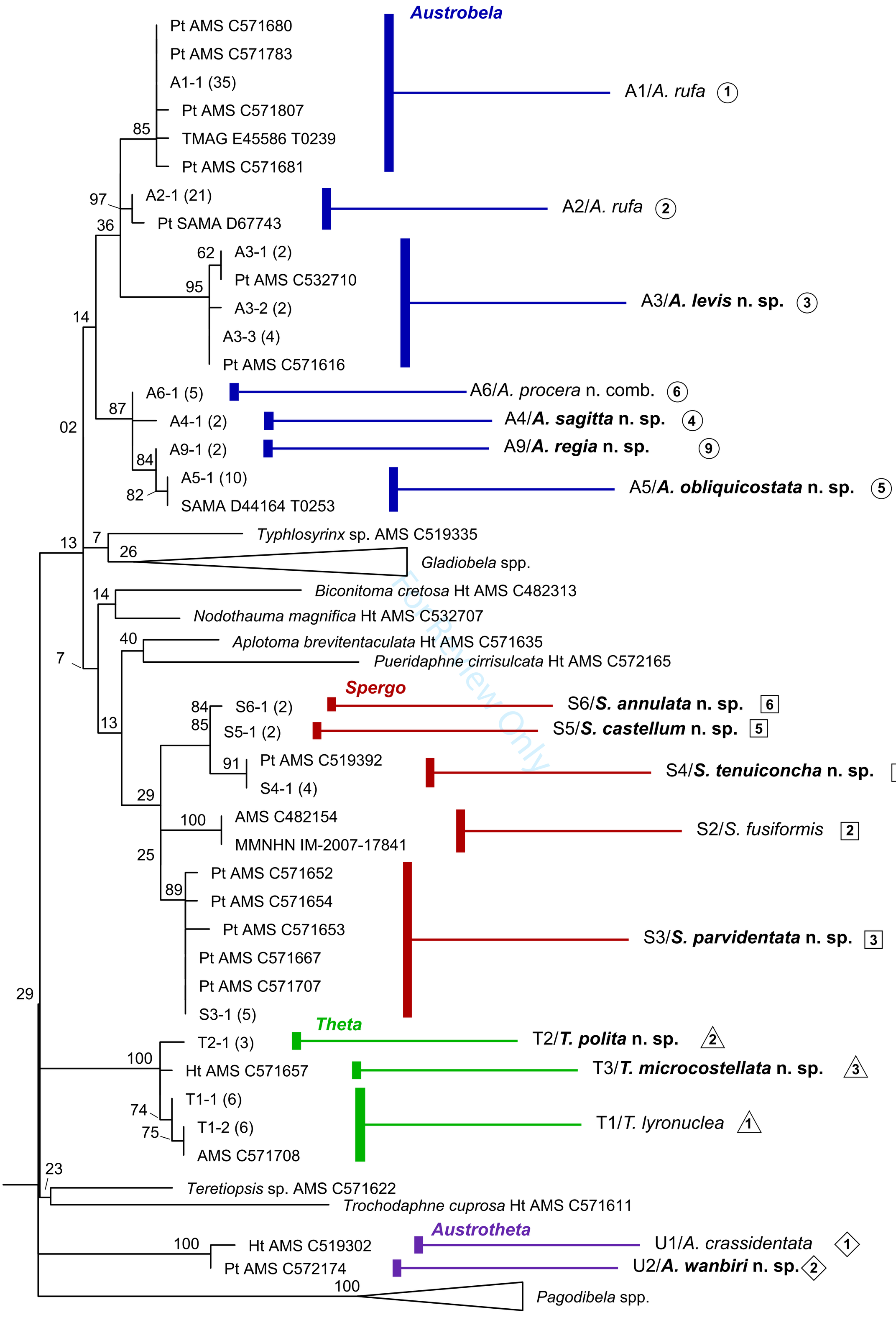
Austrobela
Pt AMS C571680
Pt AMS C571783
A1-1 (35)
Pt AMS C571807
TMAG E45586 T0239
Pt AMS C571681
A1/A. rufa 1
A2-1 (21)
Pt SAMA D67743
A2/A. rufa 2
A3-1 (2)
Pt AMS C532710
A3-2 (2)
A3-3 (4)
Pt AMS C571616
A3/A. levis n. sp. 3
A6-1 (5)
A6/A. procera n. comb. 6
A4-1 (2)
A4/A. sagitta n. sp. 4
A9-1 (2)
A9/A. regia n. sp. 9
A5-1 (10)
SAMA D44164 T0253
A5/A. obliquicostata n. sp. 5
Typhlosyrinx sp. AMS C519335
Gladiobela spp.
Biconitoma cretosa Ht AMS C482313
Nodothauma magnifica Ht AMS C532707
Aplotoma brevitentaculata Ht AMS C571635
Pueridaphne cirrisulcata Ht AMS C572165
Spergo
S6-1 (2)
S6/S. annulata n. sp. 6
S5-1 (2)
S5/S. castellum n. sp. 5
Pt AMS C519392
S4-1 (4)
S4/S. tenuiconcha n. sp. 4
AMS C482154
MMNHN IM-2007-17841
S2/S. fusiformis 2
Pt AMS C571652
Pt AMS C571654
Pt AMS C571653
Pt AMS C571667
Pt AMS C571707
S3-1 (5)
S3/S. parvidentata n. sp. 3
Theta
T2-1 (3)
T2/T. polita n. sp. 2
Ht AMS C571657
T3/T. microcostellata n. sp. 3
T1-1 (6)
T1-2 (6)
AMS C571708
T1/T. lyronuclea 1
Teretiopsis sp. AMS C571622
Trochodaphne cuprosa Ht AMS C571611
Austrotheta
Ht AMS C519302
Pt AMS C572174
U1/A. crassidentata 1
U2/A. wanbiri n. sp. 2
Pagodibela spp.
85
97
36
62
95
14
02
87
84
82
13
7
26
14
40
7
84
85
91
29
100
25
89
29
100
74
75
23
100
100
0.01

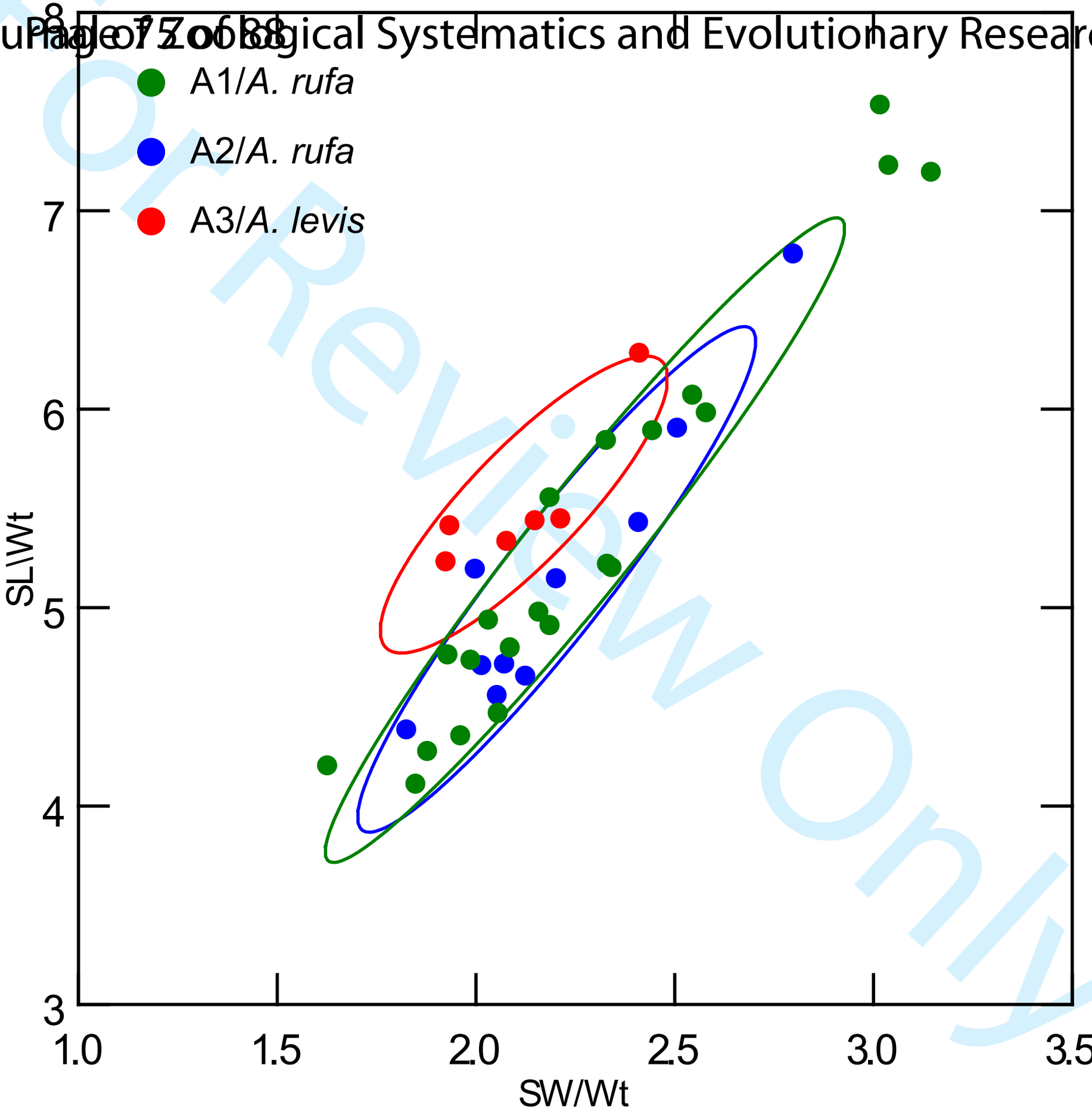

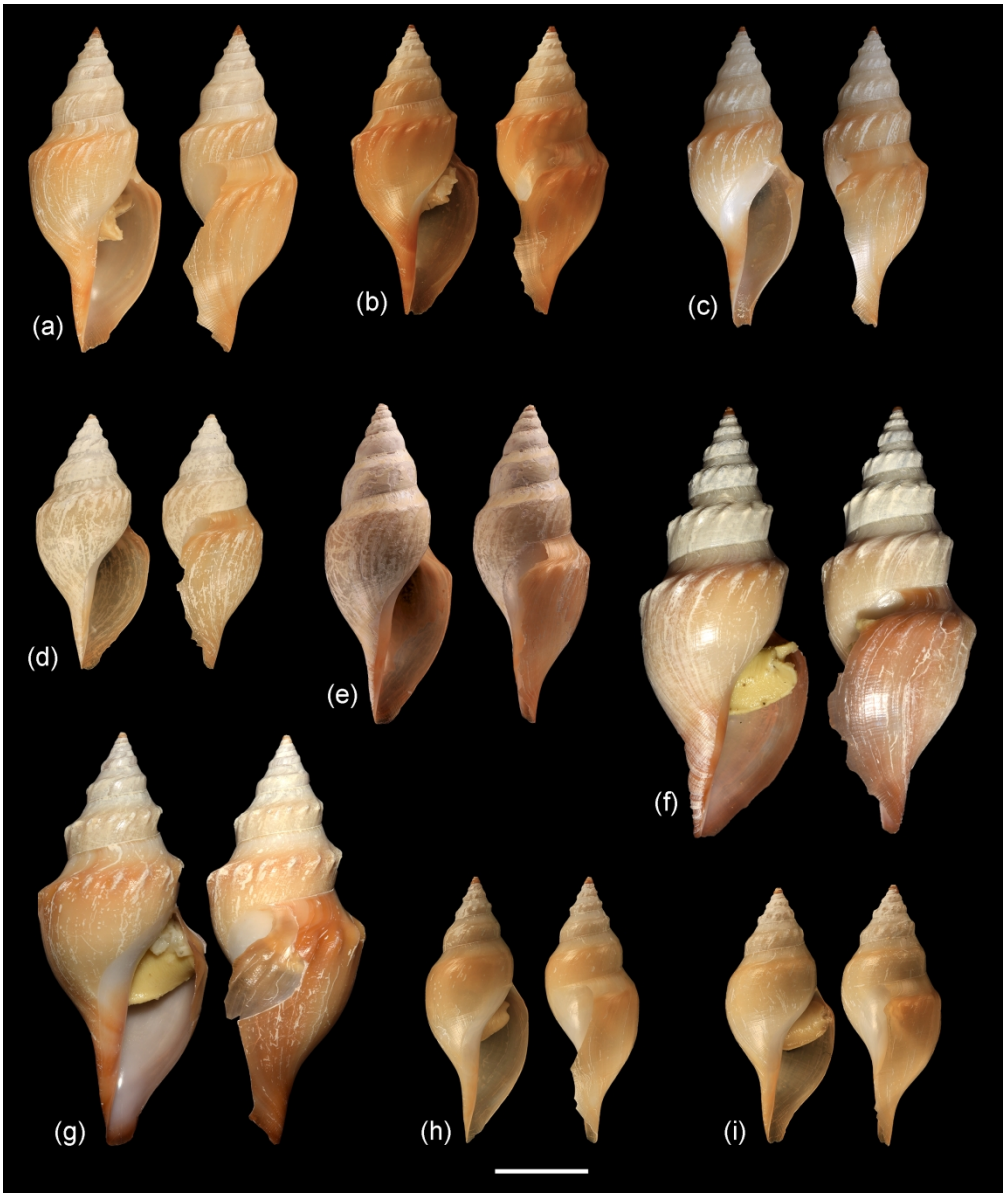

Figure 5. Shells of Austrobela rufa Criscione et al., 2020 (PSHs A1-A2). (a) Holotype AMS C.571709 (A1); (b) AMS C.571756 (A2); (c) AMS C.532684 (A2); (d) Paratype AMS C.571699 (A1); (e) Paratype AMS C.483802 (A1); (f) Paratype AMS C.574588 (A1); (g) Paratype AMS C.271201 (A1); (h) Paratype SAMA D44253 (A1); (i) Paratype SAMA D67742 (A1). Scale bar = 10 mm.

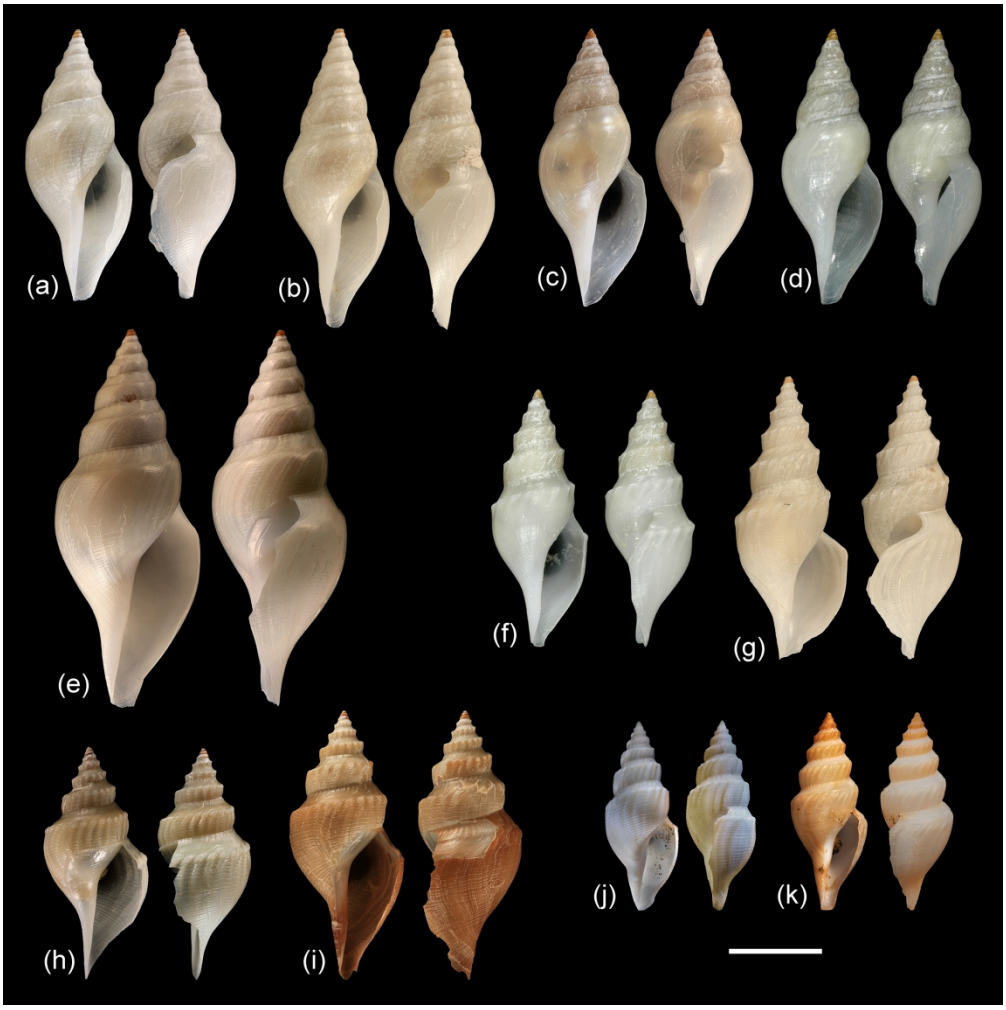

Figure 6. Shells of Austrobela PSHs/species studied herein. (a) A3/Austrobela levis n. sp., holotype AMS C.571693; (b) A3/Austrobela levis n. sp., paratype AMS C.532671; (c) A3/Austrobela levis n. sp., paratype AMS C.571694; (d) A3/Austrobela levis n. sp., paratype AMS C.571813; (e) A3/Austrobela levis n. sp., paratype SAMA D44145; (f) A5/Austrobela obliquicostata n. sp., holotype SAMA D67741; (g) A5/Austrobela obliquicostata n. sp., paratype AMS C.532689; (h) A4/Austrobela sagitta n. sp., holotype AMS C.519338; (i) A9/Austrobela regia n. sp. holotype AMS C.571682; (j) Austrobela pyrrhogramma (Dautzenberg & Fischer, 1896) n. comb., holotype MOM INV-18477; (k) A8/Austrobela pyrrhogramma (Dautzenberg & Fischer, 1896) n. comb., MNHN IM-2013-61353 . Scale bar = 10 mm.

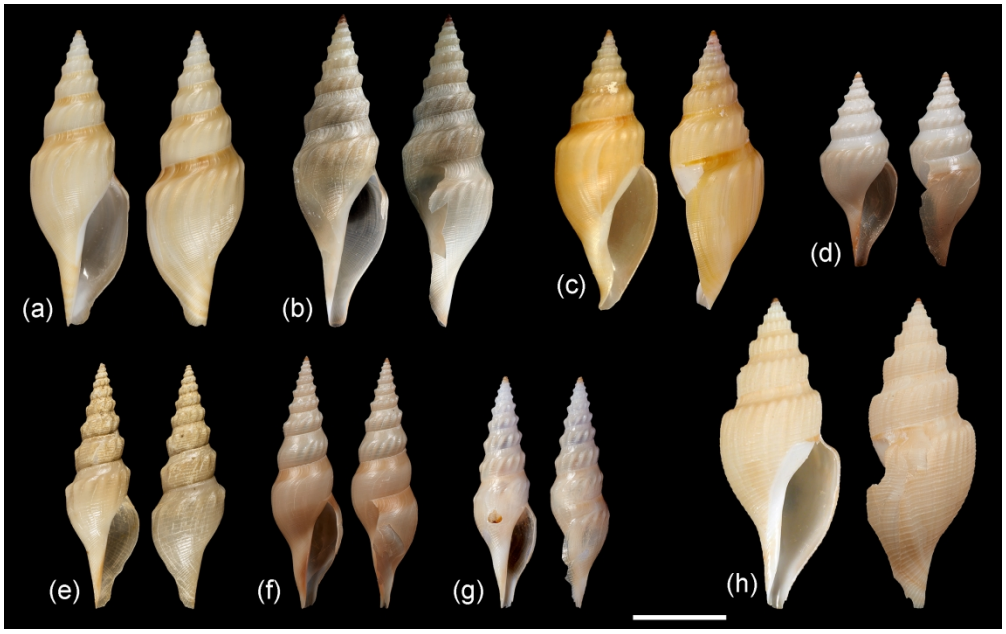

Figure 7. Shells of Austrobela PSHs/species studied herein. (a) Austrobela procera (Sysoev & Bouchet, 2001), holotype MNHN IM-2000-3188; (b) A6/Austrobela procera (Sysoev & Bouchet, 2001) n. comb., AMS C.519339; (c) Austrobela AB, MNHN IM-2009-13538; (d) Austrobela AA, MNHN IM-2013-61625; (e) Austrobela micraulax (Sysoev, 1997) n. comb., holotype MNHN IM-2000-3091; (f) A7/Austrobela micraulax (Sysoev, 1997) n. comb., MNHN IM-2013-9837; (g) Austrobela AD, MNHN IM-2009-29317; (h) Austrobela AC, IM-2007-38756. Scale bar = 10 mm.

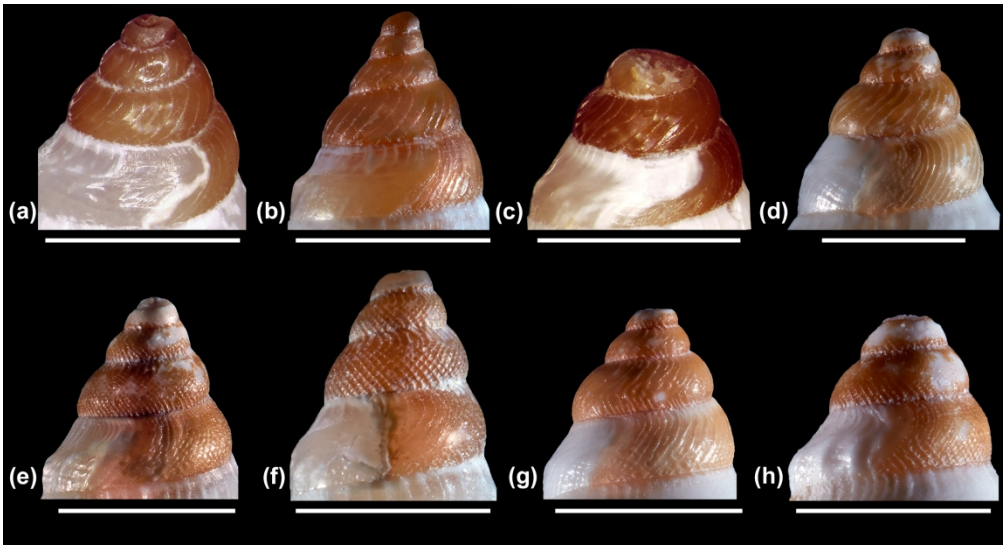

Figure 8. Larval shells of Austrobela PSHS/species studied herein. (a) A1/Austrobela rufa Criscione et al., 2020 holotype AMS C. 571709; (b) A1/Austrobela rufa Criscione et al., 2020 paratype AMS C.571681; (c) A2/Austrobela rufa Criscione et al., 2020, AMS C.571756; (d) A3/Austrobela levis n. sp., paratype AMS C.532883; (e) A4/Austrobela sagitta n. sp., paratype AMS C.519400; (f) A6/Austrobela procera (Sysoev & Bouchet, 2001) n. comb., AMS C.519275; (g) A5/Austrobela obliquicostata n. sp., paratype AMS C.572173; (h) A9/Austrobela regia holotype AMS C.571682. Scale bar = 1 mm.

Figure 9. Hypodermic teeth of Austrobela PSHs/species studied herein. (a) A1/Austrobela rufa Criscione et al., 2020, paratype AMS C.571679; (b) A2/Austrobela rufa Criscione et al., 2020, AMS C. C.575584; (c) A6/Austrobela procera (Sysoev & Bouchet, 2001) n. comb., AMS C.519339; (d) A5/Austrobela obliquicostata n. sp., paratype AMS C.571644; (e) A9/Austrobela regia holotype AMS C.571682; (f) A3/Austrobela levis n. sp., holotype AMS C.571693; (g) A4/Austrobela sagitta n. sp., holotype AMS C.519338. Scale bar = 200 µm.

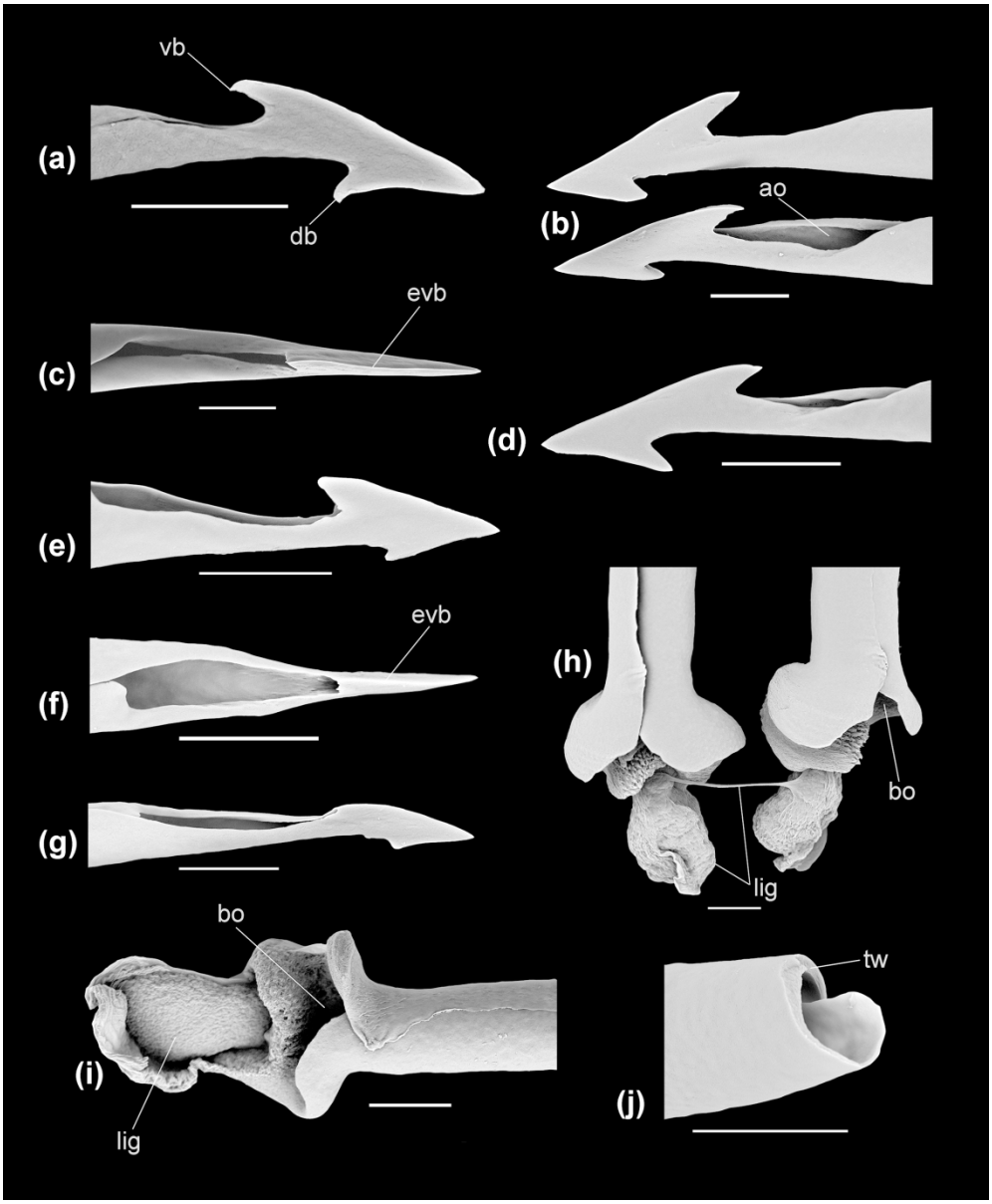

Figure 10. Radular details of Austrobela and Theta spp. (a) A3/Austrobela levis n. sp., holotype AMS C.571693; (b) A9/Austrobela regia holotype AMS C.571682; (c) A1/Austrobela rufa Criscione et al., 2020 paratype AMS C.574588; (d) A2/Austrobela rufa Criscione et al., 2020 AMS C.575584; (e) T1/Theta lyronuclea (Clarke, 1959), AMS C.571733; (f) T1/Theta lyronuclea (Clarke, 1959), AMS C.571733; (g) T3/Theta polita n. sp., paratype AMS C.532868 (h) A9/Austrobela regia holotype AMS C.571682; (i) T3/Theta polita n. sp., holotype AMS C.571657; (j) A2/Austrobela rufa Criscione et al., 2020, AMS C.571670. Scale bar = 20 μm.
Abbreviations: ao = adapical opening; bo = basal opening; db = dorsal barb; evb = edge of ventral barb; lig = ligament; tw = tooth wall; vb = ventral barb.

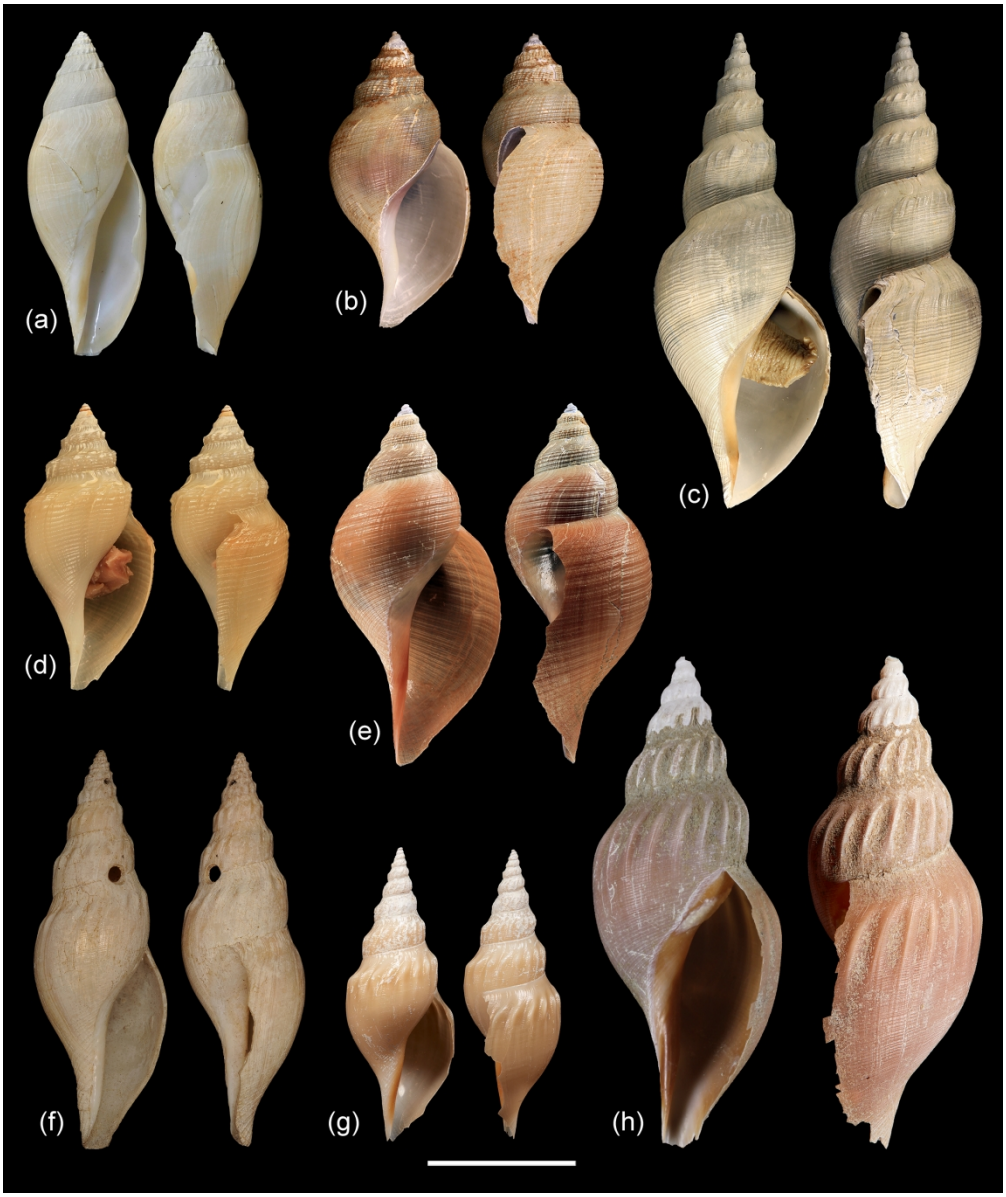

Figure 11. Shells of Spergo PSHS/species studied herein. (a) Spergo glandiniformis (Dall, 1895), holotype USNM 107013; (b) S4/Spergo tenuiconcha n. sp., holotype AMS C.482142; (c) S5/Spergo castellum n. sp. holotype AMS C.482148; (d) S3/Spergo parvidentata n. sp., holotype AMS C.519401; (e) S6/Spergo annulata n. sp., holotype AMS C.519333; (f) Spergo sibogae (Schepman, 1913), holotype NBCNL ZMA.MOLL.136847; (g) S1/Spergo sibogae (Schepman, 1913), MNHN IM-2009-16933; (h) S1/Spergo sibogae (Schepman, 1913), MNHN IM-2013-61655. Scale bar = 20 mm.

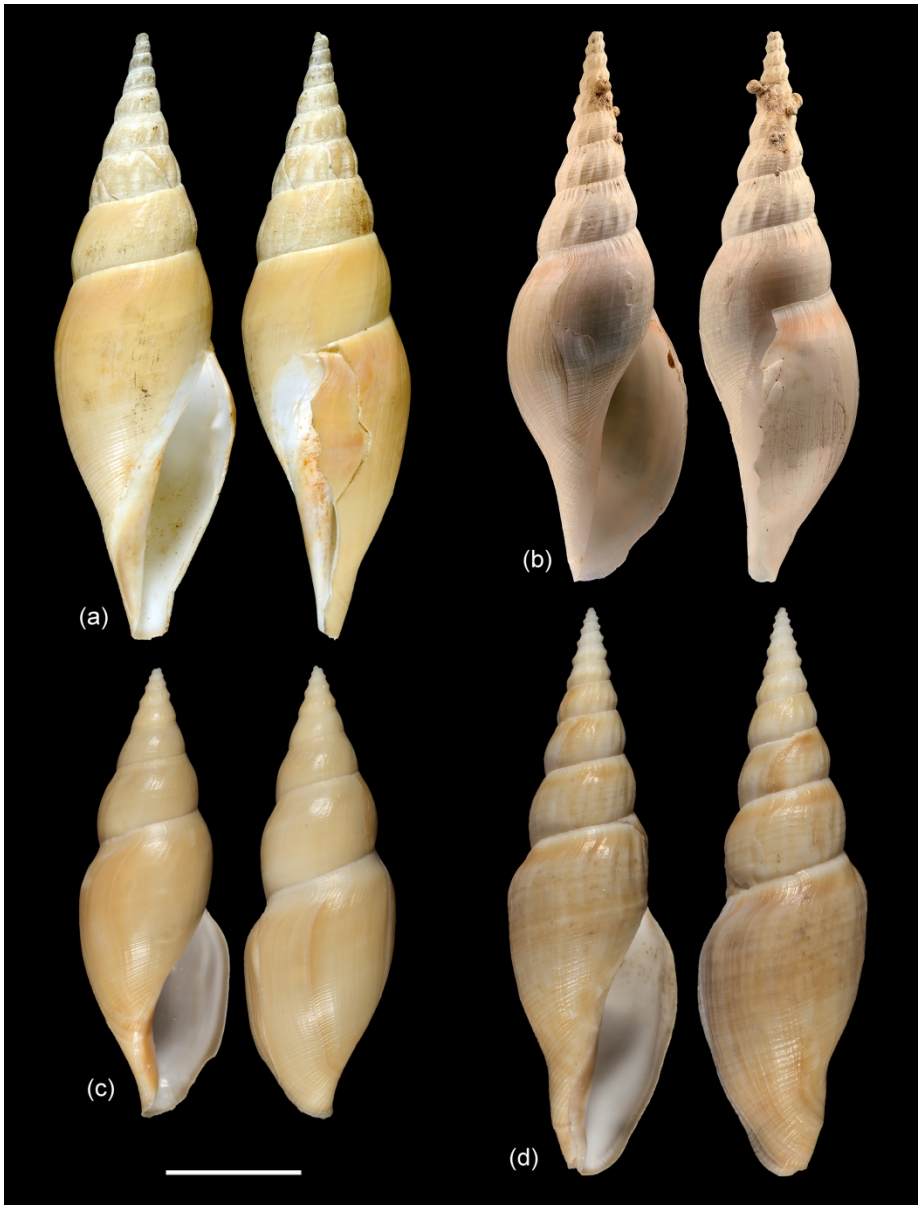

Figure 12. Shells of Spergo PSHs/species studied herein. (a) Spergo fusiformis (Habe, 1962), holotype NSMT MoR 49751; (b) S2/Spergo fusiformis (Habe, 1962), AMS C.482154; (c) Spergo aithorrhis Sysoev & Bouchet, 2001, holotype MNHN IM-2000-2742; (d) Spergo parunculis Stalschmidt, Chino & Fraussen, 2015, holotype MNHN IM-2000-30150. Scale bar = 20 mm.

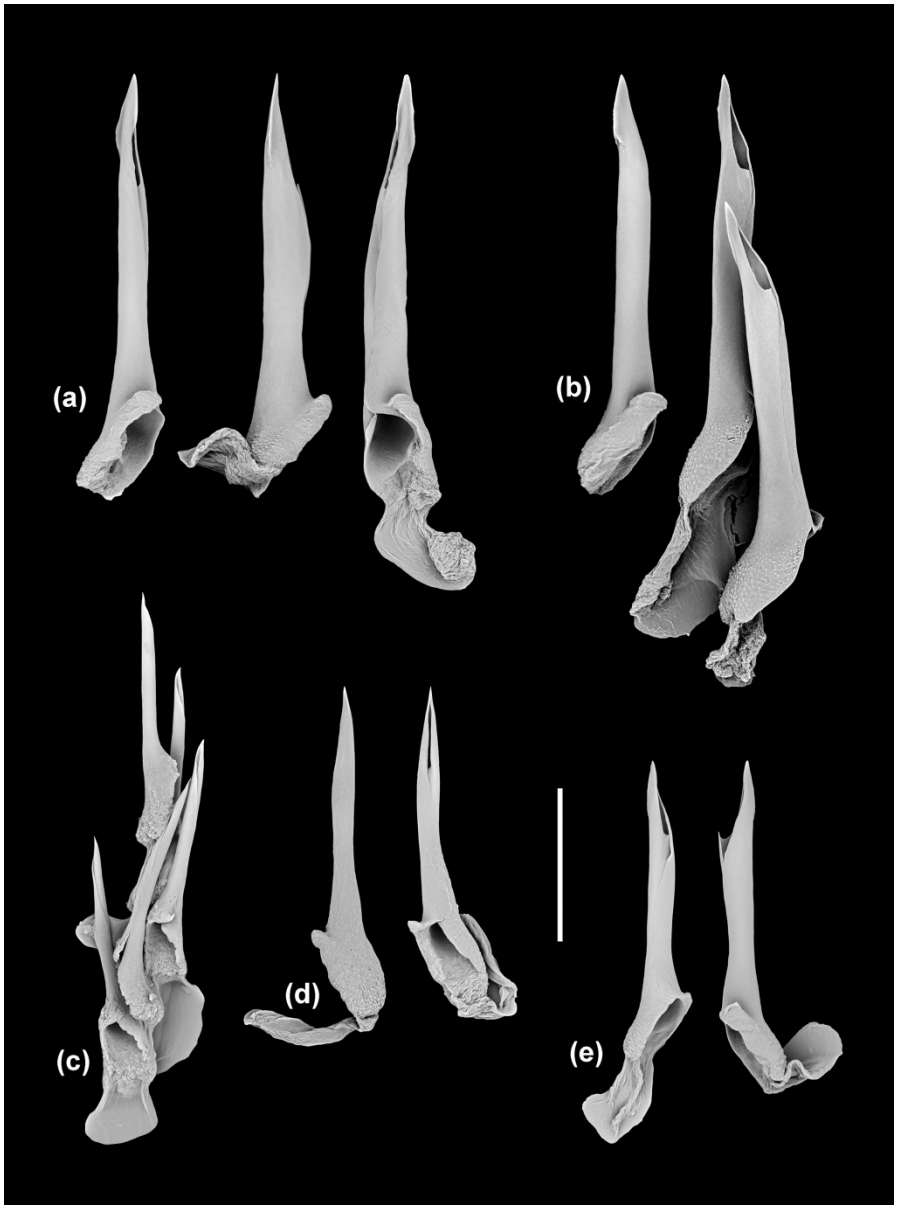

Figure 13. Hypodermic teeth of Spergo PSHs/species studied herein. (a) S5/Spergo castellum n. sp., paratype AMS C.519290; (b) S4/Spergo tenuiconcha n. sp., holotype AMS C.482142; (c) S3/Spergo parvidentata n. sp., paratype AMS C.571667; (d) S2/Spergo fusiformis (Habe, 1962), AMS C.482154; (e) S6/Spergo annulata n. sp., paratype AMS C.571638. Scale bar = 50 μm (9A, B, D & E); 30 μm (9C).

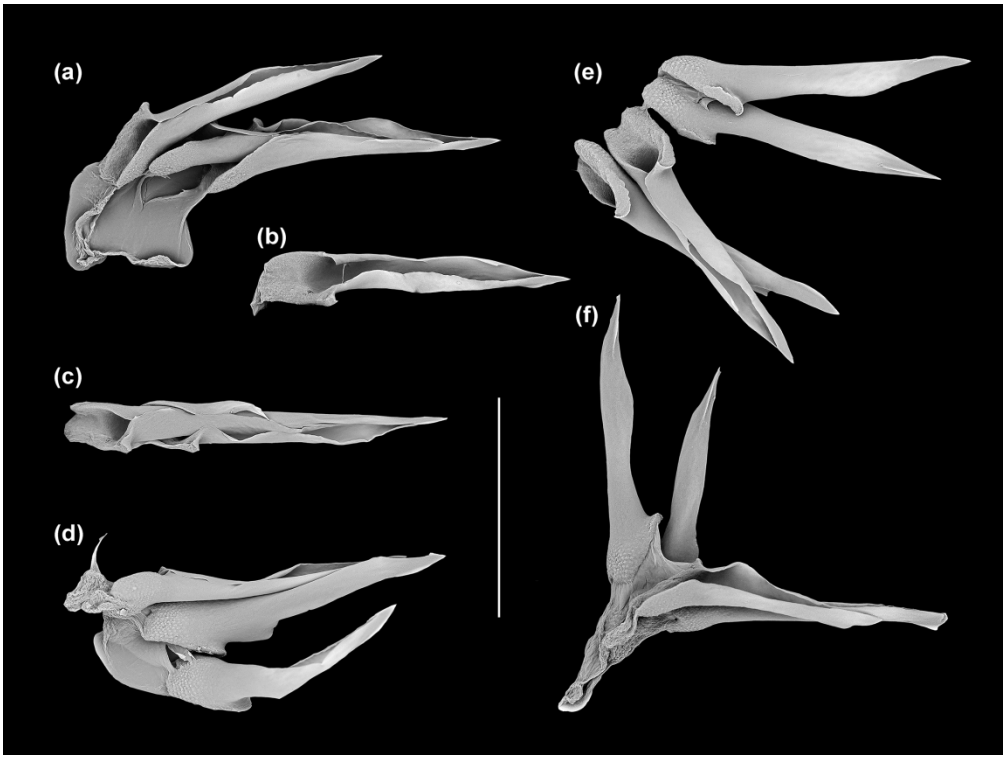

Figure 14. Variation in tooth formation in S5/Spergo castellum n. sp., holotype AMS C.482148. (a) Teeth exhibiting medium to high degree of unrolling, with two bottom teeth entangled (with one encapsulated within the other); (b) entirely unrolled tooth; (c) entangled teeth; (d) bent, possibly poorly sclerotized teeth (e) moderately to tightly rolled, straight teeth; (f) cluster of teeth with interconnecting ligaments, showing one entirely unrolled tooth. Scale bar = 100 μm.

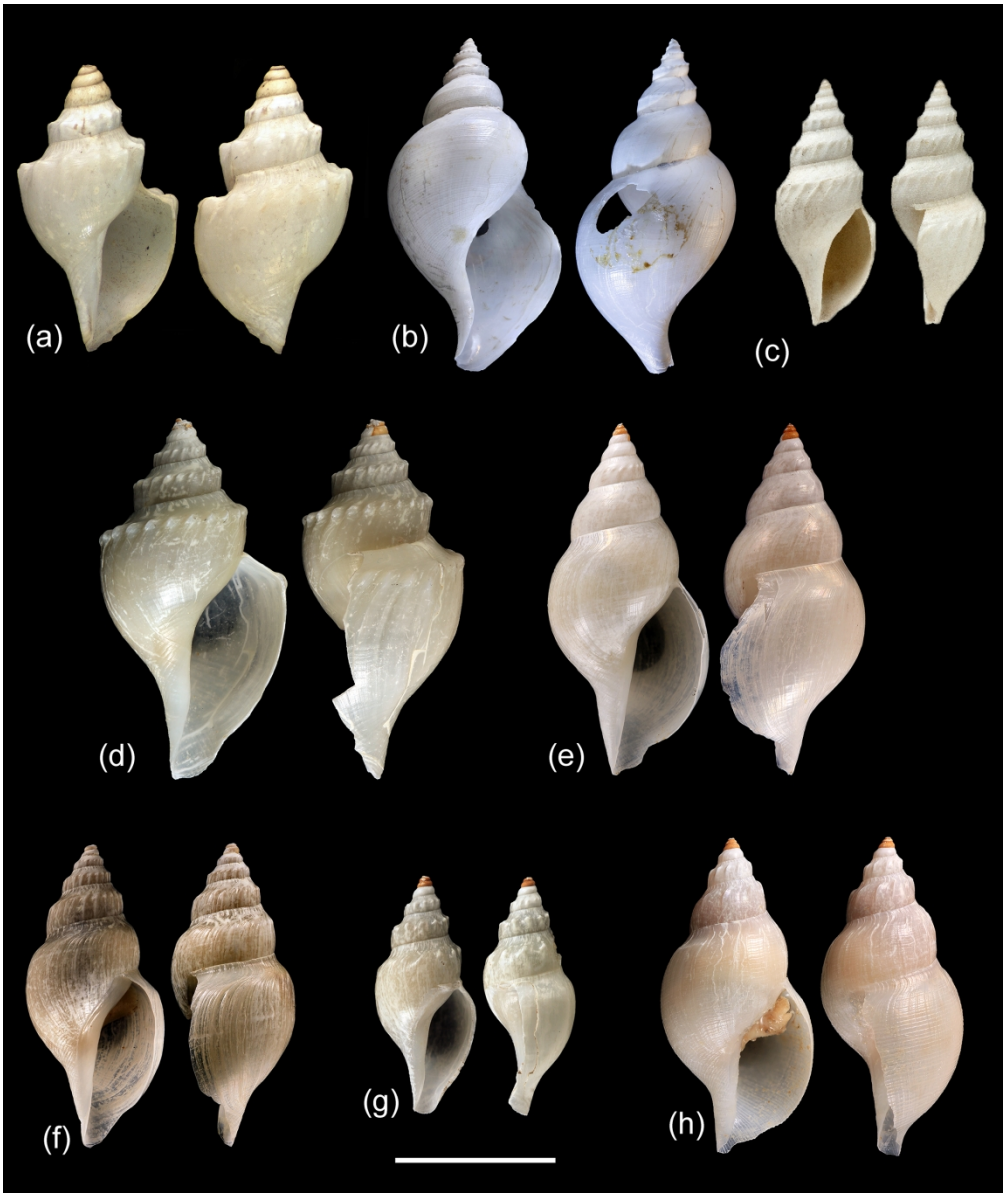

Figure 15. Shells of Theta and Austrotheta PSHs/species studied herein. (a) T1/Theta lyronuclea (Clarke, 1959), holotype MCZ 218184; (b) Theta vayssierei (Dautzenberg, 1925), holotype MOM INV-18405; (c) Theta chariessa (Watson, 1881), syntype NHMUK 1887.2.9.1098; (d) T1/Theta lyronuclea (Clarke, 1959), AMS C.571655; (e) T3/Theta polita n. sp., holotype AMS C.571657; (f) T2/Theta microcostellata n. sp., holotype AMS C.532711;
(g) U2/Austrotheta wanbiri n. sp., holotype AMS C.572174; (h) U1/Austrotheta crassidentata Criscione et al., 2020, holotype AMS C.519302. Scale bar = 5 mm (a), 10 mm (b-h).

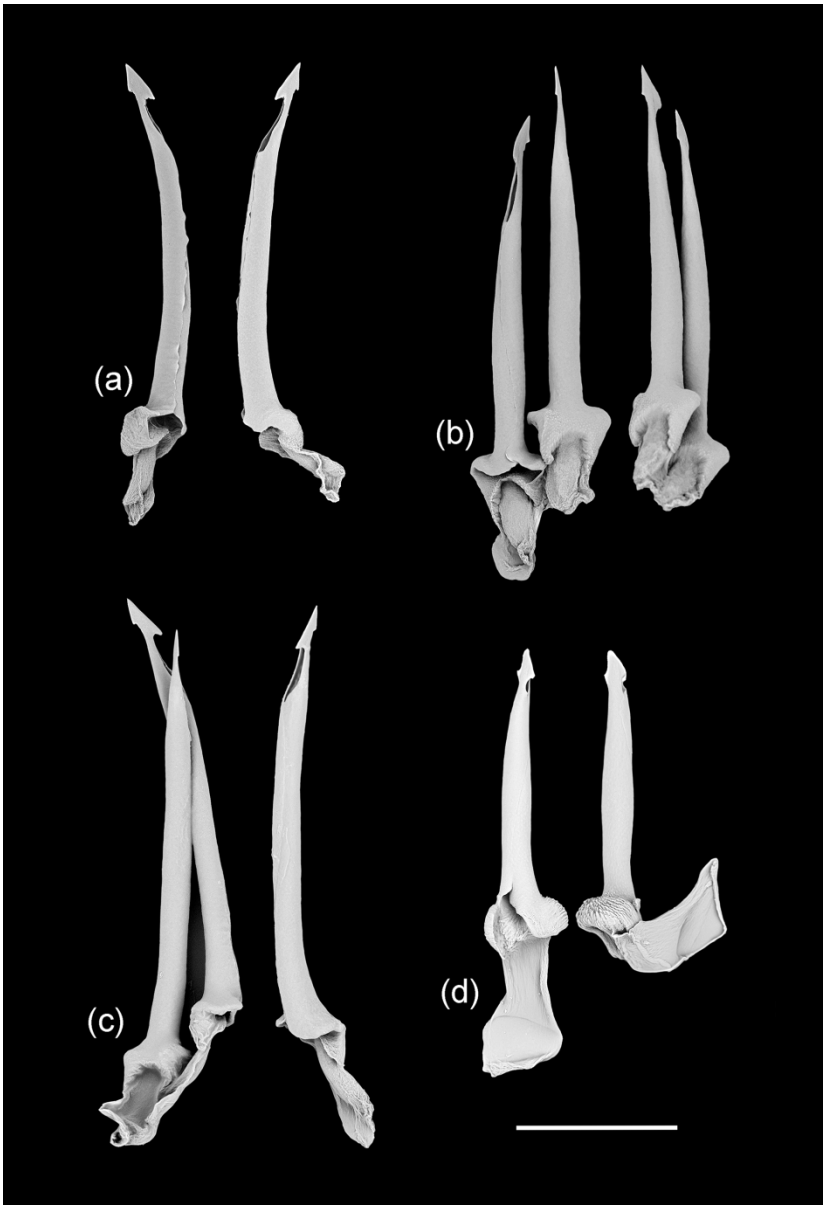

Figure 16. Hypodermic teeth of Theta and Austrotheta PSHs/species studied herein. (a) T1/Theta lyronuclea (Clarke, 1959), AMS C.571733; (b) T2/Theta polita n. sp., paratype AMS C.532868; (c) T3/Theta microcostellata n. sp., holotype AMS C.571657; (d) U1/Austrotheta crassidentata Criscione et al., 2020, holotype AMS C.519302. Scale bar = 100 μm.

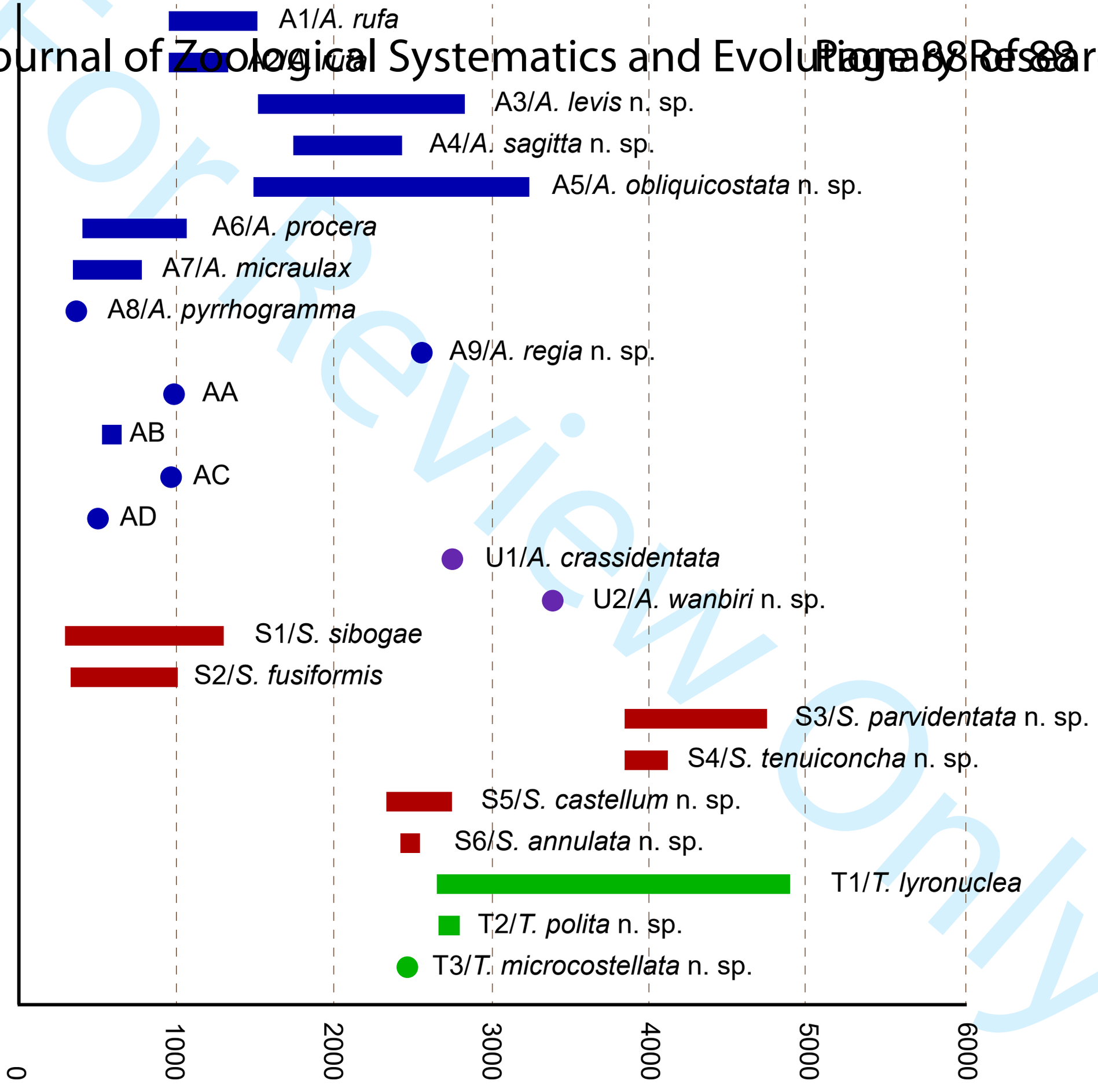

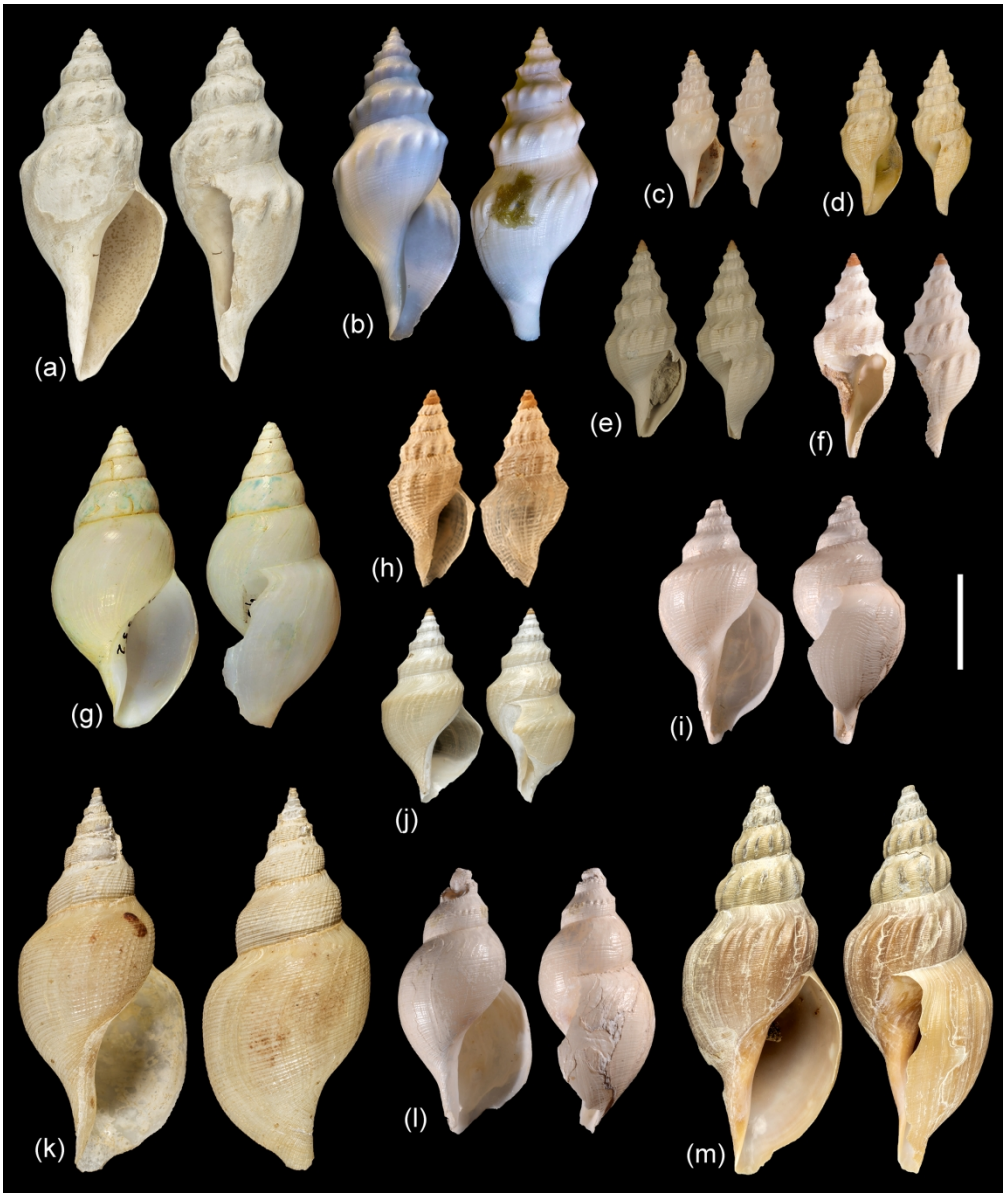

Figure 18. Shells of types of species of Raphitomidae showing typical traits of the genera studied herein. (a) Pleurotoma gypsata Watson, 1881, syntype NHMUK 1887.2.9.979; (b) Pleurotoma fulvotincta Dautzenberg & Fischer, 1896, syntype MOM INV-18461; (c) Pleurotomella dubia Schepman, 1913, syntype NBCN ZMA.MOLL.136881; (d) Pleurotoma filifera Dall, 1881, holotype USNM 596209; (e) Gymnobela petiti Garcia, 2005, holotype ANSP 412715; (f) Gymnobela nivea Sysoev, 1990, holotype ZMMU Lc-5737; (g) Pleurotomella argeta Dall, 1890, holotype UNSM 96552; (h) Pleurotomella ceramensis Schepman, 1913, syntype ZMA.MOLL.137936; (i) Gymnobela latistriata Kantor & Sysoev, 1986, holotype ZMMU Lc-22341; (j) Clathurella homeotata Watson, 1886, holotype NHMUK 1887.2.9.1115; (k) Thesbia nudator Locard, 1897, holotype MNHN IM-2000-3131; (l) Gymnobela oculifera Kantor & Sysoev, 1986; (m) Gymnobela africana Sysoev, 1996, holotype NHMUK 1993114. Scale bar = 3 mm (k), 5 mm (e-f), 10 mm (a-d, h-i, j, l), 12.5 mm (g, k, m).